U.S. DRIVE Net-Zero Carbon Fuels Technical Team Analysis Summary Report 2020

September 2021

This report is a document of the U.S. DRIVE Partnership. U.S. DRIVE (Driving Research and Innovation for Vehicle efficiency and Energy sustainability) is a voluntary, non-binding, and non-legal partnership among the U.S. Department of Energy; the United States Council for Automotive Research (USCAR), representing FCA US LLC, Ford Motor Company, and General Motors; five energy companies—BP America, Chevron Corporation, Phillips 66 Company, ExxonMobil Corporation, and Shell Oil Products US; four utilities—American Electric Power, DTE Energy, Duke Energy Corporation, and Southern California Edison; and the Electric Power Research Institute (EPRI).

The Net-Zero Carbon Fuels Technical Team (NZTT) is one of 13 U.S. DRIVE technical teams whose mission is to accelerate the development of pre-competitive and innovative technologies tenable of a full range of efficient and clean advanced light-duty vehicles, as well as related energy infrastructure.

This report was authored by John Dees[1], Hannah Goldstein[2], Gary Grim[3], Kylee Harris[3], Zhe Huang[3], Uisung Lee[4], Pimphan (Aye) Meyer[5], Ian Rowe[6], Dan Sanchez[1], A.J. Simon[2], Lesley Snowden-Swan[5], Ling Tao[3], Michael Wang[4], and Eunji Yoo[4].

For more information about U.S. DRIVE, please see the U.S. DRIVE Partnership Plan at www.energy.gov/eere/vehicles/us-drive or www.uscar.org.

---

[1] University of California, Berkeley
[2] Lawrence Livermore National Laboratory
[3] National Renewable Energy Laboratory
[4] Argonne National Laboratory
[5] Pacific Northwest National Laboratory
[6] Bioenergy Technologies Office

List of Acronyms

|	
afdw	ash-free dry weight
CCS	carbon capture and sequestration
CH_4	methane
CI	carbon intensity
CO	carbon monoxide
CO_2	carbon dioxide
CO_2e	carbon dioxide equivalent
DGS	distillers grains with solubles
DME	dimethyl ether
gge	gallon gasoline equivalent
GHG	greenhouse gas
GREET	Greenhouse gases, Regulated Emissions, and Energy use in Technologies
HOG	high-octane gasoline
HTL	hydrothermal liquefaction
LCA	life cycle analysis
MESP	minimum ethanol selling price
MFSP	minimum fuel selling price
MJ	megajoule
MMBTU	million British thermal units
MSP	minimum selling price
MT	million tonnes
N_2O	nitrous oxide
NG	natural gas
NZTT	Net-Zero Carbon Fuels Technical Team
R&D	research and development
RNG	renewable natural gas
SMR	steam methane reforming
SOT	state of technology
TEA	techno-economic analysis
TRL	technology readiness level
U.S. DRIVE	Driving Research and Innovation for Vehicle efficiency and Energy Sustainability

Executive Summary

The Net-Zero Carbon Fuels Technical Team (NZTT) is tasked with investigating the potential to generate carbon-based fuels with much lower carbon intensities (CIs) compared to those of conventional fuels, approaching or exceeding net-zero greenhouse gas (GHG) emissions. In this study, the life cycle GHG emissions of four fuel production pathways and dozens of variants on those pathways are analyzed. Additionally, the overall cost of each pathway is evaluated and calculated as minimum fuel selling price (MFSP). The four pathways and their primary variations are:

1. Conventional ethanol production with carbon capture and sequestration (CCS).
2. Production of gasoline, jet, and diesel fuel from the hydrothermal liquefaction (HTL) of algae and subsequent hydrotreating and fractionation.
3. Advanced ethanol production via syngas fermentation. Both biomass gasification and electrolytic carbon dioxide (CO_2) reduction are investigated as carbon inputs.
4. Methanol production from renewable syngas. Both biomass gasification and electrolytic CO_2 reduction are investigated as carbon inputs. Further conversion of methanol to high-octane gasoline (HOG) is evaluated as an option for drop-in fuel production.

These pathways represent a diverse set of options for producing net-zero-carbon fuels, covering a range of feedstocks, process inputs, products, coproducts, environmental impacts, and technical maturities. It is not the intention of this report to rank or compare these pathways on specific criteria or overall promise. Rather, this report is intended to show that there are multiple pathways with multiple feedstocks toward net-zero liquid fuels. Factors such as feedstock constraints, carbon disposal logistics, maturation time, capital and operating costs, and renewable energy availability will affect the technical and economic feasibility of each of these pathways. This report lays the groundwork for continual assessment of net-zero options as this landscape evolves.

Section 2 of this report describes the analysis methodologies. Life cycle analysis (LCA)—based primarily on the Greenhouse gases, Regulated Emissions, and Energy use in Technologies (GREET) LCA model—was used to calculate each pathway's CI. Our LCA considers the GHG emissions associated with the operation of upstream conversions and logistics (e.g., biomass growth and transport, fossil fuel production) and process inputs (electricity generation, hydrogen production, and reagent manufacturing), as well as the GHG consequences of all products and coproducts, including displacement credits. Carbon usage, emissions, and disposal from the core pathway are accounted for. Techno-economic analysis (TEA) based on a consistent set of assumptions about finance, capital costs, and feedstock prices is used to calculate each pathway's MFSP. Using published engineering methods and standard accounting assumptions, a discounted cash flow rate of return analysis is conducted using capital and operating cost data to calculate MFSPs.

This process is shown schematically in Figure ES-1 for a generalized process. Each case and sub-scenario has different connectivity between resources, intermediates, process configuration, and products.
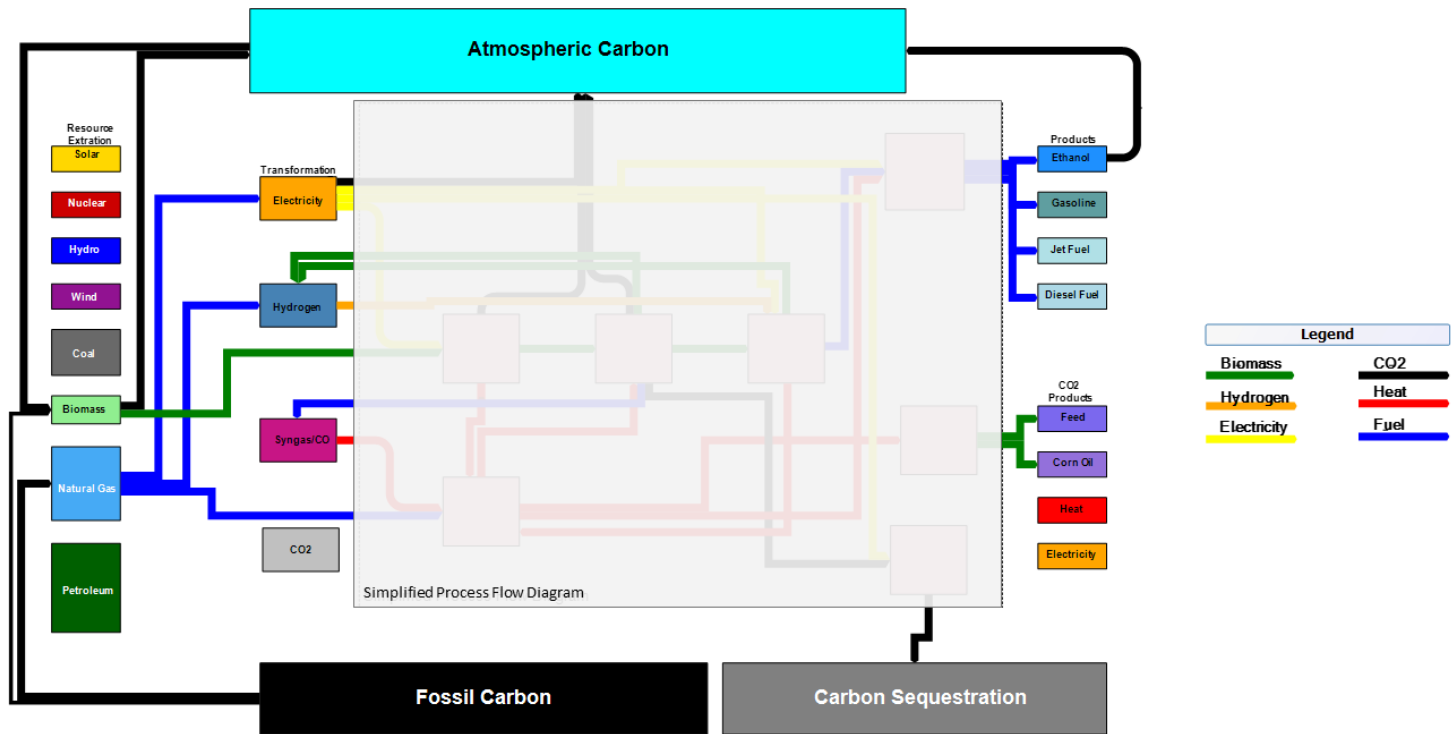
Section 3 of the report provides details related to each pathway and sub-scenario, including process design, overall mass and energy flows, LCA and TEA results. The cost impacts of CI reduction interventions are also discussed here.

Section 4 presents the results of the analysis of these four highly diverse pathways in an integrated format. The high-level results, as well as the advantages and disadvantages of each of the pathway cases, are summarized in the following paragraphs.

Case 1. Conventional ethanol with CCS of fermentation CO$_2$ emissions. This pathway has a CI of 15 to −9 g/MJ ethanol (Figure ES-2) and an MFSP of $1.86 to $2.48/gallon ethanol (equivalent to $2.83–$3.77/gallon gasoline equivalent [gge]). The technical maturity of this pathway is high, with industrial-scale deployment ongoing. Variations in this pathway that can reduce its CI include use of renewable electricity and renewable natural gas (RNG) as process inputs, as well as producing fertilizer for the corn feedstock with renewable or low-carbon inputs. The benefits of this approach are its maturity, its ability to utilize 200+ existing corn

ethanol facilities, and its potential for negative emissions. This approach also has room for additional innovation in carbon capture from other emissions streams at the biorefinery. The drawbacks to this approach are that conventional ethanol fermentation is a mature technology with little room for fundamental process improvement, the requirement that carbon capture be proximate to carbon storage, and that ethanol markets are unlikely to grow substantially without further policy intervention.

   Case 2. Drop-in fuels from HTL of algae. This case has a CI of 53 to 2 g/MJ fuel and an MFSP of $4.10 to $4.90/gge. The technical maturity of this pathway is moderate, with industrial-scale demonstrations of both HTL and algae farming currently ongoing. The CI of this pathway can be reduced by eliminating fossil natural gas by using either RNG or internal algae-derived process off-gases. Further reductions are possible by incorporating renewable electricity across the inputs to the fuel pathway and using renewable electricity to produce the hydrogen required as a process input. The benefits of this approach are its use of a novel feedstock that has the potential for significant supply growth, use of a conversion technology with demonstrated energy and cost performance, and production of drop-in fuels from a fractionated bio-crude. The drawbacks are that algae farming has not achieved commercial success, and that costs appear to be high, even for the nth-of-a-kind plants.
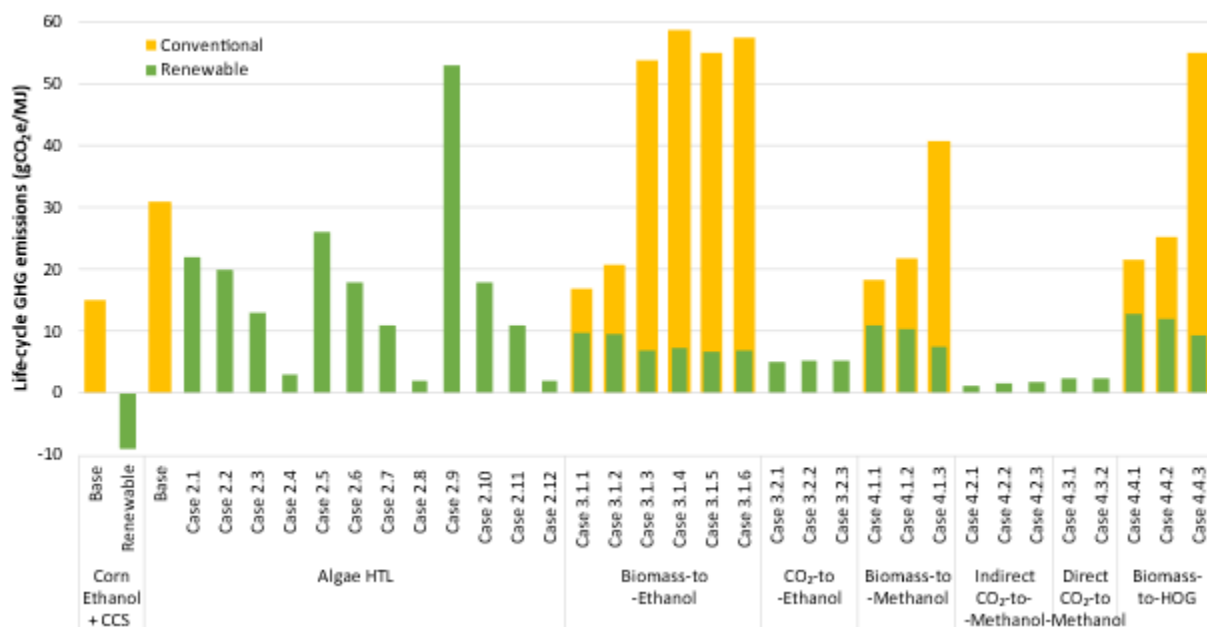

Figure ES-2. Summary of LCA results of carbon intensities of net-zero liquid fuels

   Case 3. Ethanol production from syngas fermentation. This pathway has a CI of 5.1 g/MJ to well over four times that of the fossil fuel baseline. However, if the cases where fossil energy is used to convert CO_2 to synthetic fuel are avoided, the other sub-case CIs range from 58.6 to 5.1 g/MJ. MFSP is estimated at $1.36 to $6.55/gallon ethanol (equivalent to $2.07–$9.95/gge), depending on the plant configuration. The technical maturity of the biomass-fed sub-cases is moderate, with multiple demonstration-scale syngas fermentation plants having been operated over the past decade. The technical maturity of the CO_2-fed cases is low, with CO_2 electrolysis

to carbon monoxide (CO) at a very early stage. CIs of all sub-cases can be reduced by using renewable electricity and renewable hydrogen as process inputs. Further reductions of CI follow from using RNG instead of recycled syngas from biomass gasification. The advantages of this case are its use of syngas as an intermediate, which can be produced from numerous upstream pathways, and its potential to supply low-cost ethanol. Drawbacks include this pathway's reliance on biomass gasification (mature technology with demonstrated challenges) or CO_2 reduction (immature technology) and its production of ethanol, with limited market growth potential.

   Case 4. Catalytic production of methanol or synthetic gasoline from syngas. This pathway has a CI of 40.8 g/MJ to 1.3 g/MJ, excluding cases that would use fossil energy to transform CO_2 into fuels (which have CIs in excess of two times that of the fossil baseline). MFSP is projected to be $0.35 to $1.62/kg methanol (equivalent to $2.46–$6.50/gge), or $3.09 to $3.29/gge for high-octane gasoline. The technical maturity of the biomass-fed scenarios in this pathway is high because today's fossil-derived methanol is produced from the same syngas intermediate and catalytic conversion. The technical maturity of the CO_2-fed scenarios is low, as stated previously. The pathways that produce methanol as a fuel product may be limited by the overall market for methanol, whereas the pathways that produce HOG are limited by the technical maturity of the methanol-to-gasoline process. The effects of renewable electricity and renewable hydrogen as process inputs on the CI of both pathways were evaluated. Advantages of this pathway include the optionality of producing two different products and the potential to optimize yield through hydrogen addition. Drawbacks include a relatively high projected MFSP and dependence on biomass gasification (proven, but challenging) or CO_2 electroreduction, which is immature.

Table of Contents

List of Figures

List of Tables

1. Introduction

Sustainable conversion of carbon dioxide (CO_2) to value-added chemicals or fuels shifts a linear "cradle-to-grave" chemicals or fuels manufacturing model to a circular carbon economy. A key consideration for CO_2 utilization is the economic viability and deep greenhouse gas (GHG) reductions of converting specific CO_2 sources based on factors like scale or purity. Among different CO_2 sources, the corn dry mill ethanol plant with on-site fermentation CO_2 upgrading is considered low-hanging fruit for implementing CO_2 utilization with minimum requirements for gas purification. Further, CO_2 from other conversion processes of biomass to fuels offers opportunities for significant GHG reductions by utilizing all carbon available in feedstocks.

With nearly 33 gigatonnes (Gt) of carbon emitted each year globally and 5 Gt in the United States in the form of CO_2 [1, 2], there is increasing interest in capturing and utilizing these otherwise wasted resources for economic benefit at the industrial scale. CO_2 sources range from atmospheric CO_2 with extremely low concentration at currently 415 parts per million (ppm) [3] to the nearly pure CO_2 streams released from corn ethanol plants. The total ethanol production capacity in the United States is about 16.500 billion gallons per year, with 50 million tonnes (MT) of CO_2 emissions in 2019 [4], and the fermentation CO_2 may increase over time if second-generation cellulosic ethanol becomes a reality. Although the fermentation-derived CO_2 is nearly pure, thus representing a high capture and utilization potential, most corn ethanol plants currently emit their CO_2 to the atmosphere [5]. Only a minor portion of the fermentation-derived CO_2 is used in merchant markets as feedstock in the fertilizer industry, in carbonated beverages, and for food processing and preservation. Otherwise, the fermentation-derived CO_2 can serve as a feedstock for the synthesis of fuels and chemicals.

To evaluate the technological maturity and feasibility of various renewable fuel pathways, a techno-economic analysis (TEA) is often used to provide estimates of the economic performance of complete fuel production processes. Such an analysis is done by assessing the overall material and energy inputs and outputs and costs, as well as the product potential of a process based on its current state of technology development. This information is then used to identify the parameters that most significantly impact costs while also estimating the technical readiness of the technology for deployment at a relevant scale. In this case, such an analysis can usually be presented as the cost of fuel production for a given volume.

Complementary to a TEA, a life cycle analysis (LCA) is often performed as either a "well-to-wheels" or a more extensive "cradle-to-grave" analysis to assess the environmental impacts associated with the various stages of fuel production and use, including resource extraction, feedstock growth and processing, conversion, distribution, and end use. Life cycle GHG emissions of fuel production pathways are also called as carbon intensities (CIs). Broadly speaking, CIs include emissions of CO_2, methane (CH_4), and nitrous oxide (N_2O) combined together with their global warming potentials. Together, TEA and LCA can provide insights into

potential projected costs of new fuel pathway technologies and environmental performance improvements compared to existing fuels refined from fossil sources.

The scope for the Net-Zero Carbon Fuels Technical Team (NZTT) is to investigate and propose solutions for generating liquid carbon-based fuels with a reduced CI such that, from a life cycle carbon accounting standpoint, they have a net GHG emissions profile approaching zero. NZTT will also perform process analyses to examine the conditions required for economic viability and allow eventual demonstration of the most promising technologies. As stated, the relevance of liquid fuels in the transportation sector points toward the need for carbon-based fuels derived from low-carbon-intensity sources. The main renewable option for liquid fuel is commonly considered biofuels, which are typically made from organic matter such as corn, oilseeds, algae, and woody or herbaceous biomass, or from waste materials including fats, oils, and greases; agricultural residues; and municipal solid waste. This NZTT effort will investigate both of these more "traditional" biofuels as well as more novel fuels synthesized using renewable electricity and CO_2 from point sources or captured directly from the air.

In an applied research and development (R&D) setting, where technology exploration is directly tied to practical application and possible commercial deployment, the unit operations and process design for the renewable fuel being developed are often optimized to achieve the lowest minimum fuel production cost possible. Thus, fuel pathway design is optimized first in a TEA, followed by the same parameters used to perform an LCA to determine the GHG emissions and other environmental impacts.

This project team has analyzed the environmental and economic feasibility of net-zero-carbon fuels, determining the top challenges and opportunities across and with results demonstrated using four representative pathway technologies. Key challenges and potential opportunities for transformational R&D toward net-zero-carbon fuels with economic viabilities are highlighted and reported with comprehensive LCA and TEA results, offering promising near- and longer-term commercialization opportunities.

2. Methodology

2.1 LCA

To analyze the environmental impact of various energy conversion technologies and resultant fuels and products, LCA is conducted to account for the life cycle environmental impacts, including GHG emissions through the supply chain of fuels and products. In this report, we have analyzed the life cycle GHG emissions of the four fuel production pathways using the Greenhouse gases, Regulated Emissions, and Energy use in Technologies (GREET) model developed by Argonne National Laboratory [6] and key data on energy and mass balance developed by TEA and other process modeling conducted by other national laboratories. LCA system in this study includes three major stages: feedstock production and transportation, fuel production and transportation, and fuel combustion (Figure 1). All upstream impacts of key inputs (e.g., energy or chemical inputs) are considered, as well as process emissions from each stage. For conversions of biomass feedstocks, the feedstock production stage includes farming crops and collecting biomass and/or residues. There are also processes of feedstock treatment and transportation.

Feedstock production	Feedstock transportation	Fuel production	Fuel transportation	Fuel combustion
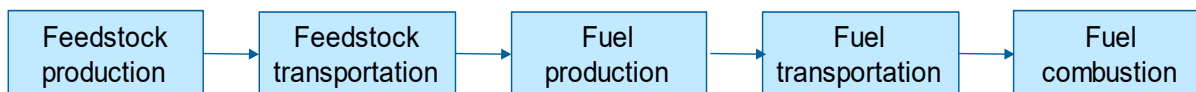
Figure 1. The schematic of LCA system boundary that consists of feedstock production, feedstock transportation, fuel production, fuel transportation, and fuel combustion stages

For CO_2 feedstocks such as fermentation CO_2 (Case 1), the feedstock production stage includes CO_2 capture and transmission processes. In this case, CO_2 is a waste stream and we assumed that CO_2 streams do not bear emission burdens before its collection. The fuel production (i.e., conversion) stage is where feedstock is converted into energy products (e.g., hydrocarbon fuels, ethanol, and methanol) with process energy and chemical inputs. For LCA Cases 2–4, two major scenarios (conventional and renewable energy supply) are considered (Table 1), mainly driven by the types of input energy sources (electricity, H_2, and natural gas [NG]). The conventional scenario represents current U.S. energy systems, whereas the renewable scenario considers alternative energy systems with further reductions in the CIs to achieve net-zero-carbon fuels.

All values in Table 1 are from GREET 2019 [6] and are used in this study. For the conventional scenario, electricity use refers to U.S. electricity grid mix in 2018 and 2030, H_2 is produced from fossil NG via steam methane reforming (SMR), and NG use means conventional fossil NG. On the other hand, for the renewable scenario, we assumed on-site renewable electricity (solar or wind) that does not have carbon emissions (0 grams CO_2 equivalent [CO_2e] per kilowatt-hour); H_2 is produced from on-site electrolysis with renewable electricity (0 gCO_2e/megajoule [MJ] H_2); and for NG, landfill-based renewable natural gas (RNG) is assumed.

Landfill-derived RNG considers avoided flaring landfill gas emissions because using landfill gas for other beneficial purposes diverts landfill gas from being flared. Note that the impact of building facilities is not considered in this study.

Table 1. The carbon intensities of electricity, H_2, and NG of two scenarios used for Case 2–4: conventional scenario and renewable scenario [6]

	Conventional scenario	Renewable scenario
Electricity	U.S. grid mix 483 gCO₂e/kWh (2018) 414 gCO₂e/kWh (2030)	Renewable electricity 0 gCO₂e/kWh
H₂	NG SMR (off-site, 50 miles) 80 gCO₂e/MJ	On-site electrolysis with renewable electricity 0 gCO₂e/MJ
NG	Fossil NG 69 gCO₂e/MJ	Renewable natural gas from landfill gas 9.8 gCO₂e/MJ

The life cycle GHG emissions were calculated in terms of CO_2e using the global warming potentials of 1, 30, and 265 for CO_2, CH_4, and N_2O, respectively, based on the fifth assessment report by the Intergovernmental Panel on Climate Change [7].

2.2. TEA

Process economic analysis includes (1) a detailed process flow diagram, informed by a conceptual-level process design based on research data and rigorous material and energy balance calculations via commercial simulation tools such as Aspen Plus; (2) capital and project cost estimations using an in-house model; (3) a discounted cash flow economic model; and (4) the calculation of minimum fuel selling price (MFSP).

The operating expense calculations are based on material and energy balance calculations using process simulations and are consistent with previously developed TEA models [8-13]. Raw materials include feedstocks, chemicals, catalysts, and utilities. In this analysis, we considered displacing fossil energy sources (such as natural gas) using renewable energy sources (such as RNG) to potentially reduce the CIs; Table 2 summarizes the prices of RNG varied by feedstock types. Prices are derived from previous reports [14].

Table 2. Summary of RNG cost sensitivity values

Feedstock		Cost Range ($/MMBTUᵃ)		
		min	avg	max
Anaerobic digestion	Landfill gas	$7.10	$13.05	$19.00
	Animal manure	$18.40	$25.50	$32.60
	Wastewater sludge	$7.40	$16.75	$26.10
	Food waste	$19.40	$23.85	$28.30

ᵃ Million British thermal units

The ranges of renewable electricity and renewable hydrogen are listed in Table 3. Note that baseline H_2 price represents the optimistic case from the Hydrogen Analysis (H2A) model [15]. All costs are adjusted to 2016 U.S. dollars (2016$) using the Plant Cost Index from Chemical

Engineering Magazine [16], the Industrial Inorganic Chemical Index from SRI Consulting [17], and labor indices provided by the U.S. Department of Labor Bureau of Labor Statistics.

Table 3. Summary of renewable electricity and renewable H_2 cost sensitivity values

Resource	Baseline	Minimum	Maximum
Renewable electricity ($/kWh)	$0.02	$0.02	$0.10
Renewable H_2 ($/kg)	$1.38	$1.38	$4.50

Material and energy balance and flow rate information is used to determine the number and size of equipment and calculate the capital expenses. Capital costs are primarily based on detailed equipment quotations from previous TEA models. For equipment not listed and for which vendor guidance is not available, the Aspen Icarus Process Evaluator is used to estimate baseline capital costs, assuming a scaling exponent term of 0.6.

Using published engineering methods, a discounted cash flow rate of return analysis was conducted using capital and operating cost data, with the financial assumptions shown in Table 4. We assume 40% equity financing and 3 years of construction plus 6 months for startup. The plant's life is assumed to be 20 years for Case 1 and 30 years for Cases 2 to 4. The income tax is 21%. Working capital is 5% of the fixed cost investment. The MFSP is the minimum price that the fuel product must sell to generate a net present value of zero for a 10% internal rate of return.

Table 4. Economic assumptions for TEA

Economic Parameters	Assumed Basis
Basis year for analysis	2016
Debt/equity for plant financing	60%/40%
Interest rate and term for debt financing	8%/10 years
Internal rate of return for equity financing	10%
Total income tax rate	21%
Plant life	20 years (Case 1, dry mill facilities) 30 years (Cases 2, 3, and 4)
Construction period	3 years
Fixed capital expenditure schedule (years 1–3)	32% in year 1, 60% in year 2, 8% in year 3
Startup time	0.5 years
Revenues during startup	50%
Variable costs during startup	75%
Fixed costs during startup	100%
Site development cost	9% of inside battery limit (ISBL), total installed cost
Warehouse	1.5% of ISBL
Indirect Costs	**% of Total Direct Costs**
Prorated expenses	10
Home office and construction fees	25
Field expenses	10
Project contingency	10
Other costs (startup and permitting)	10
Fixed Operating Cost	**Assumed Basis**

The analysis accounts for all emissions from the combustion of process fuel and non-combustion emissions from chemical reaction, leakage, venting, and others. Then, the transportation of fuels from the fuel production plant to the end-use phase is considered. The fuel combustion stage is where fuel is used while emitting combustion emissions. Note that the carbon-neutrality assumption is used because CO_2 combustion of biomass- and CO_2-derived fuels offsets biological carbon uptake during biomass growth and waste CO_2 emissions that are otherwise emitted to the atmosphere, respectively.

3. Case Studies

3.1 Case 1 – Corn Ethanol with Carbon Capture and Sequestration (CCS)

Capture and sequestration of the CO_2 from biomass fermentation represents a near-term opportunity to deliver low-, zero-, or negative-GHG liquid fuels. Conventional ethanol manufacturing already produces a pure stream of CO_2, comprising approximately one-third of the biogenic carbon input to the process. Because this carbon was drawn from the atmosphere, its sequestration can be counted as a negative emission. This approach has already attained commercial deployment, demonstrating the potential for combining bioenergy and carbon capture to attain net-zero-carbon fuels.

Many routes to further decarbonizing starch ethanol are speculative, but one approach has attained commercial deployment—biorefineries with CCS. The fermentation stage of ethanol production generates a high-purity (99%) stream of CO_2 that can be captured without solvents and sequestered in geologic formations at much lower cost than post-combustion flue gas CCS. There are currently four active projects demonstrating this intervention at commercial scale. The largest of the four active projects is Archer Daniels Midland Demonstration in Decatur, Illinois. The Illinois Basin Decatur Project, which was operational between 2011 and 2014, successfully stored 1 MT of CO_2. Capture at the Decatur plant was then scaled up, and in 2017, sequestration began at a different location at a rate of 1 MT CO_2/year [18]. The other projects are in development and include Red Trail Energy Ltd., who recently gained approval for a North Dakota refinery with CCS to sell low-CI ethanol in the Low Carbon Fuel Standard (LCFS) market. In dry mill ethanol production, we estimate that the addition of CCS can lower the life cycle CI of corn ethanol to 17–25 gCO_2e/MJ. Given the potential of biorefineries with CCS to attain CIs of <20 gCO_2e/MJ, net-zero or even negative emissions from biorefineries may be within reach, especially given strong existing incentives.

Beyond capture and sequestration of fermentation CO_2, this work assesses three additional interventions that can lower the CI of the conventional ethanol production pathway:

1. Process heat from RNG
2. Renewable electricity
3. Low-GHG-intensity fertilizer for corn farming—"green ammonia" [19].

3.1.1 Process Design

We analyzed the "well-to-wheels" (or "farms-to-wheels") life cycle GHG emissions of a dry mill corn ethanol manufacturing process with CCS of fermentation emissions and with corn oil

and distillers grains coproducts. The flow diagram to produce ethanol from corn starch with CCS of fermentation emissions is illustrated in Figure 2.
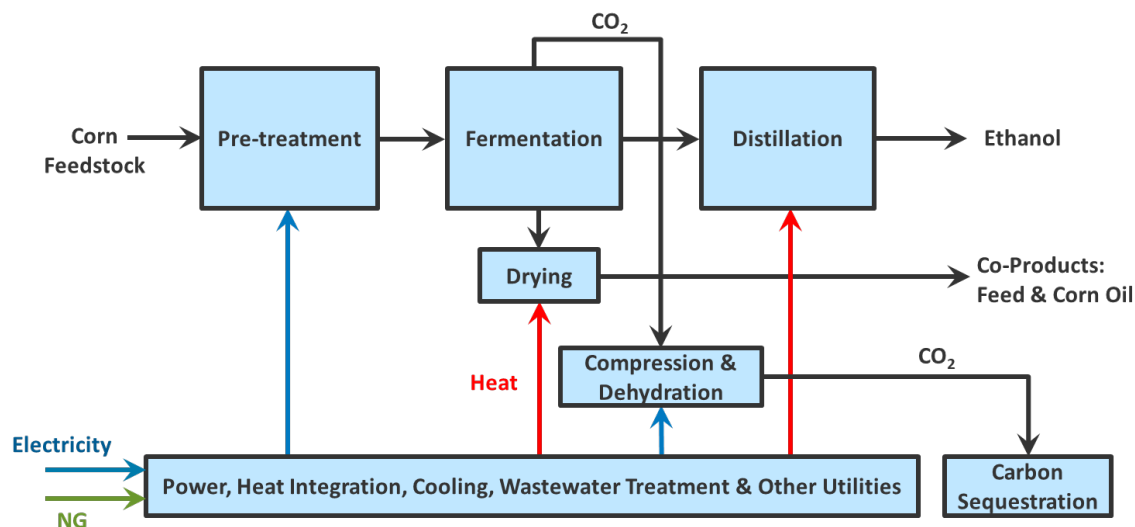
Figure 2. Baseline case: corn starch ethanol with CCS block flow diagram

Ethanol production begins with the production of feedstock, which in the United States is most commonly corn. The main assumptions used in our LCA are listed in Table 5. The existing corn logistics network typically involves transport of corn by truck to grain elevators at nodes of the broader transportation network. The grain is then shipped by rail or barge to consuming industries or to ports for international export. The Midwest is the largest corn-producing region, with Iowa ranking first in corn production and exports in 2018 [20]. Ethanol production is also largely located in the Midwest. However, due in part to California's Low Carbon Fuel Standard policy, the state has seen development of an ethanol industry with six plants located in state, co-located with growing consumption [21]. For this reason, we selected California as the location to model our production of ethanol. However, California produces less than 1% of U.S. corn [22]. The existing ethanol industry commonly sources corn from the Midwest, a trend that is likely to continue as the industry grows [23].

In order to lower the carbon intensity of the conventional ethanol production pathway with CCS (illustrated in Figure 2), we assessed three interventions: renewable natural gas, renewable electricity, and green ammonia. Three different process flowsheets were considered.

The first process flowsheet considered is the baseline case process flowsheet with process heat from RNG. The impacts from utilizing RNG on process carbon emissions and economics were evaluated, and the results are presented in the corresponding subsections. The process flowsheet for this case is presented in Figure 3.
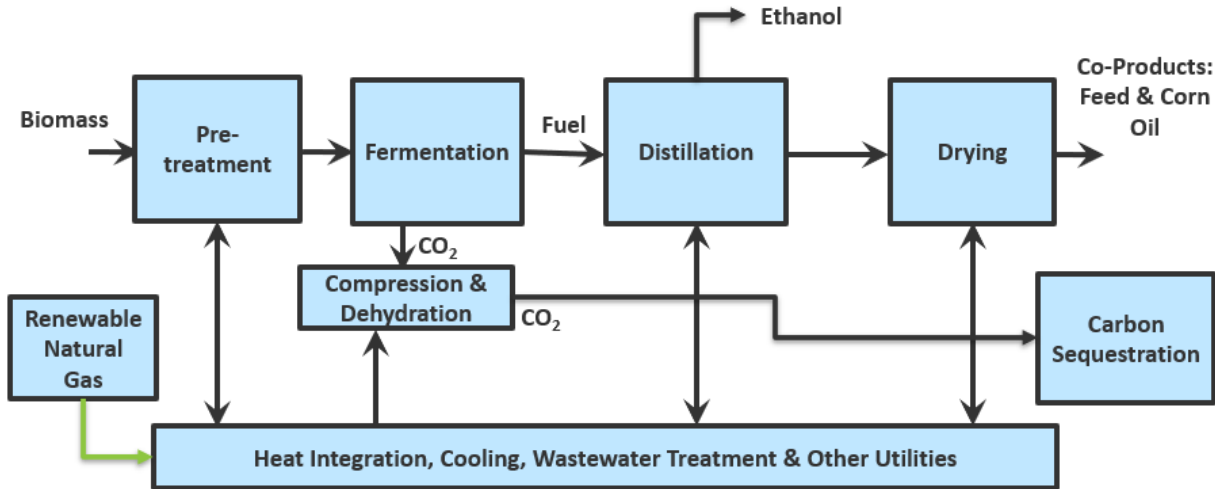
Figure 3. Corn starch ethanol with CCS and renewable natural gas block flow diagram

The next process flowsheet considered is the baseline case with renewable electricity. The impacts from utilizing renewable electricity as opposed to the Midwest grid average mix on process carbon emissions and economics were evaluated, and the results are presented in the corresponding subsections. The process flowsheet for this case is presented in Figure 4.
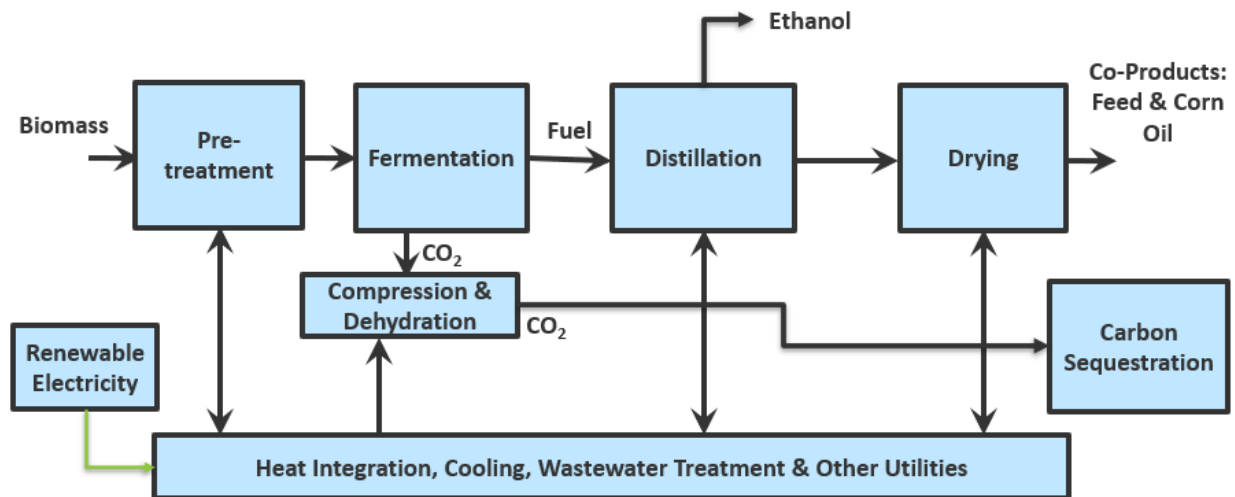
Figure 4. Corn starch ethanol with CCS and renewable electricity block flow diagram

The final process flowsheet considered is the baseline case with low-GHG-intensity fertilizer production, or green ammonia. The impacts from utilizing green ammonia in the biomass production on process carbon emissions and economics were evaluated, and the results are presented in the corresponding subsections. The process flowsheet for this case is presented in Figure 5.
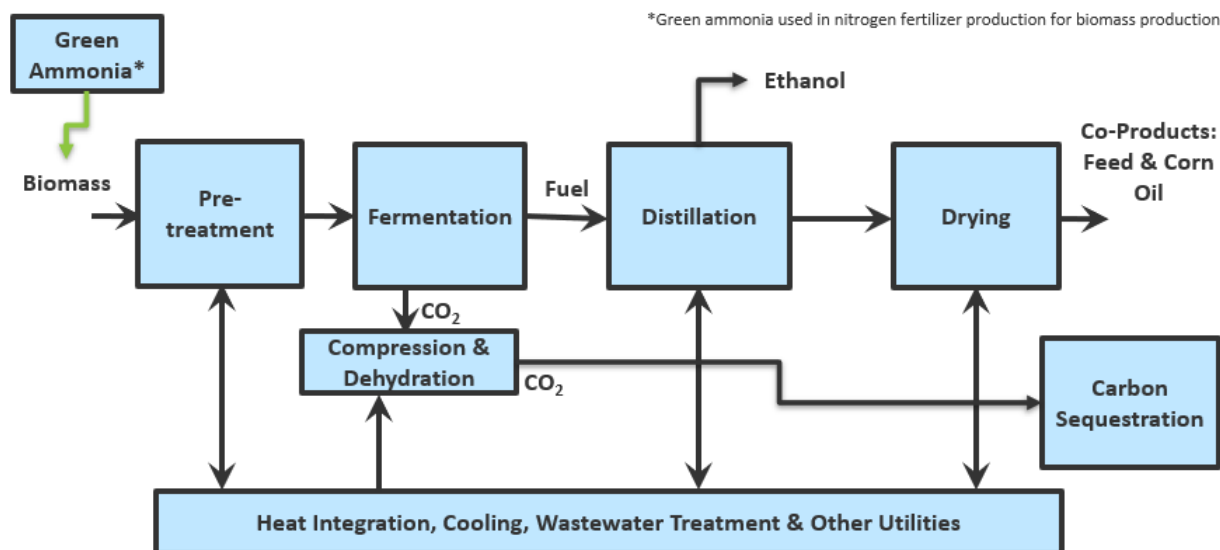
Figure 5. Corn starch ethanol with CCS and green ammonia block flow diagram

To assess the combined effects of these interventions on the baseline case corn starch to ethanol with CCS, we evaluated all three interventions together. The impacts from utilizing all three interventions on process carbon emissions and economics were evaluated and the results are presented in the corresponding subsections.

3.1.2 LCA Cases and Inventories

We analyzed the cradle-to-grave life cycle GHG emissions of a dry mill corn ethanol manufacturing process with CCS of fermentation emissions and with corn oil and distillers grains coproducts. The main assumptions used in our LCA are listed in Table 5.

Table 5. Main input assumptions for LCA

Feedstock	Corn
Feedstock location	Iowa
Feedstock electricity	Midwest grid average mix
Feedstock transport distance	1,800 miles
Feedstock transport method	Diesel rail
Ethanol plant location	California, Fresno County
Ethanol plant electricity	California grid average mix
Ethanol transport distance to bulk terminal	300 miles
Ethanol transport method to bulk terminal	Diesel rail
E85 transport distance to distribution	30 miles
E85 transport method to distribution	Heavy-duty truck

Corn Production for Biorefinery

Feedstock production is assumed to take place in Iowa, utilizing the GREET average Midwestern electric grid mix and associated transmission and distribution losses. Transportation of corn feedstock is assumed to travel 1,800 miles by diesel rail from farm to the refinery. Corn feedstock is assumed to be 45% elemental carbon by mass. This would be equivalent to approximately 1,650 kg of potential atmospheric CO_2/ton of feedstock.

GHG emissions from corn production are 259 kg CO_2e per ton feedstock (113 kg CO_2/ton from carbon dioxide), which are the result of upstream emissions in the production of the corn, specifically from the fertilizer and fossil fuel use in generating electricity. These emissions could be reduced by 36 kg CO_2e/ton feedstock by replacing the fertilizer used in corn production with low-GHG-intensity fertilizer green ammonia.

Dry Mill Corn to Ethanol Production with Corn Oil Extraction

The dry mill ethanol process was chosen as representative of the most common form of ethanol production in practice at present. The ethanol refinery is near Fresno County, which is the approximate location of several existing refineries and also proximate to nearby oil and gas fields, which we are assuming would be amenable to geological sequestration. Using lower heating values, 1 ton of feedstock is equivalent to 418.8 kg (roughly 119 gallons) of ethanol end product. We used GREET default settings for upstream model conditions with the following exceptions:

- Refinery electricity comes from an average California grid mix with associated transmission and distribution losses.
- Rather than attributing emissions to coproducts, all emissions are assigned to the ethanol product, and the coproducts instead are assumed to displace the production of equivalent products elsewhere. Distillers grains with solubles (DGS) and corn oil are coproducts of the ethanol conversion process. DGS, sold as animal feed, is assumed to displace production by mass: 78% corn feed, 30% soy meal, and 2% urea. Roughly 340 kg of DGS is assumed to be produced from 1 MT of corn. Corn oil is assumed to displace 100% by mass soy oil, with roughly 12 kg produced per MT of corn processed.

GHG emissions from ethanol production are 561 kg CO_2e/ton feedstock (539 kg CO_2/ton from carbon dioxide and 519 kg CO_2/ton net emissions after accounting for on-site credits), which are the result of fermentation (see next subsection), natural gas usage at the biorefinery for process heat, fossil fuel use in generating electricity used at the biorefinery, and upstream emissions in the production of chemicals and enzymes used in the biorefining process. Of the 247 kg CO_2e/ton feedstock not associated with fermentation, 205 kg CO_2e/ton feedstock are from natural gas usage, which can be reduced by replacing fossil natural gas with RNG. An additional 24 kg CO_2e/ton feedstock are associated with fossil fuel use in electricity production off-site, which can be reduced by procuring renewable electricity.

CO_2 Emissions from Fermentation

CO$_2$ emissions are assumed to be internally consistent with the carbon content assumptions of resources and products employed by the GREET model. GREET assumes that 45% of the mass of the corn feedstock and 52.2% of the mass of the ethanol product is elemental carbon. GREET makes no assumptions regarding the carbon content of DGS or corn oil. Figures from the literature place the carbon content of DGS and corn oil at roughly 59% and 75%, respectively [23, 24]. By mass-balance in Equation 1, we obtain the fermentation emissions rate of CO$_2$ to be roughly 316 kg/ton corn (or 86.1 kg of elemental carbon).

$$(0.45 \times 1000 kg\ Corn) - (0.522 \times 356 kg\ Ethanol) - (0.59 \times 289 kg\ DGS)$$
$$-(0.75 \times 10.1 kg\ Corn\ Oil) \approx 86.1\ \text{kg Carbon}$$

$$86.1\ kg\ C \times \frac{44.1\ kg\ CO2}{12.01\ kg\ C} \approx 316\ kg\ CO2 \qquad \text{(Equation 1).}$$

Capture and Compression of Fermentation CO$_2$

We employ a simple model of fermentation CO$_2$ capture. Fermentation CO$_2$ streams are highly concentrated at greater than 90% by mass [25]. Therefore energy-intensive separation technologies such as amine scrubbers are unnecessary. For simplicity, we model a 100% capture rate by calculating the energetic cost and associated emissions of a five-stage reciprocating CO$_2$ compressor with a suction pressure of 17.4 psia at 81°F with an inlet flow to stage one of 36,000 lb/h and a discharge pressure of 2,214 psia [25]. Assuming a pressure drop of 35 kPa/km (5.07 psia/km) and a minimum outlet pressure of 10.3 MPa (1,494 psia) [26] and excluding elevation, this pressure is sufficient to pump compressed CO$_2$ roughly 140 km. The energetic cost of this process is estimated at 100.09 kWh/ton CO$_2$ captured [25]. Emissions for this energy requirement are modeled using the same California electricity grid mix as in the aforementioned processes. The energy requirement to capture fermentation CO$_2$ is approximately 31.4 kWh/ton of corn processed, as shown in Equation 2.

$$\frac{0.10009 kWh}{kg CO2} x \frac{316 kg CO2}{t} Corn \approx 31.6 kWh/t\ Corn \qquad \text{(Equation 2.)}$$

GHG emissions from capture and compression of fermentation CO$_2$ are 8 kg CO$_2$e/ton feedstock, which are the result of fossil fuel use in generating electricity used during capture and compression. This carbon emission could be reduced by procuring renewable electricity.

Land Use Change

GREET's assumptions for land use change account for both direct (domestic) and indirect (international) land use change using the Carbon Calculator for Land Use Change from Biofuels Production (CCLUB) model. Lan use change scenarios from biofuels production are modeled using Purdue University's Global Trade Analysis Project (GTAP) model, which is a computable general equilibrium model. GTAP determines potential land use changes domestically and internationally contingent on a set of biofuel-to-ethanol production scenarios. This analysis utilizes the Corn Ethanol 2011 scenario and associated land use change elasticities. This scenario

assumes a growth in corn ethanol production from 3.41 to 15 billion gallons between 2004 and 2034, which is the end of the recommended 30-year production horizon in the CCLUB model. This expansion of ethanol production is also consistent with U.S. Department of Energy Billion-Ton Report assumptions [27]. Domestic emissions are modeled using the CENTURY model, whereas international emissions are modeled using the Winrock model. The land use change emissions amortization period is set equivalent with the production period at 30 years. The model considers 100-cm soil depth for soil organic carbon calculations, and it is assumed that, internationally, biomass is burned to clear land. Within the CENTURY model, tilling practices are set as the U.S. average, and the yield scenario assumes a 1% increasing annual yield. Where the model predicts forest conversion to cropland, the model settings adopt the Harvested Wood Products assumption from Heath et al. [28]. This setting assumes that 60% of converted forest live and dead wood will be harvested; 21% of the harvested portion will end up in durable wood products, 21% will be burned for energy, 18% will be released as CO_2 to the atmosphere, and the remaining 40% of waste wood will also be released to the atmosphere.

Ethanol End of Life

Ethanol is assumed to be combusted as an automotive fuel and its biogenic carbon returned to the atmosphere. However, due to this CO_2 being biogenic in nature, it is a net-zero emission. Non-CO_2 emissions for a purely ethanol powertrain are not readily available within the GREET framework. For the sake of simplicity, non-CO_2 emissions associated with combustion are reported from GREET for an E85 power plant in a spark-ignition internal combustion engine vehicle.

Coproduct Displacement Credits

Rather than attributing emissions to coproducts, all emissions are assigned to the ethanol product, and the coproducts instead are assumed to displace the production of equivalent products elsewhere. DGS and corn oil are coproducts of the ethanol conversion process. DGS, sold as animal feed, is assumed to displace production by mass: 78% corn feed, 30% soy meal, and 2% urea. Roughly 340 kg of DGS is assumed to be produced from a metric tonne of corn. Corn oil is assumed to displace 100% by mass soy oil, with roughly 12 kg produced per metric ton of corn processed. The combined GHG emissions displacement credit is 123 kg CO_2e/ton of feedstock, with 68 kg CO_2/ton coming from carbon dioxide emissions displacement (the remaining credits arise from N_2O and methane).

Coproduct End of Life

Both coproducts, DGS and corn oil, are assumed to be a food product for livestock or humans, respectively. Hence, there is good reason to assume some proportion of the end-of-life carbon for these products will wind up as methane emissions. If modeled as such, these emissions could significantly increase the 100-year GHG impacts (up to a maximum of 279 kg of CH_4, equivalent to 6,994 kg CO_2e). However, for the purposes of this initial analysis, we keep

the accounting simple and assume that the emissions are released as biogenic CO_2 (i.e., aerobic conditions).

3.1.3 LCA Results

As illustrated in Figure 6, photosynthetic drawdown for the feedstock stage is approximately 1,650 kg CO_2/MT of corn. However, a significant portion of this biogenic carbon is returned to the atmosphere through combustion of the ethanol and the eventual decomposition of the coproducts. These emissions are offset significantly by capture and storage of fermentation-stage CO_2 and displacement of coproduct substitutes, but it is only enough to reduce the emissions footprint of the process to 158 kg CO_2e/MT of feedstock. Capture of fermentation CO_2 decreases ethanol CI by a net 29 gCO_2e/MJ, to 15 gCO_2e/MJ. Ultimately, the case of corn to ethanol with CCS modeled here is not carbon-negative.
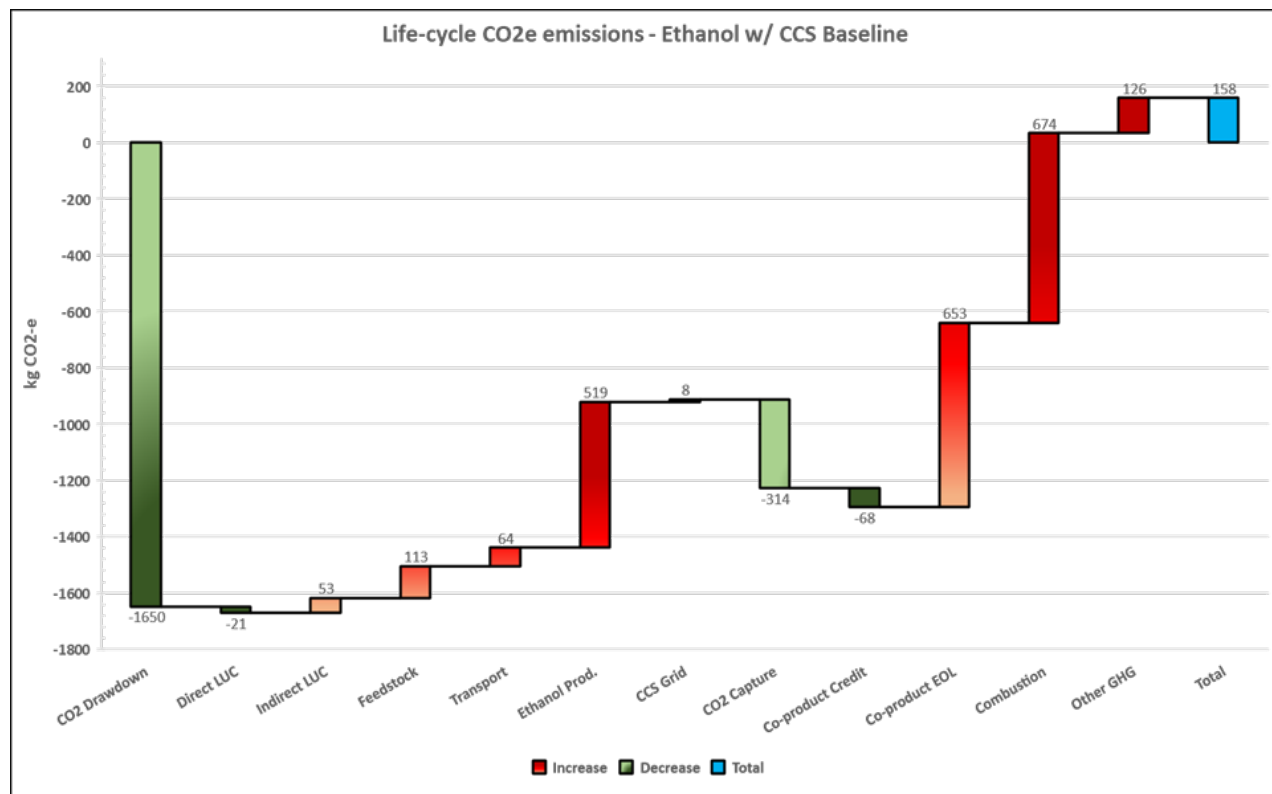
Figure 6. LCA carbon balance of fermentation with CCS only. This waterfall chart depicts the cumulative effect of each process stage and the corresponding CO_2 reduction/emissions from that stage. Green bars represent CO_2 drawdown, and the red bars represent CO_2 emissions. The blue bar on the right-hand side of the graph depicts the total emissions from the process in g/MT of corn. "Other GHG" is the net non-CO_2 emissions after accounting for all coproduct displacement credits. The remaining bars track the CO_2 component of emissions only

Although CCS of fermentation emissions does not fully offset the fossil life cycle emissions of the corn starch ethanol pathways, there are other interventions in the production pathway that, when combined, can offset the remaining 15 g/MJ. These interventions can be addressed through

procurement decisions, such as using low-carbon electricity, fuel, and fertilizer at the biorefinery and in the feedstock production. Options that were assessed include:

1. Substitution of RNG from landfill gas for conventional fossil-derived NG to serve on-site process heat requirements
2. Procurement of renewable zero-marginal-emissions electricity from solar and wind
3. Substitution of green ammonia from upstream nitrogen fertilizer production and on-site ammonia input.
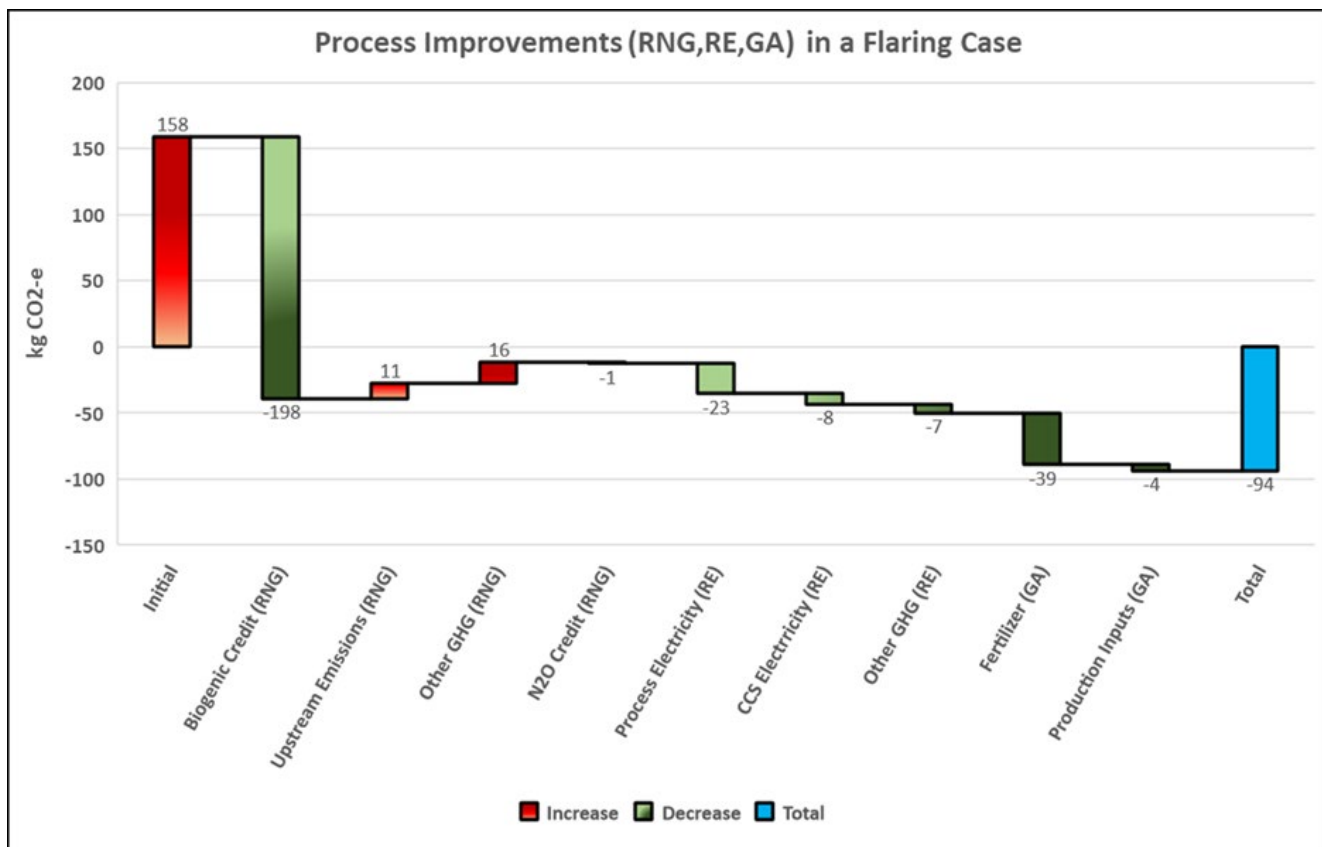
Figure 7. Life cycle assessment carbon balance of net-zero ethanol production

The life cycle emissions for RNG from landfills was based on supporting literature [29-31]. The counterfactual scenario to RNG production is flaring of landfill gas. However, GREET takes a system boundary expansion marginal approach to emissions accounting in this pathway, which accounts for the avoided flared landfill gas emissions under the business-as-usual case where landfill gas is flared that ignores the biogenic source of the fuel carbon. This pathway was recalculated in our own model for consistent tracking of biogenic emissions. Of the modeled interventions, RNG has the most significant impact because fossil process heat emissions at refinery are replaced by biogenic emissions from RNG. As shown in Figure 7, the other interventions had a much smaller impact, but collectively the interventions result in a net-negative life cycle emissions of −253 kg CO_2e/MT feedstock. Substituting RNG for on-site fossil fuel use decreases net CI by 16.3 g/MJ (172 kg/MT feedstock).

Substituting renewable (zero-carbon) electricity for on-site process electricity (including power used for CO_2 compression) decreases net CI by 3.6 g/MJ (38 kg/MT feedstock). Substituting the renewable (low-/zero-carbon) ammonia to natural-gas-based ammonia decreases net CI by 4.1 g/MJ (43 kg/MT feedstock) [19].

We incorporate electrocatalytically produced green ammonia as an input to upstream production of nitrogen fertilizer used in the corn farming stage and as a replacement for conventional ammonia used at the ethanol refinery. We select a GHG intensity of 0.30 kg CO_2e/kg of ammonia, which is consistent with the method utilizing pressure swing adsorption for N_2 production and low-temperature electrolysis of water using renewable electricity for H_2, as reported in Liu, Elgowainy, and Wang [19]. Conventional ammonia in GREET has a GHG emissions of 2.55 kg CO_2e/kg ammonia. In an effort to generate a more representative estimate of emissions reduction from green ammonia used to produce nitrogen fertilizer, nitrogen inputs at the farm level are a product of GREET's default "average mix," with 32% produced from urea-ammonium nitrate solution, 31% from ammonia, 23% from urea, 6% from diammonium phosphate, 4% from monoammonium phosphate, and 2% from ammonium nitrate and ammonium sulfate. Green ammonia is substituted for GREET's conventional ammonia pathway in each of these upstream processes, where appropriate. Green ammonia directly replaces conventional ammonia at the ethanol refinery, which utilizes 17.68 g/gallon ethanol. Substituting the renewable (low-/zero-carbon) energy inputs to fertilizer production decreases net CI by 4.1 g/MJ (43 kg/tonne feedstock) [19].

As shown in Figure 7, the collective interventions result in a net-negative life cycle emissions of −253 kg CO_2e/ton feedstock. Therefore, the corn starch ethanol from state-of-the-art technologies can be net-zero with CCS (with these interventions with a CI of −9 g/MJ).

3.1.4 TEA Results

To assess the viability for these interventions for the corn to ethanol with CCS pathway, we performed a techno-economic assessment for each of the interventions (Figure 8).
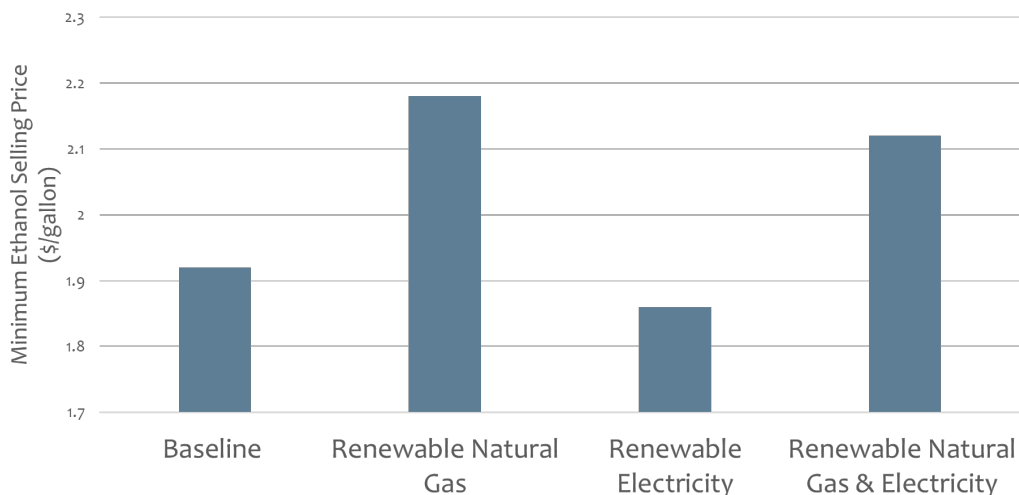
Figure 8. Techno-economic analysis results: minimum ethanol selling price (MESP)

The baseline techno-economic model of conventional ethanol production without CCS returns an MESP of $1.77/gallon ethanol. When that model is extended to include carbon capture, it returns an MESP of $1.92/gallon. Table 6 shows the key costs and coproduct prices used in the TEA to calculate the MESP. These values and assumptions are based on the United States Department of Agriculture (USDA) Dry Mill Ethanol Production Model of a 40-million-gallon-per-year plant. The CCS costs and assumptions are scaled from the Archer Daniel Midland Demonstration in Decatur, Illinois. The cost of carbon capture was calculated as $0.15/gallon ethanol or $52/MT of CO_2 without incentives or credits.

Table 6. Key costs and coproduct prices for TEA of corn ethanol refinery and CCS

Input	Price
Corn feedstock	$3.30/bushel
Electricity (Midwest)	$0.068/kWh
NG	$3.39/MMBTU
Ethanol plant TEA	USDA Dry Mill Production Model (2016)
CCS capital expenses	$9.6 million
CCS utilities and labor (scaled from ADM, Decatur, IL)	+33% and +35% of capital expenses
Coproduct	Selling price
DDGs and solubles	$139/MT
Corn oil	N/A

The values in Table 7 reflect alternative cost inputs for the TEA for each of the low-CI inventions.

Table 7. Alternate input cost assumptions for TEA of ethanol refinery with CCS with abatement interventions

Input	Price
RNG (landfill)	$12/MMBTU
Electricity (zero marginal emissions renewable)	$0.02/kWh
Corn feedstock (green ammonia)	$3.86/bushel

The USDA Dry Mill Production Model (2016) of the 40-million-gallon-per-year TEA was updated for the three intervention cases. In each case, the ethanol refinery with CCS is paired with one intervention to determine the effect on the MESP for that intervention alone. The results are presented in Table 8.

Table 8. Calculated MESP for ethanol with CCS baseline plus a single abatement intervention

Case	MESP ($/gallon ethanol)
Ethanol with CCS and RNG	$2.18
Ethanol with CCS and renewable electricity	$1.86
Ethanol with CCS and green ammonia	$2.13

In the final case, the USDA Dry Mill Production Model (2016) of the 40-million-gallon-per-year TEA was updated with all three interventions. In this case, the ethanol refinery with CCS was paired with each cost intervention from Table 7 at the same time to determine the total effect on the MESP. The MESP with CCS baseline plus each abatement intervention together is $2.33/gallon ethanol.

TEA Sensitivity Study

A sensitivity analysis is a method that determines how target variables are affected based on changes in other variables known as input variables. The variables that we analyze in our TEA sensitivity study are feedstock cost, labor, price of RNG, price of renewable electricity, and capital cost of the CCS equipment. The ranges of the input variables are presented in Table 9. The results presented in Figure 9 show that feedstock cost was the most significant determinant of MESP. The feedstock cost can increase the MESP by approximately 21%.

Table 9. Ranges of input variables for sensitivity study

Input Variables	Minimum Value	Baseline Value	Maximum Value
Feedstock cost	$2.90/bushel	$3.30/bushel	$4.50/bushel
Labor quantity	5.24	7.24	9.24
Price of RNG	$7.48/MMBTU	$12/MMBTU	$29.44/MMBTU
Price of renewable electricity	$0.02/kWh	$0.02/kWh	$0.02/kWh
CCS-related capital cost	−10%	$9.6 million	+10%
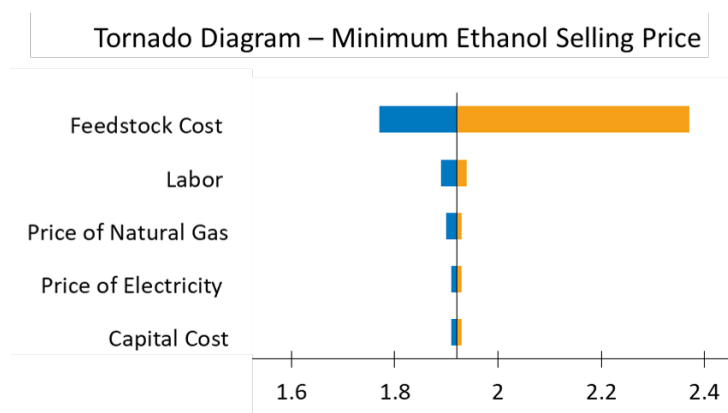
Figure 9. Techno-economic sensitivity analysis tornado graph results

3.1.5 Key Learnings

From the baseline, CCS pathway, and three intervention scenarios we constructed a preliminary abatement cost curve, shown in Figure 10. Notably, the small CI reduction from the renewable electricity intervention comes at a cost savings. This result should be considered with caution. Although we relied on cost assumptions widely used in analysis by collaborating with other national laboratories ($0.02/kWh), it is questionable whether consistent procurement at this price is possible today.

The most significant intervention on a cost and CI reduction basis is the CCS retrofit, which we estimate can lower the CI of the refinery (in California) by 33 g/MJ at a cost of $52/MT of CO_2. RNG can reduce CI by 17 g/MJ for under $200/MT CO_2, roughly commensurate with current carbon prices in the Low Carbon Fuel Standard. Green ammonia achieves a roughly 3.5-g/MJ reduction at a very high cost >$1,000/MT CO_2.
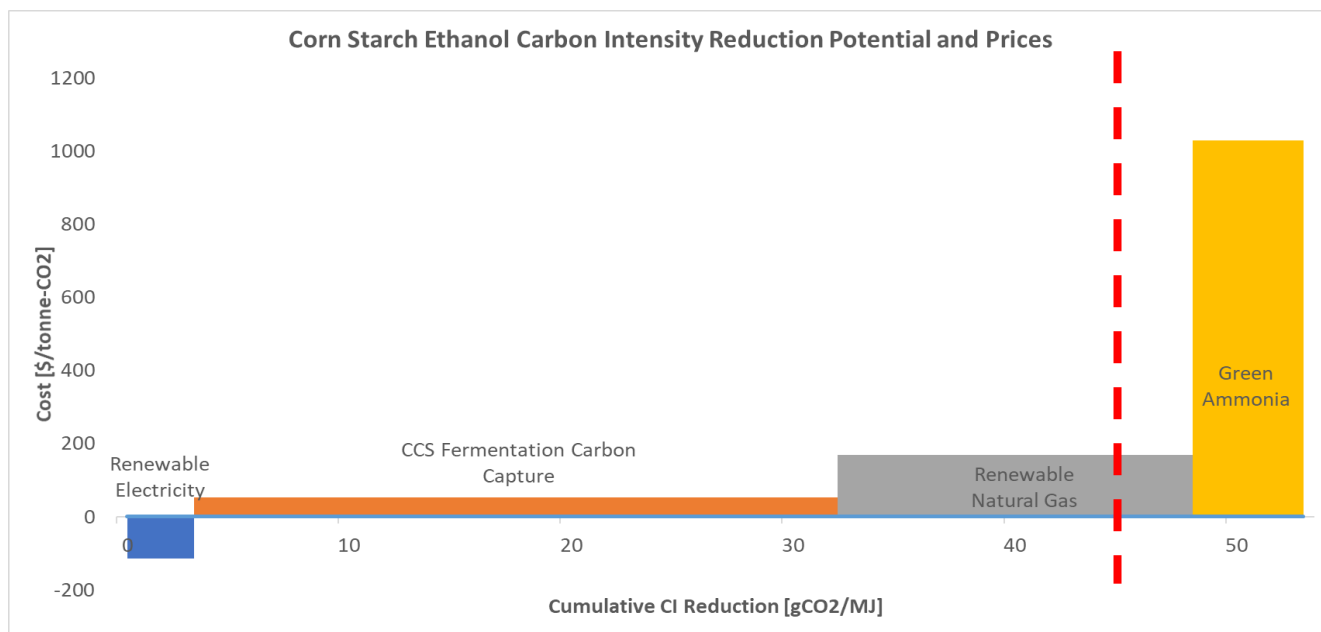
Figure 10. Carbon intensity reduction technology cost curve

3.2 Case 2 – Hydrocarbon Fuel Blendstock via Hydrothermal Liquefaction of Algae

3.2.1 Process Design

Case 2 is based on hydrothermal liquefaction (HTL) of microalgae feedstock and subsequent catalytic upgrading of the produced biocrude into hydrocarbon fuel blendstocks in the gasoline, diesel, and jet range (Figure 11 and Figure 12). The process model for the conceptual conversion plant is based on a report prepared by Pacific Northwest National Laboratory [8] and represents a future target case with improved process performance parameters and economics relative to the state of the art. The scale of the plant is 565 U.S. tons/day, ash-free dry weight (afdw) algae. As shown in Figure 11, NG is used for drying excess algae generated in the high-productivity months to be stored for use in low-productivity periods, to provide a constant feed rate to the plant. Algae dewatered to 20% solids is pumped and heated to reactor conditions (3,000 psi and 350°C) and fed to the HTL process. Products from the HTL process include a gravity separable oily phase, also known as "biocrude"; an aqueous phase; and a solid phase consisting mainly of ash with some biocrude (adhered to the particles) and char. Approximately 19% of algae carbon remains in the aqueous phase in the form of water-soluble compounds such as carboxylic acids, alcohols, and amines. This stream is processed with catalytic hydrothermal gasification at similar conditions to HTL to convert organics into a methane-rich gas product. This methane, along with hydrotreating off-gas, HTL off-gas, and supplementary NG is used to produce H_2 in an SMR unit for downstream biocrude upgrading.

Note that the H_2 gas generated from biogenic carbon (catalytic hydrothermal gasification, hydrotreating, and HTL off-gasses) provides 80% of the H_2 needed for the catalytic upgrading process, whereas the supplementary NG is used to fulfill the hydrogen requirement. Hydrogen and biocrude from HTL are fed to a hydrotreater packed with a standard hydrotreating catalyst typical for petroleum hydrotreating. The upgraded oil from the hydrotreating process is then fractionated into gasoline and diesel fractions. A heavy cut is hydrocracked into additional gasoline and diesel. A jet cut blendstock can also be produced, which is about 20% of the total product slate. Electricity is primarily used for pumping and H_2 compression at the conversion plant.
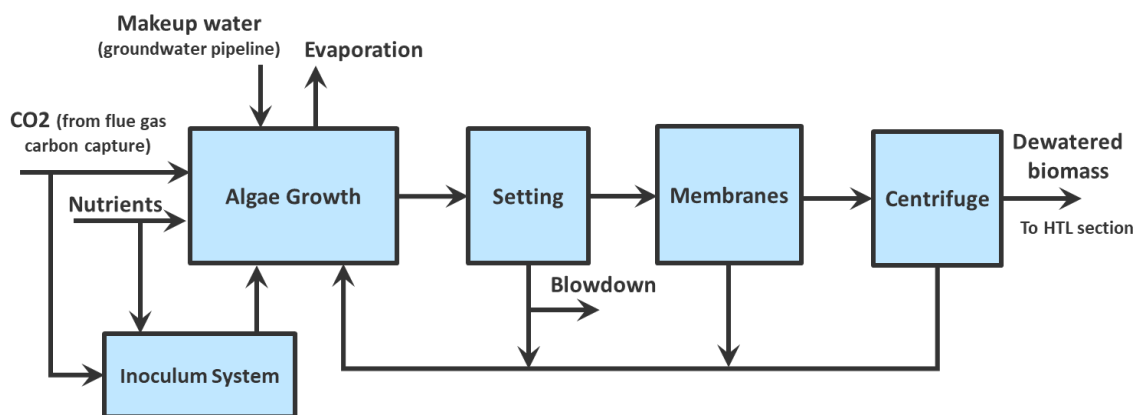
Figure 11. Algae production [10]

In order to reduce the process carbon emissions, fossil-derived resources were replaced by renewable resources, namely RNG, renewable electricity, and electrolysis-based hydrogen. Three different process flowsheets were considered. Sensitivity cases for each process flowsheet were evaluated by incrementally introducing renewable H_2 and electricity into the conversion area, algae farm, and CO_2 capture and transmission stages of the supply chain. The first process flowsheet considered is the base case process flowsheet with RNG. The impacts from utilizing RNG on process carbon emissions and economics were evaluated as the analysis of Cases 2.1–2.4. Primary process parameters for the plant are given in Jones et al. [8]. Algae feedstock cost is assumed to be \$461/dry ton when generated with the average U.S. grid electricity and \$441/dry ton when generated with renewable electricity [13]. Sensitivity cases for this flowsheet were evaluated by incrementally introducing renewable H_2 and electricity into the conversion area, algae farm, and CO_2 capture and transmission stages of the supply chain, as described in Table 10. Renewable electricity was incrementally introduced to the process flowsheet. Electricity from the grid is used in the entire process Case 2.1. Renewable electricity is only used in the conversion process for Case 2.2. Renewable electricity is used in both the conversion process area and algae production for Case 2.3. Renewable electricity is used in the entire process for Case 2.4. In addition to the base case flowsheet, two alternative flowsheet configurations were evaluated. Figure 13 shows the first alternative (flowsheet A), where NG consumption is eliminated by using a portion of the methane-rich off-gas from catalytic hydrothermal gasification for algae drying and using H_2 derived from water electrolysis for the 20% that is otherwise produced from NG (see Figure 12). Sensitivity Cases 2.5–2.8 (Table 11) are based on this flowsheet, where increasing levels of renewable electricity are introduced into the supply

chain. The second alternative flowsheet, flowsheet B (Figure 13), considers the case where all H_2 is provided through water electrolysis. In this case, process off-gas is burned, and the heat is used to produce steam that is sent to a turbine for power production. Sensitivity Cases 2.9–2.12 (Table 12) are evaluated for this flowsheet.

Table 10. Description for the base case and Cases 2.1–2.4

Case	Scenario	Conversion area (Algal HTL to HC production)		Algae farm	CO_2 capture & transmission
		H_2 source	Electricity source	Electricity source	Electricity source
Base case	2030 target case	SMR using NG and off-gas	U.S. mix	U.S. mix	U.S. mix
Case 2.1	Replacing fossil NG with RNG	SMR using RNG and off-gas	U.S. mix	U.S. mix	U.S. mix
Case 2.2	Replacing fossil NG with RNG	SMR using RNG and off-gas	Renew. electricity	U.S. mix	U.S. mix
Case 2.3	Replacing fossil NG with RNG	SMR using RNG and off-gas	Renew. electricity	Renew. electricity	U.S. mix
Case 2.4	Replacing fossil NG with RNG	SMR using RNG and off-gas	Renew. electricity	Renew. electricity	Renew. electricity
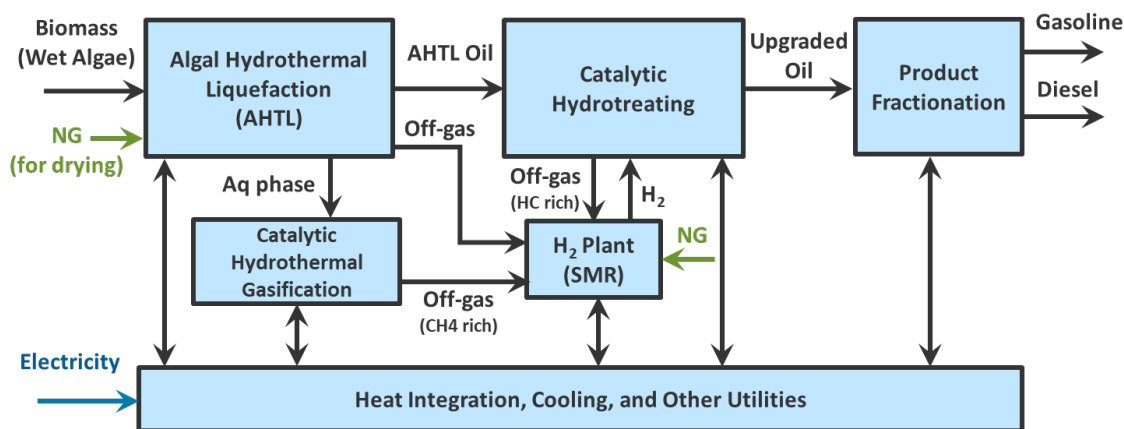
Figure 12. Base case flowsheet for the analysis of Cases 2.1–2.4
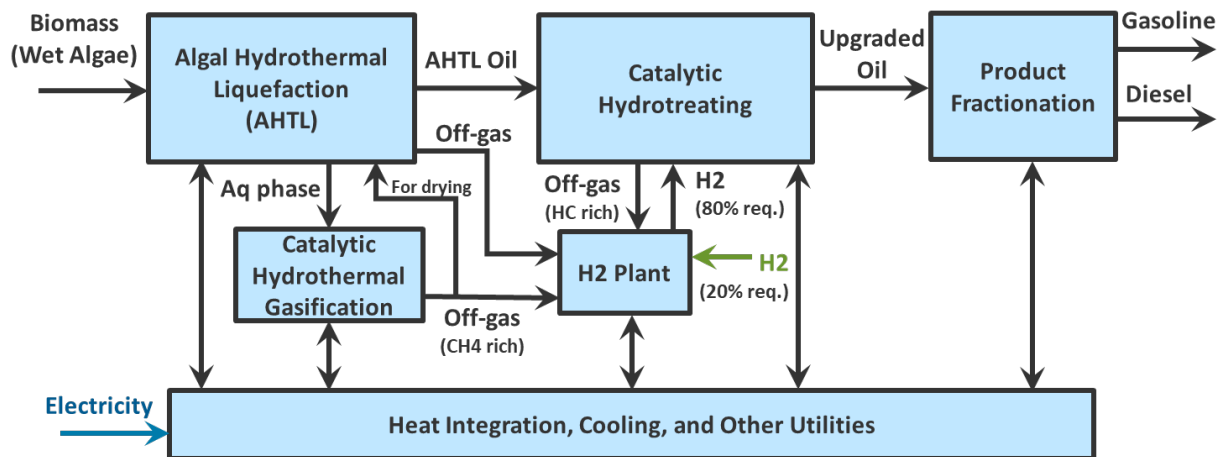
Figure 13. Flowsheet A for Cases 2.5–2.8

Table 11. Description for Cases 2.5–2.8

Case	Scenario	Conversion area (Algal HTL to HC production)		Algae farm	CO_2 capture and transmission
		H_2 source	Electricity source	Electricity source	Electricity source
Case 2.5	Eliminating NG by using off-gas for drying and electrolysis for H_2 production	SMR using off-gas + electrolysis with U.S. mix	U.S. mix	U.S. mix	U.S. mix
Case 2.6	Using renewable electricity for conversion process area	SMR using off-gas + electrolysis with renew. electricity	Renew. electricity	U.S. mix	U.S. mix
Case 2.7	Using renewable electricity for conversion and algae production	SMR using off-gas + electrolysis with renew. electricity	Renew. electricity	Renew. electricity	U.S. mix
Case 2.8	Using renewable elec. from algae to HC production	SMR using off-gas + electrolysis with renew. electricity	Renew. electricity	Renew. electricity	Renew. electricity
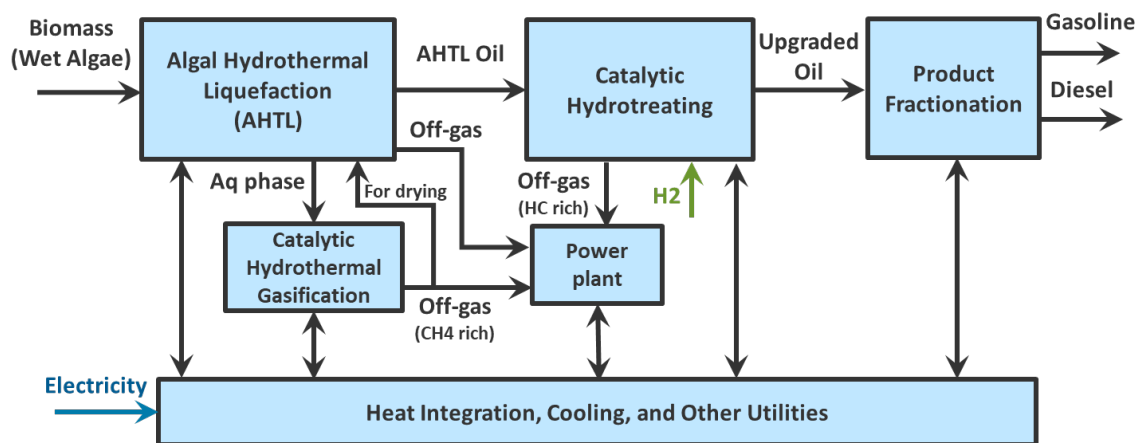
Figure 14. Flowsheet B for Case 2.9–2.12

Table 12. Description for Cases 2.9–2.12

Case	Scenario	Conversion area (Algal HTL to HC production)		Algae farm	CO_2 capture and transmission
		H_2 source	Electricity source	Electricity source	Electricity source
Case 2.9	Eliminating NG by using off-gas for drying and electrolysis for H_2 prod.	Electrolysis with U.S. mix	U.S. mix	U.S. mix	U.S. mix
Case 2.10	Using renewable electricity for conversion process area	Electrolysis with renew. electricity	Renew. electricity	U.S. mix	U.S. mix
Case 2.11	Using renewable electricity for conversion and algae production	Electrolysis with renew. electricity	Renew. electricity	Renew. electricity	U.S. mix
Case 2.12	Using renewable electricity from algae to HC production	Electrolysis with renew. electricity	Renew. electricity	Renew. electricity	Renew. electricity

3.2.2 LCA Results and Discussions

LCA Cases and Inventories

Figure 15 is the schematic flow diagram of the life cycle pathways for Case 2. CO_2 is supplied from off-site to promote algae growth, and electricity is used in the CO_2 capture and transmission processes. Algae is converted into renewable fuels through HTL processes. Although the fuel production process can convert algae into various types (i.e., diesel, gasoline, and jet), we evaluate renewable diesel for LCA. However, process emissions may not differ from each other using the energy allocation method for the energy products. The renewable diesel produced is transported to the end-use site and combusted. In addition, GHG emissions generated from upstream processes of all energy and chemicals used in each process are also accounted for life cycle GHG emissions. All cases for Case 2 are based on the 2030 target case, so we considered the U.S. electricity mix in 2030 (414 gCO_2e/kWh).
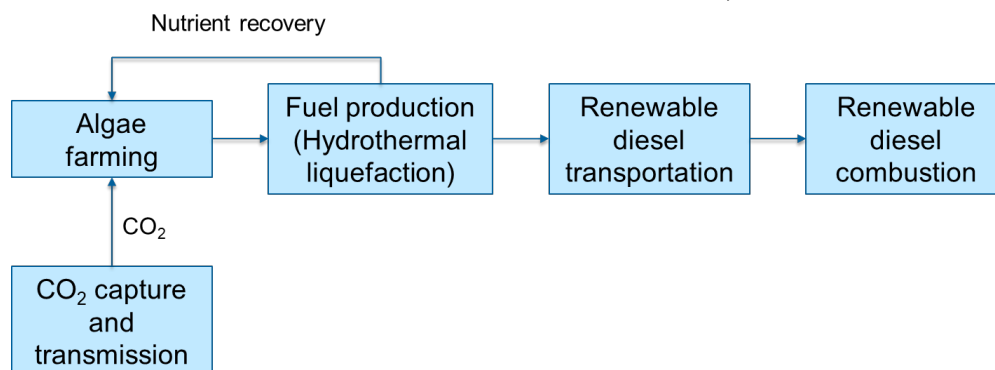
Figure 15. The schematic flow diagram of the life cycle pathways of Case 2, which includes algae farming, CO_2 capture and transmission, fuel production (HTL), fuel transportation, and fuel combustion

For algae farming, we assumed algae growth and production in 2030 [32]. The farming process energy (0.3645 kWh/afdw kg algae) is 100% electricity, which is mostly used for algal growth, pumping, dewatering, and harvesting. Although there are nutrients inputs (ammonia and $(NH_4)_2HPO_4$; 20 and 10 g/afdw kg algae, respectively—see Table 13), these are recovered during the fuel production stage, so GHG emissions from nutrient use are offset. To promote algae growth, CO_2 is supported (2.67 kg CO_2/afdw kg algae), which requires electricity of 0.1750 kWh/kg CO_2 for capture and 0.0016 kWh/kg CO_2 for CO_2 transportation from the off-site to the algae farm [32]. We assumed CO_2 is from coal power plants, where it is compressed under high pressure and transported through a pipeline; the transportation distance is assumed less than 100 miles, which does not require CO_2 recompression. Note that CO_2 emissions from algae biomass during conversion and biofuel combustion would offset carbon emissions otherwise emitted. Thus, we considered CO_2 from algae and algal biofuels carbon-neutral.

We assumed that an HTL facility is co-located with the algae farm, and Figure 15 presents the major inputs to produce 1 MJ of renewable diesel through the HTL process. There are three data sets, depending on the system configurations explained in the earlier section. NG and electricity inputs to produce H_2 required for the conversion process are the most critical inputs, although there are small amounts of catalyst and chemical inputs (i.e., sulfuric acid, HT catalyst,

hydrocracking catalyst). During the conversion process, nutrients (i.e., nitrogen and phosphorus) are recovered and sent back to the algae farms for recycling; GHG emissions credits for the nutrient recycling are considered. While the base case and Cases 2.1–2.4 require NG for H_2 production and drying, we use off-gas for H_2 and drying algae for Cases 2.5–2.8 where electricity is used for supplying the rest of the H_2 demand. In Cases 2.9–2.12, off-gas is only used for drying algae, and H_2 is supplied by electrolysis with electricity inputs.

Table 13. Life cycle inventory of the HTL conversion process for three design configurations

per 1 MJ of product		Base case, Cases 2.1–2.4	Cases 2.5–2.8	Cases 2.9–2.12
Inputs	Algae biomass (kg afdw)	0.048	0.048	0.048
	Electricity for H_2 production (kWh)		0.017	0.084
	Electricity for others (kWh)	0.0052	0.0027	0.00025
	NG for H_2 production (MJ)	0.071	0	0
	NG for drying (MJ)	0.087	0	0
	Water (gal)	0.043	0.052	0.11
	Chemicals and catalysts (g)	6.6	6.6	6.6
Recovered nutrients	Ammonia (g)	2.34	2.34	2.34
	$(NH_4)_2HPO_4$ (g)	0.27	0.27	0.27

Once produced, renewable diesel is transported from the plant to the gas station. This process is assumed to be the same as the renewable diesel transportation process in GREET [6]. As the combustion emissions of biomass-derived fuels offset the CO_2 emissions absorbed during the production of bio-feedstock, there are only small amounts of GHG emissions during the fuel combustion stage due to CH_4 and N_2O emissions.

LCA Results

LCA results are shown in terms of life cycle GHG emissions in Figure 16. Note that we have analyzed the cases with the conventional and renewable conditions presented in Table 4. First, the base case considers electricity from the U.S. grid mix, fossil NG, and H_2 by SMR with NG. As the major driver that determines the CI of algae-derived fuels is the source of electricity used for algae farms, HTL conversion, and CO_2 capture and transmission, Cases 2.1–2.12 can be divided into four groups with respect to the sources of electricity.

The 2030 base case representing the algae-derived renewable diesel production using U.S. electricity mix (in 2030) and conventional U.S. NG already shows significant life cycle GHG emission reductions; the CI of the base case is 31 gCO_2e/MJ, which is 66% lower than that of conventional petroleum diesel (92 gCO_2e/MJ). Most of GHG emissions contributions are from CO_2 capture and transmission (27%), algae production (30%), and conversion (39%), excluding the contribution of emission credits, mainly from upstream emissions of the use of fossil NG, electricity generation, and H_2 produced via SMR with fossil NG. There are GHG emission credits of recovering nutrients, which offset the nutrient inputs included in the "conversion of algal biomass to biofuels" category.
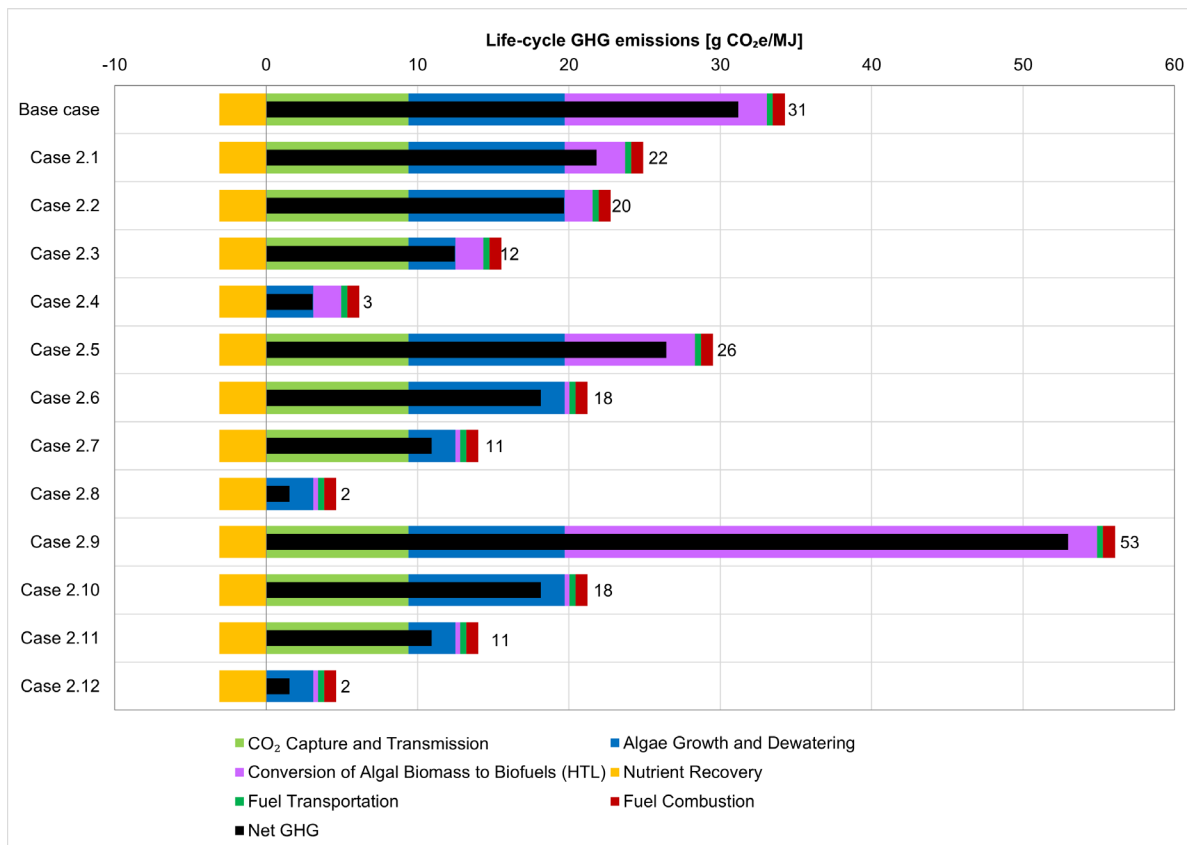
Figure 16. Life cycle GHG emission results of Case 2

For Cases 2.1, 2.5, and 2.9, we assumed U.S. electricity mix is used as the base case; for Cases 2.2, 2.6, and 2.10, we considered renewable electricity is used for the conversion process, keeping the other two using the U.S. electricity mix. For Cases 2.3, 2.7, and 2.11, we considered both algae farm and fuel production use renewable electricity whereas CO_2 capture and transmission are supported by the U.S. electricity mix. Lastly, Cases 2.4, 2.8, and 2.12 assume the use of renewable electricity for all stages.

Case 2.1 uses landfill gas-derived RNG for H_2 production needed for the HTL process, which reduces 9.4 gCO_2e/MJ of the GHG emissions during the conversion process compared to the base case. On the other hand, Case 2.5 uses both off-gas and electricity for H_2 production, which is slightly lower than the CI (5 gCO_2e/MJ) from the base case; GHG emissions of the conversion process (8.6 gCO_2e/MJ) is generated from the upstream of electricity. As Case 2.9 relies on electricity for H_2 production, it leads to having the highest CI value, mainly due to upstream emissions of U.S. mix electricity for H_2 for the conversion process.

GHG emissions led by the HTL process can be further reduced by using renewable electricity instead of the U.S. electricity mix. For Cases 2.2, 2.6, and 2.10, GHG emissions are reduced by 2.1, 8.3, and 35 gCO_2e/MJ, respectively, compared to Case 2.1, 2.5, and 2.9. Whereas Case 2.2 uses H_2 from RNG SMR, Cases 2.6 and 2.10 rely on electricity for H_2 production (and internally generated off-gas in Case 2.6), which is why Cases 2.6 and 2.10

almost eliminate the HTL-associated GHG emissions by utilizing renewable electricity. Using renewable electricity for algae growth and dewatering can reduce 7.2 gCO$_2$e/MJ of GHG emissions in Cases 2.3, 2.7, and 2.11. Furthermore, using renewable electricity for CO$_2$ capture and transmission, an additional 10.3 gCO$_2$e/MJ of GHG emissions can be eliminated in Cases 2.4, 2.8, and 2.12.

Note that LCA results of Cases 2.6–2.8 and Cases 2.10–2.12 become identical because they have the same amount of chemical/catalyst inputs, algal biomass inputs, and CO$_2$ inputs; although electricity inputs are different from each other, the LCA results are not affected because the CI of renewable electricity is 0.

LCA results from the analysis of flowsheets A and B are also shown in Figure 16. Process GHG emissions are expected to be reduced by eliminating NG in both flowsheets. However, the life cycle GHG for Case 2.9 is higher than the base case, which uses NG. This is because the amount of electricity consumption for electrolysis is very high, especially when it is nonrenewable electricity. The results basically show that the process GHG emissions could be improved by renewable electricity. The life cycle GHG emissions could be near zero (Cases 2.8 and 2.12) when NG is eliminated and renewable electricity is used throughout in both the algae production and the conversion step.

3.2.3 TEA Results and Discussions on Key Metrics (Carbon Efficiency, Energy Efficiency, and Cost)

TEA results of Case 2 are summarized in Figure 17. The results are shown in terms of MFSP in dollars per gallon gasoline equivalent (gge) when the MFSP of the base case study was reported at \$4.3/gge [27]. Uncertainty on cost of the renewable resources—namely NG, electricity and H$_2$ (as listed in Table 2)—are considered and showed as error bars in Figure 17. When fossil-based NG and electricity from the grid are replaced by RNG and renewable electricity (for Cases 2.1 and 2.4), the selling price of hydrocarbon fuel product increase from the base case. This is because prices of RNG are assumed to be approximately 2–10 times more expensive than NG. Flowsheet A results in slightly more favorable process economics for Cases 2.5–2.8 when NG is replaced by internal process off-gases and electrolysis-based H$_2$ is used. On the other hand, using internal process off-gases for on-site electricity generation and purchased renewable H$_2$ in flowsheet B provides the least economically attractive scenarios. Analysis of the three different process flowsheets shows consistent results when renewable electricity is used for the entire process (Cases 2.3, 2.4, 2.7, 2.8, 2.11, and 2.12). For example, MFSPs from Cases 2.3 and 2.4 are approximately \$0.20/gge less than Cases 2.1 and 2.2. The reduced MFSP primarily results from the less-expensive feedstock, which utilizes renewable electricity. Algae production is highly energy-intensive itself. The feedstock cost is reduced from \$461/ton (afdw) to \$441/ton (afdw) when electricity from the grid (\$0.0682/kWh) is replaced by renewable electricity (\$0.02/kWh).
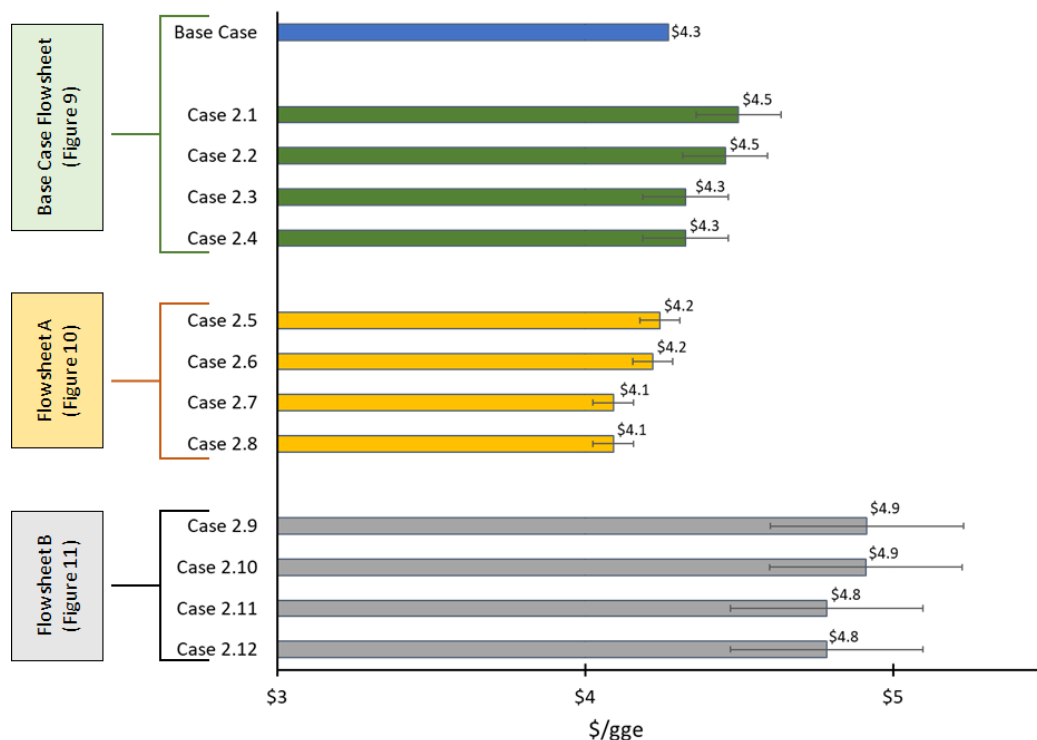
Figure 17. TEA results for sensitivity Cases 2.1–2.12 for the algae HTL pathway

Carbon efficiency and thermal efficiency were evaluated for the conversion step only (algae HTL to hydrocarbon fuel). Carbon efficiency is defined as the ratio of carbon content of hydrocarbon fuel product to carbon from algae plus NG, as expressed in Equation 3. The thermal efficiency (lower heating value basis) calculation is shown in Equation 4. It is the ratio of the heating value of hydrocarbon fuel product to the heating value of algae plus NG and electricity. Both carbon and thermal efficiencies are summarized in Table 14.

Carbon efficiency

$$Ceff = \frac{C_{HC\,fuel\,product}}{C_{Algae} + C_{NG}} \qquad \text{(Equation 3)}$$

Thermal efficiency

$$Ther_{eff} = \frac{LHV_{HC\,fuel\,product}}{LHV_{Algae} + LHV_{NG} + Electricity} \qquad \text{(Equation 4)}$$

The results in Table 14 were generated under the assumption of comparable carbon content and energy content between NG and RNG. Because carbon efficiency depends on carbon input (algae and natural gas) and output (hydrocarbon), the carbon efficiency is kept constant in each process flowsheet configuration (base case, flowsheet A and flowsheet B) even though renewable resource is incrementally applied. The carbon efficiency of flowsheet A is the same as flowsheet B and better than the base case flowsheet. The overall carbon efficiency can be improved if NG or RNG is eliminated. On the other hand, thermal efficiency depends on the energy content of feed (algae and natural gas) and product (hydrocarbon fuel) and process

electricity usage. Correspondingly, the thermal efficiency remains constant in each flowsheet even though additional renewable resources were introduced. Compared to the base case flowsheet, thermal efficiency was improved by flowsheet A because of the elimination of NG usage. However, the thermal efficiency is decreased when the process off-gases is used to produce electricity (in flowsheet B) rather than to produce H_2 (in flowsheet A). This is because electricity usage is significantly increased when all the required H_2 is exclusively produced by electrolysis.

Table 14. Carbon efficiency and thermal efficiency for conversion process

Case	Carbon efficiency	Thermal efficiency	Note
Base case	0.64	0.85	NG for drying and SMR
Cases 2.1 to 2.4	0.64	0.85	Base case flowsheet: RNG for drying and SMR
Cases 2.5 to 2.8	0.70	0.87	Flowsheet A: Eliminate NG. Additional H_2 from electrolysis
Cases 2.9 to 2.12	0.70	0.73	Flowsheet B: Eliminate NG. Additional H_2 from electrolysis

3.2.4 Key Learnings

Using biomass is a good starting point to achieve near-zero-carbon fuels. LCA results suggest that a near-net-zero algae HTL process could be possible if NG and electricity are replaced by RNG and renewable electricity throughout from algae production to hydrocarbon fuel production. However, with the scenarios of using electrolysis H_2, GHG emissions are increased quite significantly if the grid electricity mix is assumed. Therefore, it is far better to use off-gasses from algae conversion for H_2 production than for power and heat if using grid mix electricity. The results show the potential of net-zero-carbon fuels when multiple renewable energy options are considered in biofuel production pathways. Renewable electricity and RNG for meeting power and heat demand can help reduce the CI. The renewable diesel production from algae via HTL can achieve the lowest GHG emissions (1 gCO_2e/MJ) by using renewable energy systems, which is 99% lower than the CI of petroleum diesel.

Replacing fossil-based NG by RNG could improve the LCA, but its economics might not be favorable. Flowsheet A of incorporating H_2 from electrolysis instead of from NG for the 20% needed beyond what is supplied by process off-gas (that is biomass-derived) does not significantly affect economics of the process. By substituting flowsheet B of diverting process off-gases to heat and power and using all electrolytically derived H_2 increased MFSP by about 20%–25%. This is due to the fact that it is much more efficient to use process off-gas for H_2 production (which is inherently renewable) than for power generation.

3.3 Case 3 – Carbon Conversion to Ethanol

Case 3.1 examines the production of ethanol via fermentation of biomass-derived syngas. In this pathway, syngas is produced via indirect gasification of woody biomass per the performance metrics outlined for the 2022 projection case in the National Renewable Energy Laboratory's 2019 State of Technology Report [12]. The fermentation step is based on published literature

from LanzaTech. In accordance with the goals of this analysis, several process modifications were tested to determine the key drivers that could result in improved energy efficiency, carbon efficiency, and cost. The six scenarios employed for Case 3.1 were (Table 15):

- Case 3.1.1 benchmark case
- Case 3.1.2 RNG import
- Case 3.1.3 renewable H_2 import; an additional subset of Case 3.1.3 was studied to understand the impact of varying the amount of H_2 imported
- Case 3.1.4 renewable H_2 import and RNG import
- Case 3.1.5 renewable H_2 and renewable electricity import
- Case 3.1.6 renewable H_2, RNG import, and renewable electricity import.

Case 3.2 investigates the potential of using a hybrid bio-electrochemical process to convert waste CO_2 streams from corn dry mill facilities into ethanol and demonstrates the impact of CO_2 utilization on the biorefinery economics. The bio-electrochemical CO_2 conversion process combines water electrolysis to H_2, electrolysis of CO_2 to CO, and gas fermentation to ethanol. With on-site CO_2 conversion, total ethanol yield can be potentially improved by 45%. In this study, variations of H_2:CO ratio ranging from 0 to 5 are explored to understand the impact of gas mixture composition on economic viability. The TEA results show single-pass carbon yield in the biological conversion step can be potentially improved up to 100% when using H_2 as an alternative energy source.

3.3.1 Process Design

The process description for Case 3.1 (Figure 18) demonstrates the production of ethanol via fermentation of syngas. The front end of the process (biomass to scrubbed syngas) is produced identically to the National Renewable Energy Laboratory's indirect liquefaction to high-octane gasoline 2022 projection [12]. However, because CO_2 can be fermented in addition to CO, there is no acid gas removal step. Thus, the whole syngas stream is compressed and fed to the fermentation.
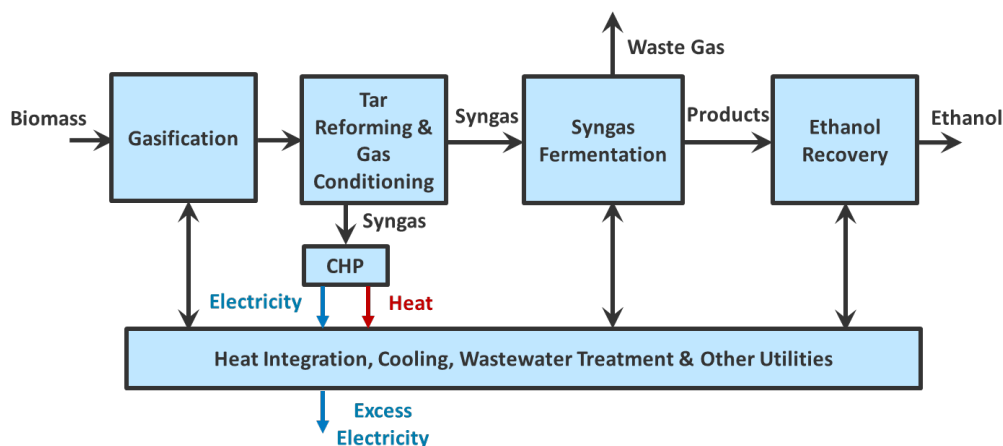
Figure 18. Block flow diagram of biomass to ethanol via syngas fermentation, Case 3.1

Fermentation processes and conditions were based on published literature from LanzaTech and INEOS/BRI. Fermentation is governed by the following equations:

$$1.61\ H_2 + CO \rightarrow 0.435\ EtOH + 0.305\ H_2O + 0.13\ CO_2 \qquad \text{(Equation 5)}$$
$$6\ H_2 + 2\ CO_2 \rightarrow EtOH + 3\ H_2O \qquad \text{(Equation 6)}$$
$$2\ CO + 4\ H_2 \rightarrow EtOH + H_2O \qquad \text{(Equation 7)}$$
$$3\ CO + 5\ H_2 \rightarrow Bacteria + 2\ H_2O \qquad \text{(Equation 8)}$$
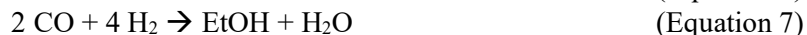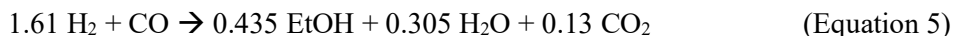
Table 15. Descriptions of scenarios for Case 3.1

3.1.1: Benchmark	Fermentation yields were determined by Equation 5 and Equation 8. It was assumed that there was 90% conversion of CO to ethanol (Equation 5) and 1.29% conversion of CO to bacteria growth (Equation 8). The molar ratio of H_2 to CO in biomass syngas is 1.61:1. This was used to determine the stoichiometry of the base case's governing equation. Additional assumptions include that all heat and power to the plant is provided by diverting a portion of the biomass syngas, and no additional NG or electricity is imported.
3.1.2: Import RNG	Has the same governing equations and fractional conversions as defined in the benchmark scenario. However, in this case no syngas is diverted for heat and power; instead, enough RNG is imported to satisfy the plant's heat and power demands. Bacteria is still produced at the same rate as Scenario 3.1.1.
3.1.3: Import renewable H_2	Through observation of the governing equations (Equations 5–8), it is apparent that the fermentation yield is limited by H_2 availability in the syngas stream. A maximum theoretical limit was therefore imposed on Scenario 3.1.3 where enough renewable H_2 is imported to have a fractional conversion of 90% for both CO and CO_2 as determined by Equations 2 and 3. Bacteria is still produced at the same rate as Scenario 3.1.1. A subset of scenarios was completed to determine the impacts of sequentially lowering CO_2 conversion (while maintaining a CO conversion of 90%), therefore lowering the H_2 demand on cost and carbon efficiency. In the Scenario 3.1.3 studies, biomass syngas is diverted to provide heat and energy to the plant.
3.1.4: Import renewable H_2 and RNG	Determine the "maximum H_2 import" while also not diverting any biomass syngas for heat or power. Instead, RNG is imported to meet the heat and power demands of the plant.
3.1.5: Import renewable H_2 and renewable electricity	Similar to Scenario 3.1.4, but a portion of biomass-derived syngas *is* diverted to meet the heat demands of the plant. However, the remaining power demands of the plant are met by importing renewable electricity.
3.1.6: Import renewable H_2, RNG import, and renewable electricity	A combination of the previous scenarios to attempt to determine if there is an optimization between the use of RNG or renewable electricity for powering the plant.

Process description for Case 3.2. (Figure 19) demonstrates the production of syngas from electrolysis of CO_2 and water, then ethanol production via fermentation of syngas. The off-gases produced in the ethanol fermentation process consist of almost pure CO_2 (over 99 vol%) with very few impurities [25]. A CO_2 purification system is not required for the downstream upgrading process in this study, and gas fermentation technology is used to convert the gaseous carbon waste streams into ethanol. For the gas fermentation step, gas feedstocks at different H_2:CO ratios have been demonstrated at scale [33] using CO as both a carbon and energy source, or also utilizing H_2 as a supplemental energy source if presented in the input gas blend. Thus, we investigate three cases with H_2:CO ratio ranges from 0 to 5 (Figure 19).
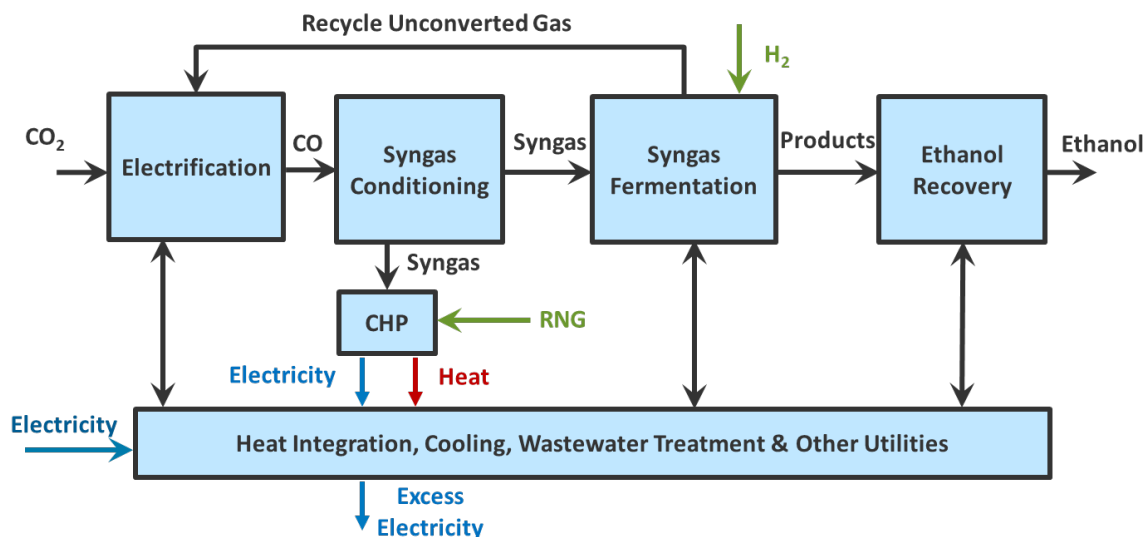
Figure 19. Process flow diagram of Case 3.2

In Case 3.2.1, the CO_2 stream from a corn dry mill facility first splits equally, and half of the CO_2 stream flows into a CO_2 electrolyzer to make CO. All the H_2 needed in the waste CO_2 upgrading process is produced via water electrolysis. The CO_2, CO, and H_2 gas mixture is fermented following Equation 6.

In Case 3.2.2, the entire CO_2 stream from a corn dry mill facility flows into a CO_2 electrolyzer directly to make CO. Then the CO and H_2 gas mixture is fermented following Equation 7.

In Case 3.2.3, similar to Case 3.2.2, all the waste CO_2 stream from a corn dry mill facility first flows into a CO_2 electrolyzer to make CO, and the CO gas is fermented following Equation 8, without H_2. Only one-third of the CO gas is converted to ethanol and two-thirds of the CO gas is oxidized to CO_2 via microbial respiration. The unconverted CO_2 is then recycled back to CO_2-to-CO electrolysis.

A standard fermentation media including macronutrients and micronutrients is used for the gas fermentation process [34]. Process productivity is a principal determinant of capital cost, and ethanol productivity of 195 g/L/d (8 g/L/h) has been reported [35]. The final ethanol titer in the fermentation broth is 60 g/L [36]. Trace amounts of other coproducts are produced in the fermentation. The ratio of ethanol to coproduct and the identity of the coproducts can be varied substantially by modifications to the process. For all CO_2 upgrading cases, gas utilization efficiency is assumed to be 95% with 100% ethanol selectivity. The fermentation broth is then pumped to the distillation columns for ethanol purification.

For the electrolysis process, critical operating metrics include cell voltage, current density, and faradaic efficiency. The cell voltage refers to the thermodynamic potential required, the activation overpotentials at both electrodes, and the ohmic overpotential associated with resistances in the electrodes and electrolyte. The current density is defined as the current flow

divided by the active electrode area. The current density is a measure of the electrochemical rate per area of electrode and is used to determine the overall size needed to obtain a desired reaction rate. Therefore, a higher current density is desirable to minimize the total capital cost of the electrolysis system, achieving a given product formation rate. The faradaic efficiency (Equation 9) is the percentage of charge passed in the electrolyzer that is directed toward the formation of the target product.

$$\varepsilon_{Faradaic} = \frac{z \cdot n \cdot F}{Q} \qquad \text{(Equation 9)}$$

A higher faradaic efficiency is desired to minimize electricity expenses and downstream separation processes. The required electricity consumption, E, in a given period, t, is calculated by Equation 10:

$$E = I \cdot V \cdot t = Q \cdot V = \frac{Z \cdot n \cdot F}{\varepsilon_{faradiac}} \cdot V \qquad \text{(Equation 10)}$$

where I is the current, V is the cell voltage, z is the number of required electrons to produce one mole of product ($z = 2$ to produce CO and H_2), n is the number of moles of the given product, F is Faraday's constant, and Q is the total charge passed.

Currently there is no standard design for a CO_2 electrolyzer, and many different configurations have been reported [37, 38]. Electrochemical CO_2 electrolysis is in many ways analogous to H_2O electrolysis, and thus a commercial CO_2 electrolyzer is expected to share many design features with an H_2O electrolyzer. To provide an estimate for the capital costs of an electrolyzer system, water electrolysis is used as a representative model. A U.S. Department of Energy H_2 Analysis (H2A) project has published case studies for H_2 production [39], and uninstalled capital costs of an alkaline H_2O electrolyzer are $400/kW. Therefore, the installed cost for a CO_2 electrolyzer is $1,400/m² based on the typical operating conditions of 175 mA/cm² and 1.75 V for the Norsk Hydro Atmospheric Type No. 5040 alkaline electrolyzer [40]. Single-pass conversion of CO_2 within the electrolyzer is assumed to be 20%, which would vary depending on reactor design [41].

3.3.2 LCA Results and Discussions

LCA Cases and Inventories

Case 3 has two main pathways generating ethanol, one starting from biomass (Case 3.1) and the other from a waste CO_2 stream (Case 3.2), as presented in Figure 20.

1) Biomass feedstock to ethanol

Feedstock	Ethanol production

Biomass collection → Biomass transportation → Preprocessing

Biomass gasification → Syngas fermentation → Ethanol recovery → Ethanol transportation & distribution → Ethanol combustion

- **Biomass feedstock**:
  50 wt.% forest residue
  50 wt.% clean pine
- **Ethanol production:**
  Woody biomass-to-ethanol via gasification and syngas fermentation

2) Waste CO_2 to ethanol

- **CO_2 feedstock:**
  high-purity waste CO_2 from bio-refinery
- **Ethanol production:**
  Waste CO_2 to ethanol via syngas fermentation

CO_2 to ethanol conversion → Ethanol transportation & distribution → Ethanol combustion

NG, H_2, electricity, chemicals/catalysts

Figure 20. The system boundaries of LCA of Case 3, which includes feedstock production and transportation, ethanol production, fuel transportation, and fuel combustion using two feedstocks (biomass and waste CO_2)

For Case 3.1, biomass feedstock is first assumed to be 50% clean pine and 50% forest residues (by mass). Woody biomass has ample feedstock supply potential for renewable fuel production with lower CIs than first-generation biofuels. The supply chain of clean pine starts from pine growth, followed by harvesting and collection. Because forest residues are waste, the supply chain starts from the collection of residues. Once feedstock is collected, forest residues and clean pine are transported to the ethanol plant by truck [13]. Electricity is consumed for receiving, handling, and depot preprocessing of the feedstock by conveyors, dryers, and dust collection operations [32]. Note that it is relatively difficult to change the energy sources used for the collection of forest residues, clean pine production, and feedstock transportation, whereas energy sources for the preprocessing can be converted to renewable electricity.

Biomass goes through biomass gasification, syngas fermentation, and ethanol recovery processes, which require electricity, H_2, NG, chemicals, and catalysts. We analyzed six sub-cases (Table 16) with different heat and power requirements for the ethanol production process by using an intermediate gas or supplying external energy, as explained earlier. In Case 3.1.1, it is assumed that heat and power demand are internally met using biomass during the ethanol production process. There is a small amount of coproduced electricity for Cases 3.1.1 and 3.1.2, the balance after meeting the electricity requirements; we accounted for the emission credits by assuming the displacement of the U.S. electricity grid mix. In Case 3.1.2, imported NG provides heat and power demand for the plant. Therefore, NG inputs (0.077 MJ NG/MJ) lead to a 4.6% reduction in feedstock inputs compared to Case 3.1.1. In Cases 3.1.3–3.1.6, waste CO_2 from the syngas production process is converted into additional ethanol by supporting additional H_2. CO_2 utilization can improve the yield of ethanol with the same amount of feedstock. In other words, the feedstock inputs decrease for 1 MJ of ethanol production. Therefore, in Case 3.1.3, with the

addition of 0.42 MJ of H_2, the feedstock input decreases by 35% compared to Case 3.1.1. In Case 3.1.5, power demand is supplemented by the external electricity, and the heat demand still comes from the biomass. Note that Cases 3.1.4 and 3.1.6 use external NG, whereas Cases 3.1.3 and 3.1.5 do not.

Table 16. Life cycle inventory of Case 3: biomass-to-ethanol and CO_2-to-ethanol pathways

Per 1 MJ of ethanol	Biomass-to-ethanol						CO_2-to-ethanol		
	Case 3.1.1	Case 3.1.2	Case 3.1.3	Case 3.1.4	Case 3.1.5	Case 3.1.6	Case 3.2.1	Case 3.2.2	Case 3.2.3
Feedstock									
Blended woody (MJ)	2.01	1.92	1.30	1.17	1.23	1.17			
Waste CO_2 (g)							74.0	73.6	73.6
Energy inputs									
Electricity (MJ)	0	0	0	0	0.014	0.012	3.11	1.11	0.60
NG (MJ)	0	0.077	0	0.085	0	0.044	0.36	0.38	0.38
H_2 (MJ)	0	0	0.423	0.424	0.423	0.424		0.88	1.08
Water (gallon)	0.05	0.049	0.038	0.036	0.037	0.036	0.013	0.006	0.006
Nutrients (g)	0.38	0.36	0.24	0.22	0.23	0.22	0.14	0.15	0.14
Coproduced electricity (MJ)	0.002	0.006							

For Case 3.2 of CO_2 feedstock to ethanol pathways, we assumed ethanol is produced from an on-site, high-purity CO_2 emission that is otherwise emitted, so there are no CO_2 transmission processes required.

Case 3.2 is divided into three sub-cases (Cases 3.2.1–3.2.3) with different CO, CO_2, and H_2 input ratios as explained earlier. Table 16 shows major inputs for the CO_2-to-ethanol process such as CO_2 feedstock, electricity, NG, H_2, and nutrients. Because Case 3.2.1 takes CO_2 and H_2O, it does require significant electricity inputs to convert CO_2 to CO, although it does not need H_2 inputs. Case 3.2.2 requires one-third of CO compared to Case 3.2.1, so the electricity inputs for CO electrolysis are reduced by 64%, while 0.88 MJ of additional H_2 needs to be supported to produce 1 MJ of ethanol. Further, Case 3.2.3 reduces CO input by half and increases H_2 input by 1.2 times compared to Case 3.2.2. For all these biomass- and CO_2-derived ethanol production cases, we considered conventional and renewable scenarios using different energy sources (electricity, NG, and H_2) as described in Table 4. For ethanol transportation, we considered typical ethanol transportation and distribution used in GREET [6]. Note that ethanol can be further processed to become aviation fuels through additional processes.

LCA Results

The life cycle GHG emissions of the ethanol production pathways from biomass via gasification followed by syngas fermentation and from CO_2 via syngas fermentation are presented in Figure 21. For conventional scenarios, the biomass-to-ethanol pathways show potential reductions in GHG emissions even compared to that of conventional corn ethanol (54 gCO_2e/MJ). Case 3.1.1 brings the lowest CI (16.8 gCO_2e/MJ) because the pathway relies highly on the energy supported by biomass rather than using external energy sources such as NG, electricity, and H_2. Thus, most of the GHG emissions occur during the feedstock production

processes (15.2 gCO$_2$e/MJ). Case 3.1.2 uses external NG to provide heat and electricity for ethanol production. As feedstock inputs decreased, GHG emissions during the feedstock production stage decreased by 0.7 gCO$_2$e/MJ, and the emission credit by coproduced electricity can further reduce 0.5 gCO$_2$e/MJ of GHG emissions. However, GHG emissions increased by 5.3 gCO$_2$e/MJ due to the NG input, so total GHG emissions increased 4 gCO$_2$e/MJ compared to Case 3.1.1.

For Cases 3.1.3–3.1.6, these use external H$_2$ produced from fossil NG SMR to convert CO$_2$ from biomass into additional ethanol. Although these generate 1.5–1.7 times more ethanol from the same amount of biomass compared to Case 3.1.1 by using CO$_2$ that is otherwise released, their CIs are higher than non-CO$_2$ utilization cases (estimated at 54–59 gCO$_2$e/MJ), mainly led by the upstream emissions of the H$_2$ inputs.
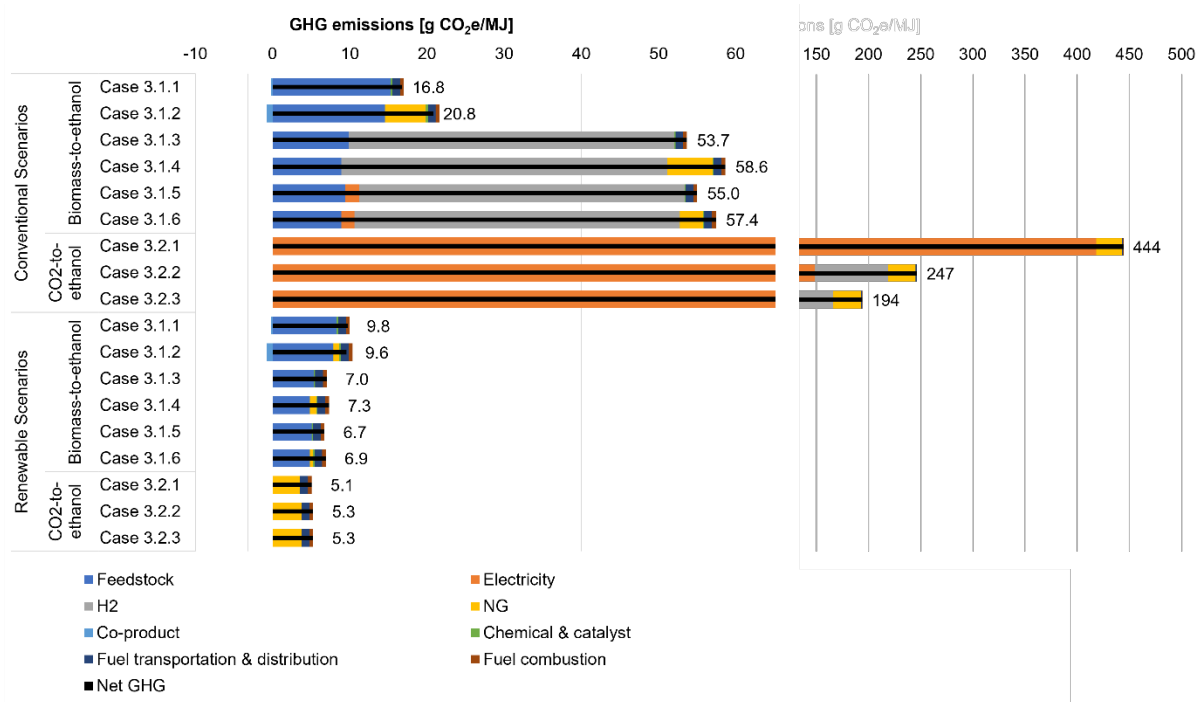
Figure 21. Life cycle GHG emissions (gCO$_2$e/MJ) of ethanol production pathways from biomass and CO$_2$ via syngas fermentation and/or biomass gasification using two scenarios (conventional/renewable)

The CO$_2$-derived ethanol production pathways consume much more electricity than biomass pathways per MJ ethanol production basis (Table 16) because of the CO electrolysis process. Therefore, the CIs of CO$_2$-derived ethanol highly depend on the CIs of electricity and H$_2$ production. With the conventional scenario that uses U.S. electricity mix, fossil NG, and H$_2$ from NG SMR, the upstream GHG emissions are substantial, which leads to the CI of ethanol 4–8 times higher (194–444 gCO$_2$e/MJ) than that of corn ethanol; these even exceed the CIs of fossil-based fuels. With different CO, CO$_2$, and H$_2$ input ratios, the upstream GHG emissions of electricity are estimated at 418, 149, and 80 gCO$_2$e/MJ and the upstream GHG emissions of H$_2$ are 0, 70, and 86 gCO$_2$e/MJ for Cases 3.2.1, 3.2.2, and 3.2.3, respectively.

By incorporating renewable energy inputs, the CIs of biomass-derived ethanol can be significantly reduced. For Cases 3.1.1–3.1.6, 46% of GHG emissions in the feedstock stage can be reduced using renewable electricity for feedstock preprocessing. For Cases 3.1.2, 3.1.4, and 3.1.6, landfill-derived RNG with lower CI than fossil NG can help reduce 86% of GHG emissions led by NG input. For conventional scenarios, Cases 3.1.3–3.1.6 that convert CO_2 from biomass into additional ethanol have higher CIs compared to Cases 3.1.1 and 3.1.2 that only generate ethanol from biomass. However, when renewable energy inputs are used, the CIs of Cases 3.1.3–3.1.6 become lower (CIs of ~7 gCO_2e/MJ) than Cases 3.1.1 and 3.1.2 (CIs of ~10 gCO_2e/MJ) because of their 1.5–1.7-times-higher ethanol yields, while the conversion process does not incur additional GHG emissions by using renewables. Therefore, with the renewable scenarios, the CIs of biomass-derived ethanol can be reduced by 82% compared to corn ethanol (54 gCO_2e/MJ) and 89% compared to petroleum gasoline (with 10% corn ethanol blended) (91 gCO_2e/MJ).

The reduction impact becomes more dramatic for CO_2-to-ethanol pathways. Although no CO_2-to-ethanol pathways provide GHG emissions benefits when conventional energy sources are used, ethanol produced through Cases 3.2.1–3.2.3 all becomes near-zero carbon fuel (CI of ~5 gCO_2e/MJ) using renewables, which are even lower than the CIs of biomass-derived ethanol. It is mainly because it is difficult to further reduce the biomass production-associated emissions as these are led by fertilizer and fossil liquid fuel use during farming, collection, and transportation. On the other hand, CO_2-derived ethanol that highly relies on electricity and H_2 can significantly reduce the CI of the final product by decarbonizing the upstream. Note that we assumed landfill gas-derived RNG is used for heat demand for ethanol purification for Cases 3.2.1–3.2.3 in Figure 21, which reduces the NG contribution in Case 3.2.1 of the conventional scenario from 24.8 to 3.5 gCO_2e/MJ of the renewable scenario.

3.3.3 TEA Results and Discussions on Key Metrics (Carbon Efficiency, Energy Efficiency, and Cost)

TEA Results for Case 3.1

The benchmark scenario (3.1.1) resulted in an MESP of $1.60/gallon ethanol and a carbon efficiency of 35.5%. To address uncertainty and variability in renewable resource cost, a minimum, baseline, and maximum cost sensitivity analysis was conducted. For each scenario beyond the benchmark case, both cost and carbon efficiency improvements were observed at the baseline costs. However, at high resource cost, the MESP tends to exceed the benchmark value, indicating some risk involved in the incorporation of that modification. Table 17 summarizes the results of each scenario discussed for Case 3.1. The case with the best performance on both cost and carbon efficiency was Case 3.1.6, with an MESP of $1.38/gallon ethanol (a 14% reduction from the benchmark) and a carbon efficiency of 60.9% (a 72% increase relative to the benchmark case).

Table 17. Summary of Case 3.1 TEA results.

	Case	MESP ($/gallon)	Production (MMgal/yr)	Carbon Efficiency
3.1.1	Benchmark	1.60	74.2	35.5%
3.1.2	RNG import – min ($7.48/MMBTU)	1.58	77.8	37.3%
	RNG import – baseline ($12.00/MMBTU)	1.60		
	RNG import – max ($29.44/MMBTU)	1.71		
3.1.3	H$_2$ import – baseline ($1.38/kg)	1.43	114.8	54.9%
	H$_2$ import – max ($4.50/kg)	2.33		
3.1.4	H$_2$ import ($1.38/kg) + RNG import ($7.48/MMBTU)	1.39	127.1	60.9%
	H$_2$ import ($1.38/kg) + RNG import ($12.00/MMBTU)	1.42		
	H$_2$ import ($4.50/kg) + RNG import ($29.44/MMBTU)	2.43		
3.1.5	H$_2$ import ($1.38/kg) + electricity import ($0.02/kWh)	1.38	121.0	57.9%
	H$_2$ import ($4.50/kg) + electricity import ($0.10/kWh)	2.30		
3.1.6	H$_2$ ($1.38/kg) + electricity ($0.02/kWh) + RNG ($7.48/MMBTU)	1.36	127.1	60.9%
	H$_2$ ($1.38/kg) + electricity ($0.02/kWh) + RNG ($12.00/MMBTU)	1.38		
	H$_2$ ($4.50/kg) + electricity ($0.10/kWh) + RNG ($29.44/MMBTU)	2.36		

Case 3.1 results are also represented in Figure 22. For each scenario, the MESP was plotted with bars indicating the change in MESP due to cost sensitivity analysis. From Cases 3.1.1 to 3.1.6, the carbon efficiency tends to trend upward, with a slight decrease in Case 3.1.5. This is because a portion of biomass-derived syngas is diverted to support heat in Case 3.1.5, decreasing the carbon efficiency observed in Case 3.1.4 by about 3%.
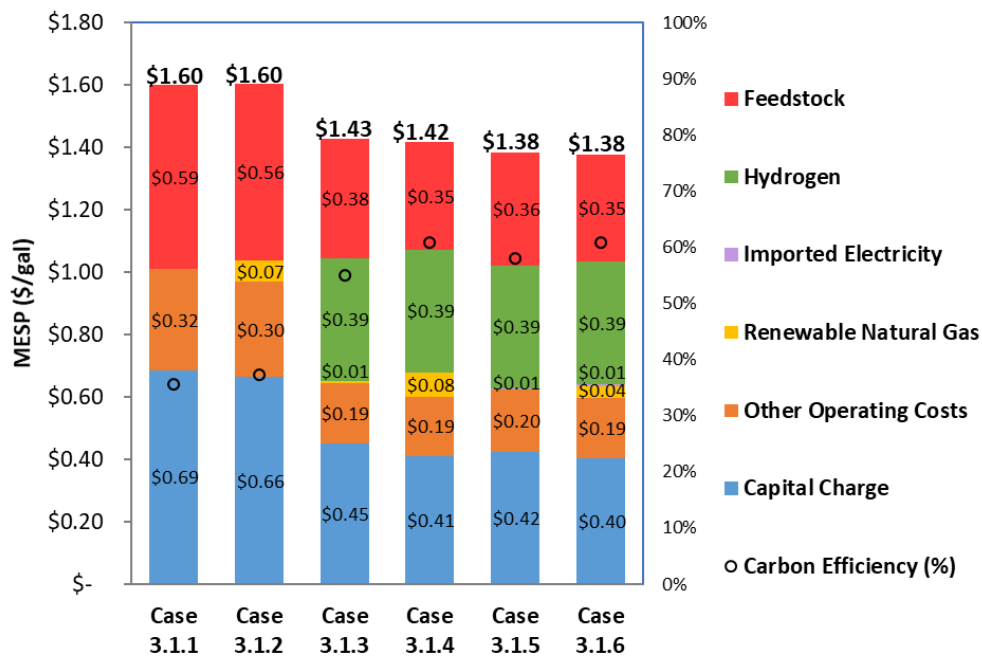
Figure 22. Graphical representation of Case 3.1 TEA results: breakdown of MESP

Further analysis was conducted to identify the impact of renewable resource cost on the MESP of ethanol. Figure 23 highlights each sensitivity case. Scenarios with multiple renewable imports were broken down into sub-cases (e.g., 3.1.4a and 3.1.4b) to investigate the effect of manipulating one or multiple sensitivity variables at a time. The cost of RNG was studied from multiple feedstocks, as discussed in Section 2.1; these cases are shown in blue. The plotted error bars indicate the minimum or maximum cost for each resource. Each scenario from 3.1.1–3.1.6 showed high sensitivity to the cost of renewable H_2 and very low sensitivity to the cost of RNG.
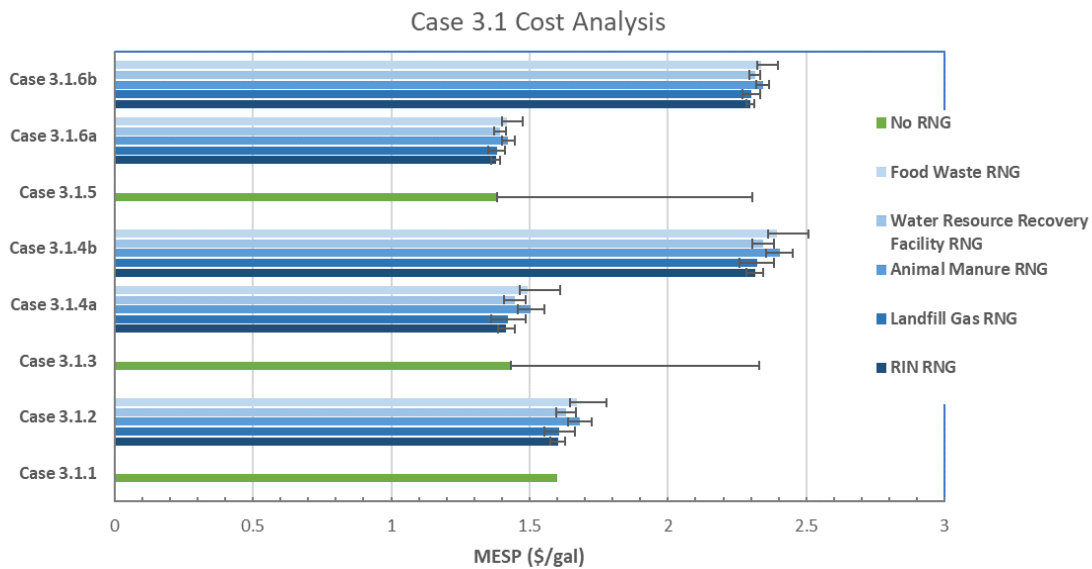
Figure 23. Detailed cost sensitivity analysis for Case 3.1

Another key process metric investigated for Case 3.1 was energy efficiency. Energy efficiency was calculated as ratio of the total energy out of the process as ethanol to the sum of all energy inputs (biomass, H_2, RNG, and electricity). As indicated in Figure 24, energy efficiency increases in each sequential scenario, corresponding with increasing carbon efficiency in each scenario as well. The key contributors to energy efficiency are also broken down in Figure 24 with the biomass feedstock contributing the largest percentage in every scenario.
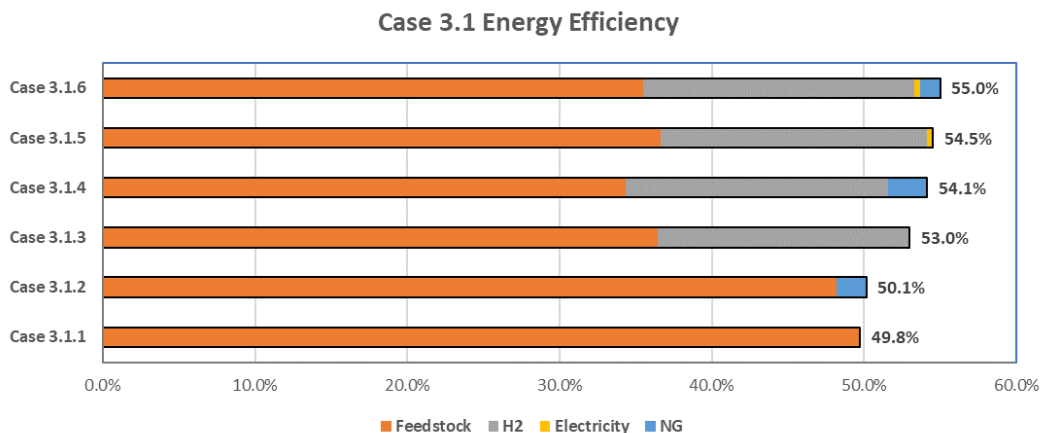
Figure 24. Case 3.1 energy efficiency summary

Case 3.1.3 represents a maximum achievable yield process where 90% of both CO and CO_2 are converted to ethanol through the stoichiometric import of renewable H_2. Additional cases were run to determine the consequence of decreasing CO_2 conversion, lowering the H_2 demand and the carbon efficiency simultaneously. The results of this study are shown in Figure 25 with MESP, carbon efficiency, and energy efficiency plotted as a function of H_2:C molar ratio at H_2 cost scenarios. The molar flow of H_2 is the sum of existing biomass-derived H_2 and imported renewable H_2.
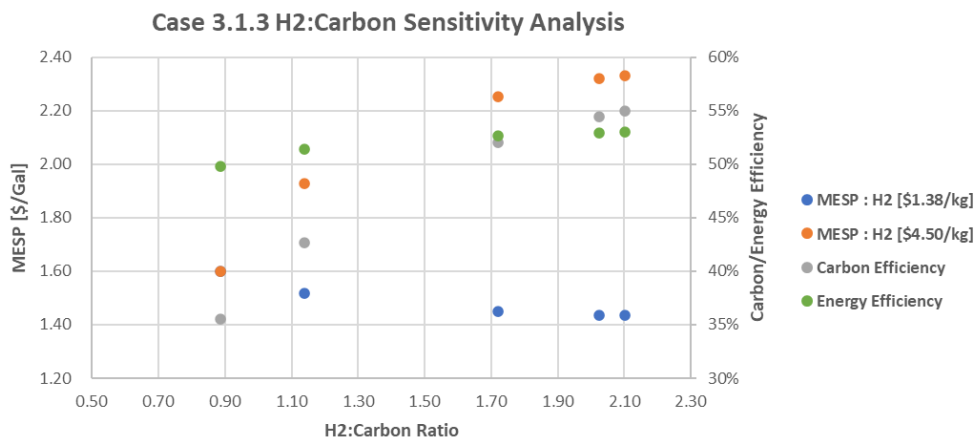
Figure 25. Effect of varying H_2:C ratio into fermenter on MESP, carbon efficiency, and energy efficiency

Increasing H_2:C ratio corresponds to significant increases in carbon efficiency and slight increases in energy efficiency. The results of this analysis also indicate that for higher-cost H_2 ($4.50/kg H_2), the increase in production does not offset the increase in operating expenses due to H_2 import. However, for a lower-cost scenario ($1.38/kg H_2), the import of H_2 is offset by the increase in ethanol production. Therefore, if the import of renewable H_2 is also supported by favorable LCA results and low-cost H_2 is readily available, this modification may be an effort worth further experimental investigation.

TEA Results for Case 3.2

Using a 10% discount rate, the MESP with CO_2 upgrading processes can be estimated similar to previous TEA approaches [42, 43]. MESP is presented using electrolysis cost, variable operating costs, fixed operating costs, capital depreciation, average income tax, and average return on investment, shown in Table 18 and Figure 26. Note that without CO_2 upgrading, annual ethanol production is about 39 MMgal/yr. Thus, the reported production in Table 18 includes both sugar- and CO_2-derived ethanol productions.

With state-of-technology (SOT) technical parameters and an electricity price of $0.0682/kWh, all three CO_2 upgrading cases are calculated to have relatively higher MESPs (Table 18). Specifically, under SOT conditions, Case 3.2.1 exhibits the highest MESP ($9.96/gge at $0.068/kWh) among the three cases due to low single-pass carbon efficiency with H_2 input (using Equation 6) and high CO_2 separation/recycle stream. Calculated MESP of Case 3.2.2 ($7.26/gge at $0.068/kWh) is slightly lower than Case 3.2.1 due to lower CO_2

separation/recycle stream as all the CO_2 stream flows into a CO_2 electrolyzer, as shown in Equation 7. Case 3.2.3 shows the lowest MESP ($6.50/gge at $0.0682/kWh) due to the highest theoretical single-pass carbon efficiency (100% as shown in Equation 8) with lowest CO_2 separation/recycle stream. Both annual ethanol production (million gallons per year) and carbon efficiencies are also listed in Table 18. Low electricity prices could reduce the MESP to $3.05/gge for Case 3.2.3.

Table 18. Summary of Case 3.2 TEA results

Case			MESP ($/gallon)	MESP ($/gge)	Production (MMgal/yr)	Carbon efficiency
3.2.1	Equation 6. 6 H_2 + 2 CO_2 →ethanol + 3 H_2O	Electricity – min ($0.020/kWh)	3.21	4.87	74.3	93.6%
		Electricity – baseline ($0.068/kWh)	6.55	9.96		
		Electricity – max ($0.100/kWh)	8.79	13.35		
3.2.2	Equation 7. 2 CO + 4 H_2→ ethanol+ H2O	Electricity – min ($0.020/kWh)	2.26	3.44	74.6	94.1%
		Electricity – baseline ($0.068/kWh)	4.78	7.26		
		Electricity – max ($0.100/kWh)	6.45	9.81		
3.2.3	Equation 8. 3 CO + 5 H_2 → Bacteria + 2 H_2O	Electricity – min ($0.020/kWh)	2.01	3.05	74.8	94.3%
		Electricity – baseline ($0.068/kWh)	4.27	6.50		
		Electricity – max ($0.100/kWh)	5.79	8.79		
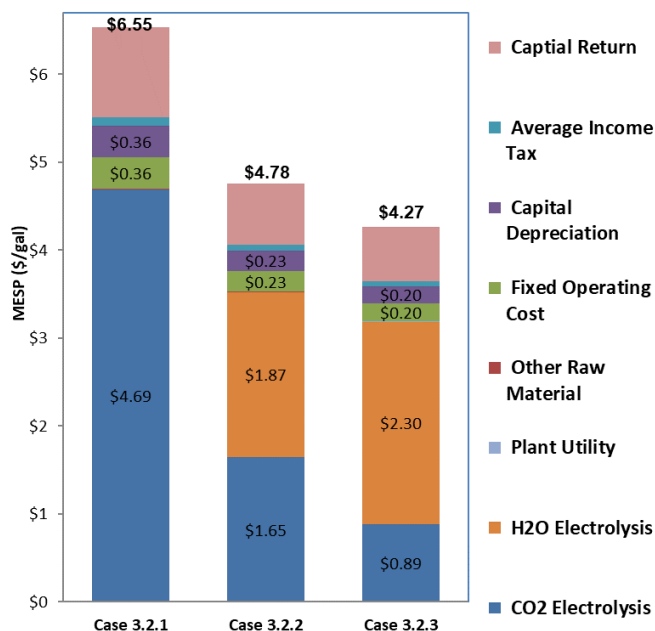
Figure 26. Cost breakdown of three scenarios

We performed sensitivity analysis for the three CO_2 upgrading cases to identify the cost drivers of the integrated waste CO_2 upgrading concept. The cost drivers are consistent for the three cases (i.e., price of electricity, electrolyzer onstream factor, and CO_2 single-pass conversion). Because Case 3.2.3 exhibits the lowest MESP with SOT assumptions, it is used as the benchmark. The resulting tornado chart is shown in Figure 27.
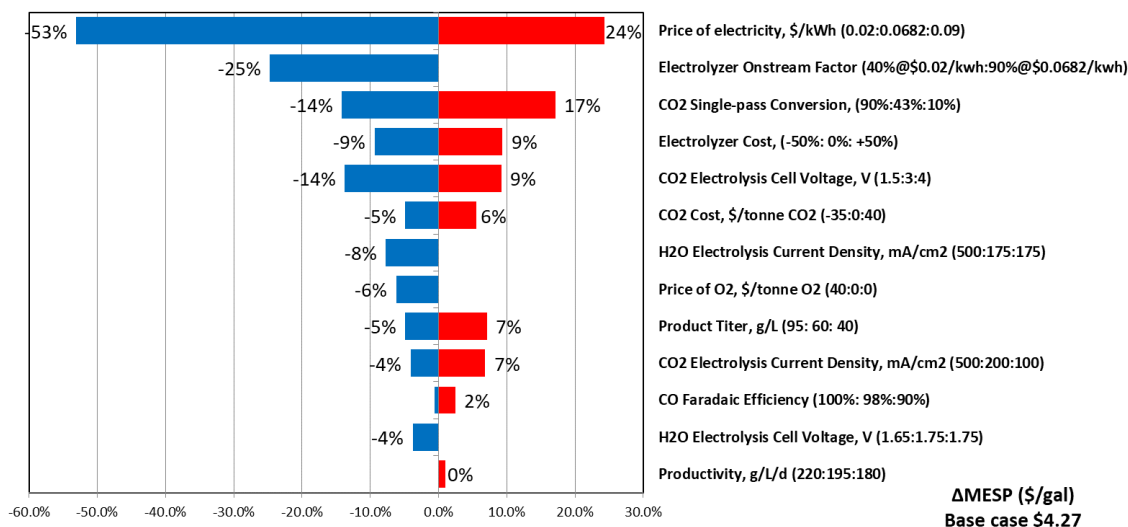
Figure 27. Tornado chart for CO_2 to ethanol using Case 3.2.3, with values of key parameters for cost penalties (red bars) and for cost benefits (blue bars)

The top five cost drivers are electricity price, electrolyzer onstream factor, CO_2 single-pass conversion, electrolyzer cost, and CO_2 electrolysis cell voltage for Case 3.2.3. The MESP is decreased to $3.05/gallon when electricity price is as low as $0.02/kWh [40]. Therefore, it is critical to have a sustained supply of low-cost electricity. Similarly, intermittent operation of electrolyzer with low-cost electrons (40% capacity, $0.02/kWh) reduces the MESP by 25%. These findings illustrate that the operating cost savings from low-cost electrons can offset the lack of production and charges incurred from capital costs. Improving the CO_2 single-pass conversion from current 43% to 90% results in a decrease in the MESP by 14% with less CO_2 separation and recycle. Current alkaline electrolyzer capital cost is $400/kW [39], and the MESP can decrease by 9% if the electrolyzer capital cost goes down from $400/kW to $200/kW. Reducing the cell voltage improves cost by reducing the electricity demand. MESP reduces by 14% when the applied voltage decreases from 3.0 V to 1.5 V [44].

The rest of studied metrics still impact MESP, but to a lesser extent. For instance, for the gas fermentation process, MESP varies within 3% with reported product titer ranges (40–95 g/L) [45]. Finally, as the demonstrated productivity is as high as 195 g/L/d [46], MESP varies within 1% over the reported range of the productivities (180–220 g/L/d) [45]. As a result, for the integrated waste CO_2 upgrading concept, technical metrics of the gas fermentation step have little overall effect on the process economics and our focus needs to primarily be on effective electron utilization.

Strategies To Achieve Cost Competitiveness

Because the addition of CO_2 upgrading results in a higher MESP ($4.27/gallon) than the current market price of fuel ethanol, improvements on electrolysis technology would be needed to increase the economic competitiveness. To answer the question of under what conditions

could CO_2 upgrading improve the economics of existing corn ethanol biorefineries, key metrics with proposed future parameters are compared with SOT values in Table 19.

The MESP for the future case is calculated at $1.39/gallon, implying a potential for cost competitiveness (Figure 28). The critical process metrics to realize the economic benefits include electricity price, single-pass CO_2 conversion, electrolyzer cost, and CO_2 electrolysis cell voltage. In locations with abundant wind and solar sources, discounted and in some cases negative energy prices due to curtailment [47] present an opportunity for the electroreduction of CO_2 to be economically viable in the future. Optimizing the reactor configuration can help increase single-pass CO_2 conversion efficiency. Continuous "flow-cell" membrane-electrode-assembly configurations that leverage specialized gas-diffusion electrodes show promise for scale-up. For electrolyzer cost, previous studies [48, 49] show that the stack is the largest contributor, and ongoing catalyst work can help decrease both the electrolyzer cost and the overall cell voltage needed.

Table 19. CO_2 upgrading system SOT and future scenarios

Parameters	SOT	Future
CO_2 electrolysis cell voltage	3.0 V	2.0 V [44]
CO_2 electrolysis current density	250 mA/cm^2	500 mA/cm^2 [50]
CO electrolyzer cost (uninstalled)	$600/kWh	$200/kWh [39]
CO faradaic efficiency	98%	98% [51]
Electrolyzer single-pass CO_2 conversion	20%	50% [52]
H_2O electrolysis cell voltage	1.75 V	1.65 V [39]
H_2O electrolysis current density	175 mA/cm^2	200 mA/cm^2 [39]
H_2O electrolyzer cost (uninstalled)	$400/kWh	$200/kWh [39]
Price of electricity	$0.0682/kWh	$0.02/kWh [40]
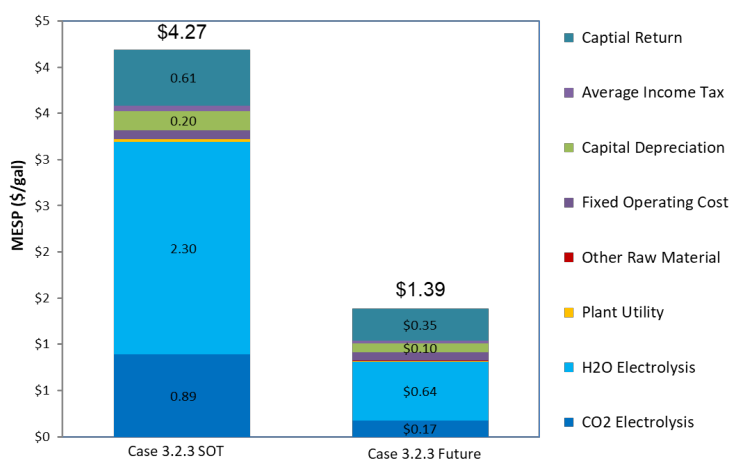
Figure 28. MESP for the base case, SOT, and future scenario with CO_2 conversion

Comparative Discussions on Case 3.1 and Case 3.2

TEA for Case 3.1 indicates low-cost production of ethanol at $1.60/gallon ethanol in the baseline scenario with the potential to reduce the MESP to as low as $1.36/gallon. However,

gasification technologies are inhibited by carbon loss to tars and chars, which are combusted for process heating, and carbon is ultimately lost as CO_2 in a flue gas stream. Even with high carbon conversion in the fermentation step, this study finds a maximum carbon efficiency of about 61%. Comparatively, Case 3.2 capitalizes on the readily available and high-purity CO_2 streams from corn dry mill facilities and reincorporates the otherwise "waste" carbon to achieve very high carbon efficiencies (on the order of 94%). The high carbon efficiency comes at high MESP, with the Case 3.2 SOT cases ranging from \$4.27–\$6.55/gallon ethanol. High MESP for Case 3.2 stems from low technology readiness level (TRL) (~4) of CO_2 electrolysis to CO and large H_2 and electricity demand.

Case 3.1 and Case 3.2 exhibit trade-offs in cost and carbon efficiency metrics. Both pathways are highly dependent on external factors such as renewable H_2 and renewable electricity. Therefore, for both scenarios, careful consideration of cost fluctuations and availability intermittency of these resources is required. Case 3.1 utilizes technologies with comparatively higher TRL than Case 3.2, suggesting an easier path to near-term commercialization. However, Case 3.2 presents attractive environmental benefits, and analysis on future scenarios suggests that competitive MESPs (\$1.39/gallon) can be achieved given enough technological development.

3.3.4 Key Learnings

Key Learnings – TEA

- Biomass-derived ethanol, such as that discussed in Case 3.1, has technological potential for near-term deployment. Current market emphasis on cost over environmental factors benefit biomass-derived ethanol in that the relatively lower carbon efficiency may be tolerated as a result.
- CO_2 to ethanol studied in Case 3.2 requires technological development to increase process efficiency and decrease the size and cost of the CO_2 electrolysis process. Potentially very high carbon efficiencies and the utilization of CO_2 as a waste-to-energy feedstock, however, could act as a driving force to continue developmental efforts of this technology.
- Cases 3.1 and 3.2 also highlight the importance of considering the potential for improving on key metrics while simultaneously considering the barriers associated with those changes. Some barriers illuminated from these efforts include time for development, reliance on external factors (such as renewable electricity intermittency), and market forces.

Key Learnings – LCA

- Biomass-derived ethanol via gasification and gas fermentation using conventional energy inputs can achieve 89% of life cycle GHG emissions reduction compared to

petroleum gasoline (91 gCO$_2$e/MJ), which can be a near-term GHG emission mitigation approach.

- CO$_2$ from biomass gasification can be further converted into ethanol with the help of H$_2$. This can increase the yield of ethanol production, which leads to reducing the feedstock stage emissions burdens per MJ basis. However, in order to reduce the CI during the conversion process, it is essential to use green hydrogen based on renewable electricity.

- With the current energy systems (e.g., U.S. electricity mix and H$_2$ from NG SMR), CO$_2$-derived ethanol does not provide any GHG emissions reduction benefits because the pathways require significant amounts of electricity and/or H$_2$ inputs.

- However, CO$_2$-derived ethanol shows substantial GHG emissions reduction potential through decarbonized electricity and H$_2$. By using renewable electricity and renewable H$_2$, CO$_2$-derived ethanol becomes net-zero-carbon fuel, which can be a long-term GHG mitigation strategy.

3.4 Case 4 – Carbon Conversion to Methanol and High-Octane Gasoline (HOG)

3.4.1 Process Design

This section considers three sustainable methanol synthesis pathways: biomass gasification to methanol, indirect conversion of CO$_2$ to methanol via a CO intermediate, and direct conversion of CO$_2$ to methanol via electrolysis. The three methanol pathways are also presented in a recent publication [53]. A fourth pathway is also considered in which further processing steps are added to the biomass gasification to methanol pathway to produce a high-octane gasoline product. Each pathway was modeled in Aspen Plus V10 and utilized the economic assumptions presented in Section 2.1. Further details of the conceptual process designs are included below.

Case 4.1 – Biomass to Methanol

In the biomass to methanol design [9, 11] (Figure 29), biomass is converted to syngas via indirect gasification and syngas is catalytically converted to methanol. Biomass was assumed to be 50% clean pine and 50% forest residues and fed at a rate of 2,000 dry MT per day.

Through gasification, the biomass deconstructs to syngas (CO, CO$_2$, H$_2$), tars, and chars. Tars and chars are combusted as the primary source of heat for the gasifier, which is operated at 1,595°F (867°C) and 2.4 atm, and syngas is routed to a gas cleanup and quench step. A portion of the syngas is diverted from the process stream and combusted to provide heat and power. Following gas cleanup, the syngas is sent to an acid gas removal unit, where CO$_2$ concentration in the syngas is limited to about 5%. Methanol synthesis is then operated isothermally at 482°F

(250°C) and 49.7 atm over a commercial copper/zinc oxide/alumina catalyst [11]. Methanol is condensed and separated from the unreacted gases, which are recycled to the synthesis reactor (Figure 29). The biomass to methanol case also investigated three scenarios, detailed in the following subsections.
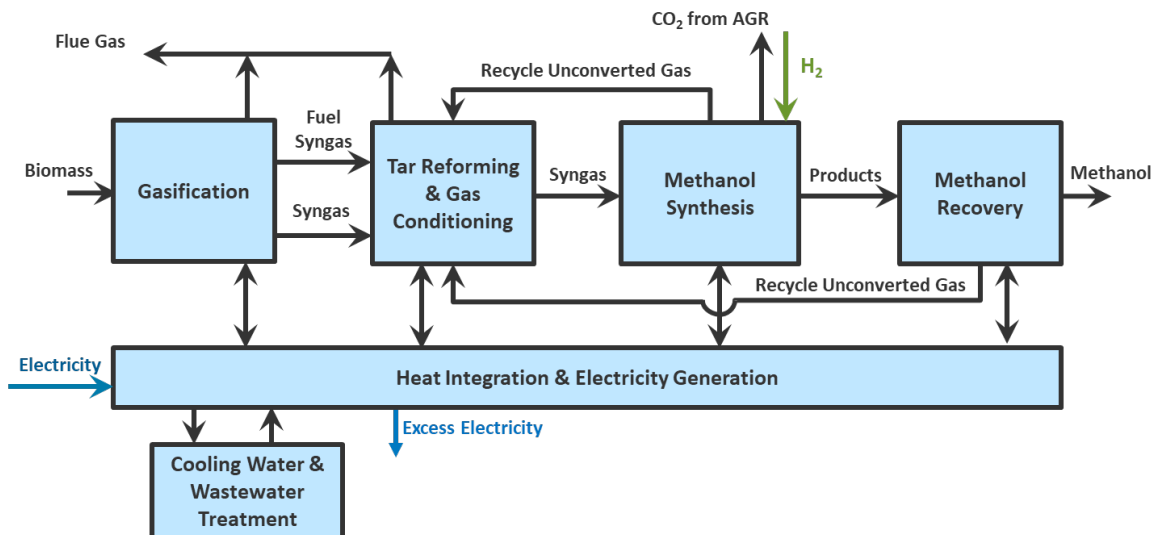
Figure 29. Block flow diagram of biomass to methanol via syngas benchmark scenario, Case 4.1

Case 4.1.1 Benchmark

The metrics for benchmark to produce methanol via lignocellulosic biomass were derived from National Renewable Energy Laboratory reports [54, 55]. The key metrics set in the benchmark scenario and held constant in other scenarios are collected in Table 20.

Table 20. Biomass to methanol key metrics

Metric	Assumed Value	Ref.
Feedstock		
Type	Biomass: 50% clean pine, 50% forest residues	[55]
Cost	$60.58/dry U.S. ton	[55]
Feed rate	2,000 dry tonnes/day	[54]
Gasification		
Temperature	1,595°F (867°C)	[54]
Pressure	2.4 atm	[54]
Tar Reforming		
Temperature	1,605°F (874°C)	[54]
Pressure	1.95 atm	[54]
Methanol Synthesis		
Temperature	437°F (250°C)	[54]
Pressure	49.7 atm	[54]
Methanol De-Gassing and Recovery		
Crude methanol purity (mol%)	97.0%	[54]
Methanol product purity (mol%)	99.4%	[54]

Case 4.1.2 – Renewable Electricity Import

In the benchmark case, biomass syngas is diverted from methanol synthesis to provide fuel to the combined heat and power system, which generates enough power for the entire plant (i.e., net power import/export = 0). The renewable electricity case minimizes the diversion of biomass syngas by diverting only enough syngas to meet the heat requirements of the plant. The resulting power demand is supplemented by the renewable electricity grid.

Case 4.1.3 – Renewable H_2 Import and CO_2 Utilization

Syngas derived from biomass contains significant amounts of CO_2, which is typically removed from the syngas stream before methanol synthesis via an acid gas removal step. This scenario reincorporated CO_2, which is typically lost to the atmosphere by importing renewable H_2 and implementing a reverse water gas shift step described by Equation 11.

$$CO_2 + H_2 \rightarrow CO + H_2O \qquad \text{(Equation 11)}$$

Case 4.2 – Indirect CO_2 to Methanol via Syngas Intermediate

Indirect CO_2 to methanol uses a hybrid approach of low-temperature CO_2 electrolysis combined with conventional methanol synthesis (Figure 30). Each model was scaled to have annual methanol production of about 96 million gallons. Under the SOT conditions [56], CO_2 is reduced over a carbon-nanotube-doped Ag electrocatalyst reaching a faradaic efficiency and whole cell voltage of 98% and 3 V, respectively. A future scenario considers technical improvements including reduced cell voltage to 2 V and a faradaic efficiency of 95%. In both cases, renewable H_2 produced from polymer electrolyte membrane H_2O electrolysis [57] is imported and mixed with the CO to create a syngas mixture, which then undergoes traditional methanol synthesis and purification as described in Case 4.1. In addition to the SOT and conceptual future case, additional scenarios were run under SOT conditions investigating the effect of H_2:CO ratio in the methanol synthesis loop. The three sub-scenarios highlighted in this analysis are under SOT conditions with H_2:CO ratios of 1 (Case 4.2.1), 1.6 (Case 4.2.2), and 2 (Case 4.2.3). Key assumptions for Case 4.2 design parameters are highlighted in Table 21.

Table 21. Key metrics for CO_2-to-CO and H_2O electrolysis

Pathway/Metric	Assumed Value	Ref.
CO_2-to-CO electrolysis		
Cell voltage (V)	3.0	[56]
Faradaic efficiency (%)	98.0	[56]
Current density (mA/cm^2)	350.0	[56]
Polymer electrolyte membrane H_2O electrolysis		
Cell voltage (V)	2.0	[57]
Faradaic efficiency (%)	99.0	[57]
Current density (mA/cm^2)	1600.0	[57]
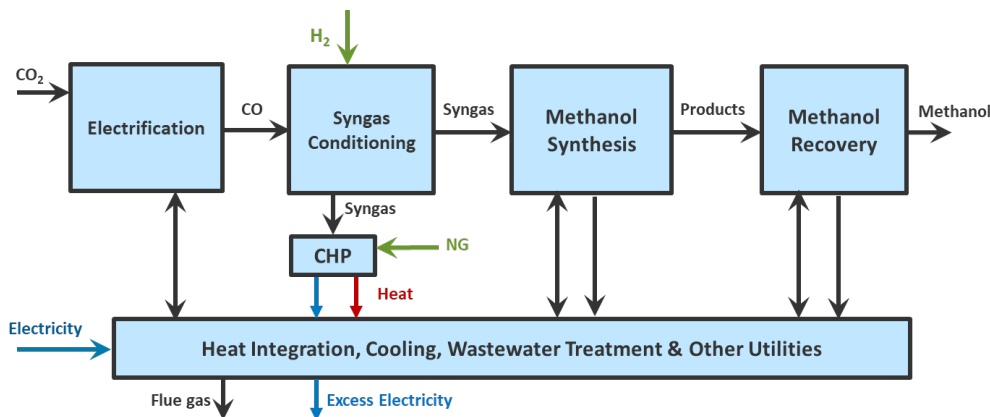
Figure 30. Block flow diagram of indirect CO_2-to-methanol, Case 4.2, H_2:CO ratio = 2

Case 4.3 – Direct CO_2-to-Methanol Electrolysis

In the direct CO_2-to-methanol electrolysis pathway shown in Figure 31, CO_2 is reduced to methanol in a single step over a copper selenide electrocatalyst. A summary of key process metrics is included in Table 22. At near-ambient reaction conditions, current SOT studies (Case 4.3.1) have reported faradaic efficiencies of over 77% at cell voltages of 2.67 V, reaching total current densities of 41.5 mA/cm^2 [58]. Reported byproducts during methanol synthesis include H_2, CO, and HCOOH, which are subsequently purified via pressure swing adsorption and distillation stages and recovered for sale. Like the electrosynthesis of CO noted in Case 4.2, direct methanol synthesis is an emerging immature technology that is likely to benefit from future R&D. Consequently, we also consider a future scenario (Case 4.3.2) that accounts for technological improvements, reaching faradaic efficiencies of 95%, cell voltage of 1.8 V, and current density of 1,500 mA/cm^2.

Table 22. Key metrics for CO_2-to-methanol electrolysis

Pathway/Metric	Assumed Value	Ref.
Cell voltage (V)	2.7	[58]
Faradaic efficiency (%)	77.8	[58]
Current density (mA/cm^2)	41.5	[58]
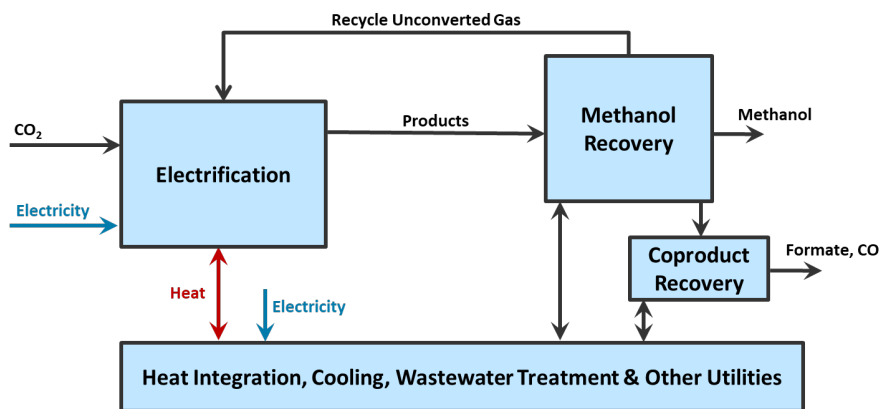
Figure 31. Block flow diagram of direct CO_2-to-methanol, Case 4.3

Case 4.4 – Biomass to HOG

In the biomass to HOG pathway (Figure 32), lignocellulosic biomass is indirectly gasified to syngas, and syngas is converted to methanol under the same assumptions provided in Case 4.1 (biomass to methanol). Following methanol synthesis, methanol undergoes a dehydration reaction to dimethyl ether (DME) over a gamma-alumina catalyst at 482°F (250°C) and 9.5 atm. DME is fed to a reactor containing the National Renewable Energy Laboratory's CuBEA zeolite catalyst at an inlet temperature and pressure of 355°F (179°C) and 8.8 atm. A high-level process flow diagram is shown in Figure 32. Single-pass conversion and product selectivity of DME to HOG were held constant in each scenario and are compiled in Table 23. Further detail on all process design assumptions are detailed in the National Renewable Energy Laboratory's 2019 SOT report [55] under the 2022 assumptions. Additional scenarios conducted on the biomass to HOG pathway are consistent with those described in Case 4.1 and include a benchmark (Case 4.4.1), a renewable electricity import scenario (Case 4.4.2), and a renewable H_2 import for CO_2 utilization scenario (Case 4.4.3).

Table 23. Key metrics for DME to HOG conversion

Process Parameter	2022 Projection [55]
Hydrocarbon synthesis reactor temperature	225°C
Single-pass DME conversion	40.0%
Productivity of hydrocarbon synthesis catalysis (kg/kg-cat/h)	0.10 (total)
Carbon selectivity to C5+ product	58%
Carbon selectivity to aromatics	0.5% aromatics (0.5% Hexamethylbenzene)
H_2 addition to hydrocarbon synthesis	Yes
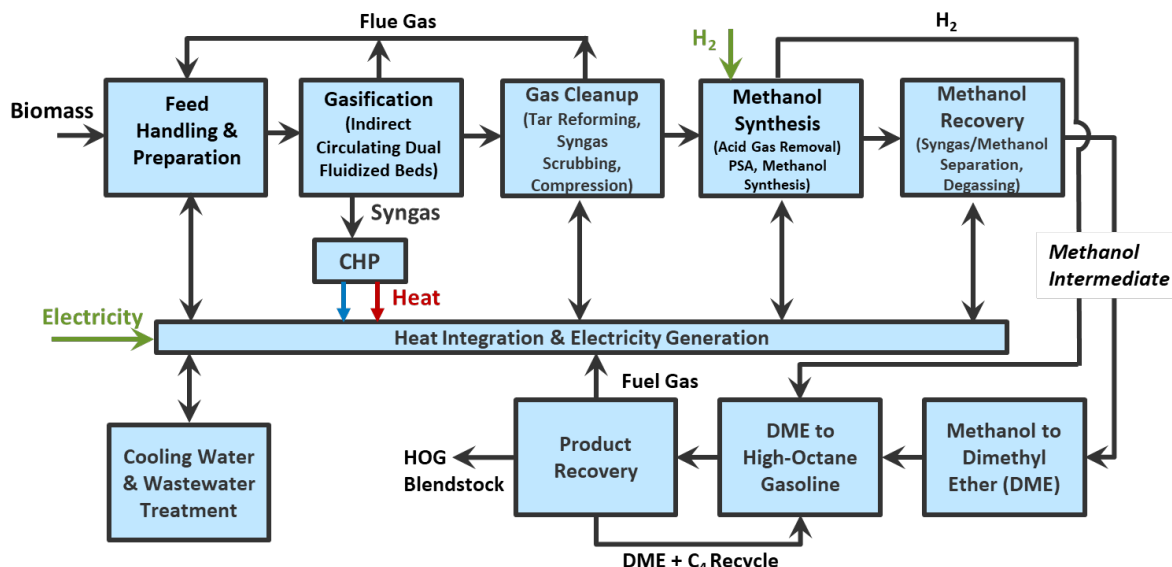
Figure 32. Block flow diagram of biomass to HOG, Case 4.4

3.4.2 LCA Results and Discussions

LCA Cases and Inventories

Case 4 generates methanol from biomass or waste CO_2 (Figure 33). There are three sub-cases: biomass-derived methanol via gasification and methanol synthesis, and two CO_2-derived methanol production technologies (i.e., indirect and direct conversion processes). Biomass feedstock consists of 50% clean pine and 50% forest residues (by mass). For clean pine, the supply chain starts with clean pine production, followed by harvesting and collection, whereas forest residues are considered as waste, which only accounts for the collection stage in the feedstock production stage. Collected biomass feedstock is transported to a methanol plant by truck [13], and then electricity is used for depot preprocessing of the feedstock for moving, drying, grinding, and dust collection [32]. For CO_2-to-methanol, we assumed using on-site separated CO_2; no CO_2 transmission processes are considered.

1) Biomass feedstock to methanol

- **Biomass feedstock**:
  50 wt.% forest residue
  50 wt.% clean pine
- **Methanol production:**
  Woody biomass-to-methanol via
  gasification and methanol synthesis

2) Waste CO_2 to methanol (Indirect)

- **CO_2 feedstock:**
  high-purity waste CO_2
  from bio-refinery
- **Methanol production:**
  Waste CO_2 to syngas
  conversion and syngas to
  methanol conversion

3) Waste CO_2 to methanol (Direct)

- **CO_2 feedstock:**
  high-purity waste CO_2
  from bio-refinery
- **Methanol production:**
  Waste CO_2 to methanol
  conversion

Figure 33. The system boundaries of LCA of methanol production (Case 4.1 and Case 4.2), which includes feedstock production and transportation, methanol production, fuel transportation, and fuel combustion using two feedstocks (biomass and waste CO_2). For CO_2-derived methanol, two conversion technologies (indirect and direct) are considered.

For the indirect CO_2-to-methanol cases, CO_2 and H_2O (or H_2) is converted into syngas composed of CO and H_2, which is then synthesized into methanol. Because H_2:CO ratios highly influence the conversion process, we considered three H_2:CO ratios varying from 1 to 2. As the H_2:CO ratio increases, the amount of CO required to produce 1 MJ of methanol decreases, resulting in a reduction of electricity (for CO electrolysis) and CO_2 feedstock inputs. Instead, the NG inputs increase, used for the combustor for boosting a reaction.

Unlike the indirect methanol production, the direct CO_2-to-methanol produces methanol by reacting CO_2 and H_2 with much more NG inputs to boost a reaction. We analyzed two conditions—SOT and future—according to the technology level in 2018 and expected in 2030. With the technological improvement in 2030, the future case has a lower CO2 input and lower electricity and NG inputs than those of the SOT case. Note that electricity for the direct cases in Table 24 is used both for CO and H_2 production. For the direct cases, NG requirement is up to 56 times higher compared to the indirect cases to support heat for methanol synthesis.

Table 24. Life cycle inventory of Case 4: biomass-to-methanol and CO_2-to-methanol pathways

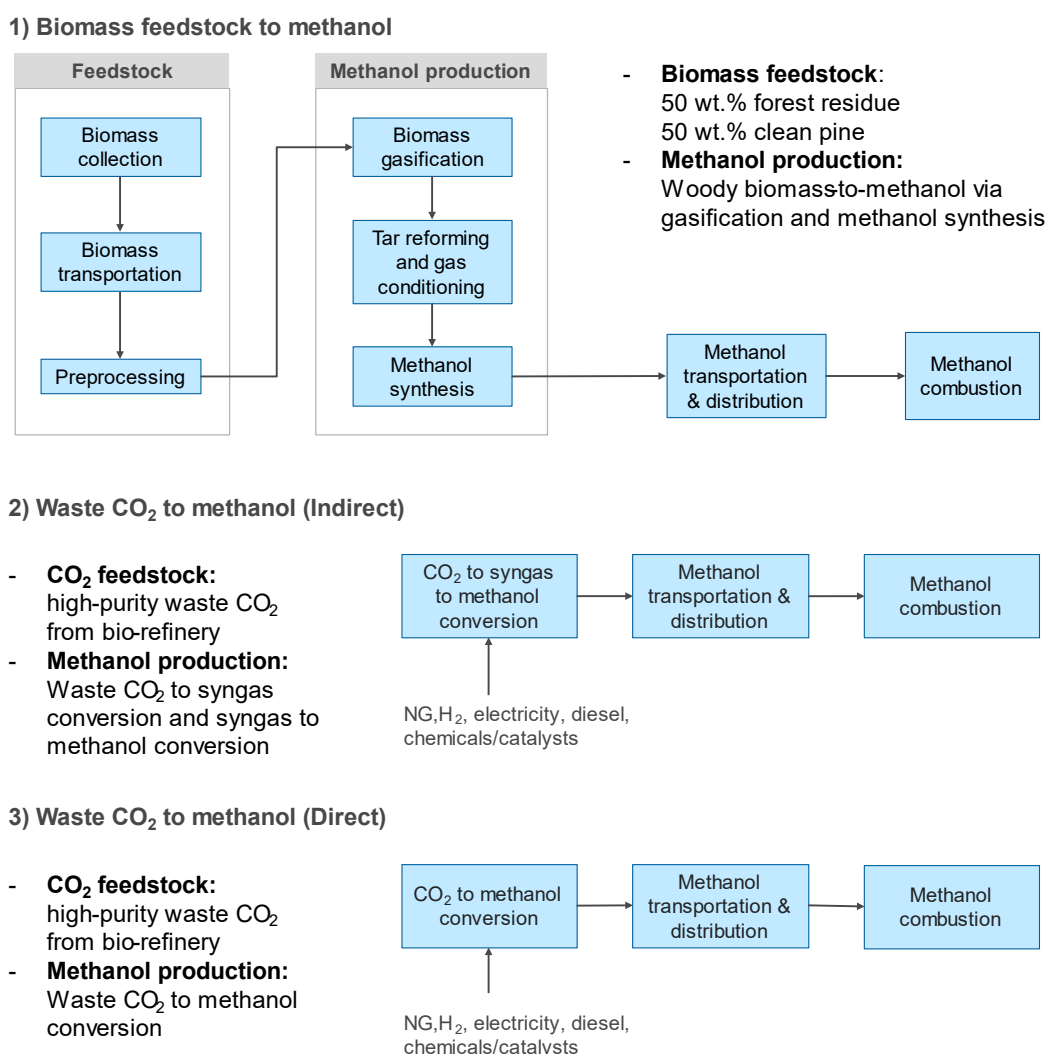| Per MJ of methanol	Biomass-to-methanol: Case 4.1			CO_2-to-methanol: Cases 4.2 and 4.3				
	Case 4.1.1	Case 4.1.2	Case 4.1.3	Indirect			Direct	
				Case 4.2.1	Case 4.2.2	Case 4.2.3	Case 4.3.1	Case 4.3.2
Feedstocks								
Blended woody (afdw kg)	0.114	0.081	0.105					
CO_2 (g)				158.2	93.7	75.8	82.2	76.1
Energy inputs								
Electricity (kWh)	0	0.0097	0	0.59	0.35	0.28	0.89	0.47
H_2 (MJ)	0	0	0.30	0.87	0.83	0.83		
NG (MJ)				0	0.05	0.06	0.28	0.20
Diesel (MJ)	0.002	0.002	0.002	0.002	0.002	0.002		
Chemicals/catalysts (g)	0.47	0.26	0.40	0.011	0.003	0.004		
Water (gallon)	0.021	0.012	0.018	0.033	0.033	0.033	0.024	0.023

Like previous cases, two conditions in Table 4 (conventional and renewable scenarios) are considered for external energy inputs (electricity, H_2, and NG). Once methanol is produced, it is transported and distributed to end applications as in GREET [6]. Note that methanol can be further processed to become HOG through additional processes. As shown in Figure 34, methanol dehydration and DME to HOG conversion processes are added to biomass to methanol pathways for Case 4.4.

Table 25 shows the life cycle inventory of biomass to HOG pathways. Compared to Case 4.1, Case 4.4 requires more feedstocks and energy/material inputs due to additional processes. In Case 4.4.1, heat and power are internally supplied by using biomass feedstocks, whereas imported electricity provides power demand for the plant in Case 4.4.2. In Case 4.4.3, imported H_2 and waste CO_2 from the syngas are converted into additional methanol. Additional methanol is converted into HOG, so Case 4.4.3 has the highest yield and the lowest required feedstock inputs.

Biomass feedstock to HOG
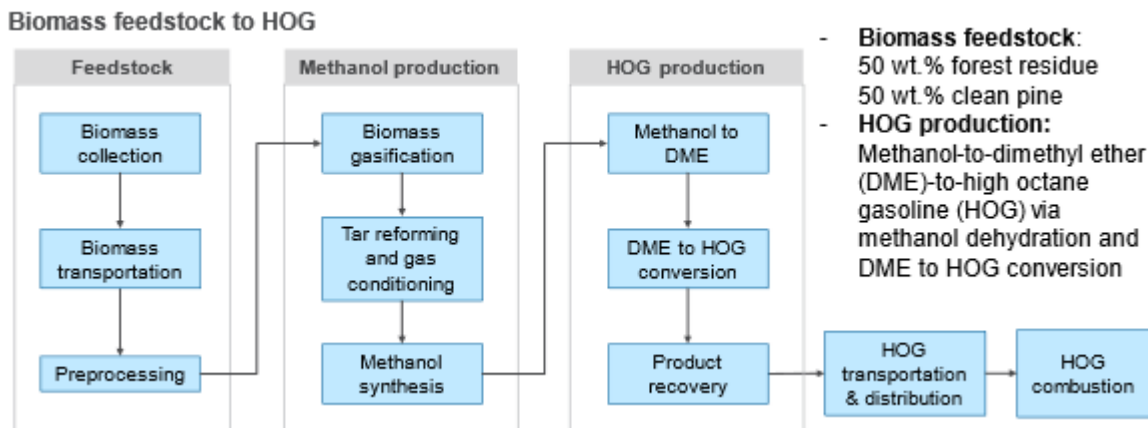
Figure 34. The system boundary of LCA of Case 4.4, which includes feedstock production and transportation, methanol production, HOG production, fuel transportation, and fuel combustion

Table 25. Life cycle inventory of Case 4.4: biomass-to-HOG pathways

Per MJ of HOG	Biomass-to-HOG: Case 4.4		
	Case 4.4.1	Case 4.4.2	Case 4.4.3
Feedstocks			
Blended woody (afdw kg)	0.135	0.124	0.102
Energy inputs			
Electricity (kWh)	0	0.0109	0
H_2 (MJ)	0	0	0.41
Diesel (MJ)	0.002	0.002	0.002
Chemicals/catalysts (g)	0.54	0.5	0.35
Water (gallon)	0.023	0.021	0.014

LCA Results

The CI of the baseline biomass-derived methanol production case using conventional energy sources (Case 4.1.1) is estimated at 18.3 gCO_2e/MJ, which is 80% lower than that of the CI of conventional fossil methanol (94 gCO_2e/MJ), mainly due to biogenic carbon uptake (Figure 35). In addition, Case 4.1.1 mostly relies on the energy in biomass not requiring external energy inputs other than biomass feedstocks, which does incur only biomass production-related emissions (15.9 gCO_2e/MJ). Case 4.1.2 uses external electricity, which brings an additional 4.7 gCO_2e/MJ. Instead, there is no biomass required for power generation, so feedstock inputs decreased slightly, and GHG emissions from the feedstock stage are reduced by 1.3 gCO_2e/MJ compared to Case 4.1.1. In Case 4.1.3, CO_2 emissions from biomass are used for additional methanol synthesis. Using imported H_2, we can produce 1.4 times more methanol from the same amount of biomass. However, the imported H_2 produced by fossil NG SMR leads to having an additional 28 gCO_2e/MJ. Thus, although feedstock production emissions are reduced, the overall CI of Case 4.1.3 with conventional scenario increases, becoming 40.8 gCO_2e/MJ. Note that this is still 56% lower than the life cycle GHG emissions of conventional fossil methanol production.
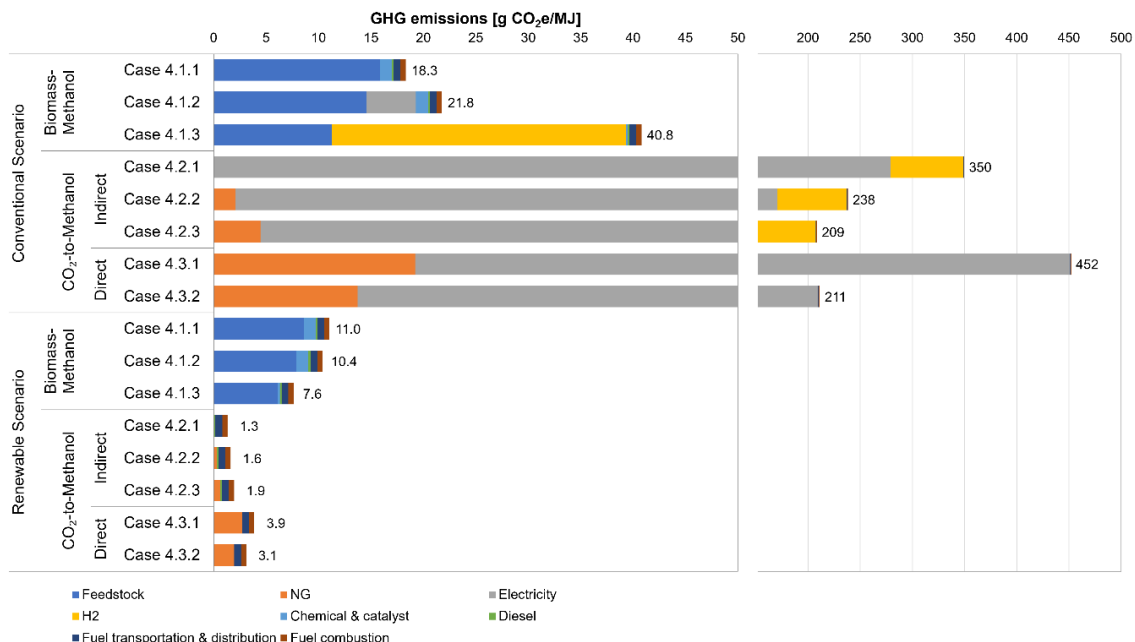
Figure 35. Life cycle GHG emissions (gCO₂e/MJ) of methanol production pathways from biomass and CO_2 via methanol synthesis using two scenarios (conventional/renewable)

Even though there are no feedstock-related GHG emissions for waste CO_2, the CO_2-to-methanol pathways with U.S. electricity mix, NG SMR H_2, and fossil NG significantly increase the CIs of methanol production due to their high energy requirements. For Cases 4.2.1–4.2.3, GHG emissions by electricity upstream is highest in Case 4.2.1, and GHG emissions by NG input is highest in Case 4.2.3, whereas H_2 inputs are similar among three cases. For Cases 4.3.1–4.3.2, energy efficiency improvement leads to the 53% of GHG emissions reduction by the lower electricity and NG inputs. In addition, the lower CI of electricity in 2030 (414 gCO₂e/kWh) from 2018 (483 gCO₂e/kWh) helps the GHG emissions reduction in the future case. Comparing the indirect and direct CO_2 to methanol production pathways, we found the latter case requires more NG input. Due to their high electricity and/or H_2 inputs, all CO_2-to-methanol cases have much higher CIs when conventional scenarios are considered, even compared to fossil methanol.

When we consider renewable electricity, 46% of GHG emissions from feedstock processes can be reduced for biomass-to-methanol cases. The CI of Case 4.1.1 of the renewable scenario is estimated at 11.0 gCO₂e/MJ, which is 88% lower than that of the conventional methanol production pathway (94 gCO₂e/MJ). Importing renewable electricity with zero CI can improve the yield and reduce the GHG emissions in Case 4.1.2. Case 4.1.3 has the lowest CI (7.6 gCO₂e/MJ) among the three biomass-to-methanol cases due to the highest yield and using renewable H_2 with zero CI. Therefore, the CIs of biomass-to-methanol (Cases 4.1.1–4.1.3) with renewable scenarios are 88%–92% lower than that of fossil methanol.

For CO_2-to-methanol cases, renewable scenarios present a significant reduction by eliminating upstream GHG emissions of energy sources (electricity, H_2, and NG). Because the

cases use waste CO_2 as feedstock, it does not involve feedstock production-related emissions. Thus, regardless of the conversion technologies, these cases can be near-zero-carbon fuels with the CIs ranging from 1.3–3.9 gCO_2e/MJ, which are 97–99% lower than the methanol from fossil NG. The remaining GHG emissions are caused by transportation and combustion of methanol and landfill-derived RNG.

Biomass-derived methanol with the renewable scenario can reduce GHGs up to 90% compared to conventional methanol. However, it is difficult to further reduce GHG emissions during biomass production and transportation. On the other hand, because CO_2-derived methanol production pathways require significant electricity, CO_2-derived methanol can become net-zero-carbon fuel (99% reduction) linked with renewable energy sources.

Figure 36 shows life cycle GHG emissions of biomass-derived HOG with the conventional and renewable scenarios. In Case 4.4, the conversion of methanol to HOG follows after the biomass-to-methanol process of Case 4.1. Due to the additional processes, feedstock, energy, and material consumptions for the plant increased, leading to an increase in CIs of 15%–30% compared to Case 4.1.

For conventional scenarios, the CI of baseline biomass-derived HOG (Case 4.4.1) is 76% reduced compared to the CI of conventional fossil HOG (E10) (92 gCO_2e/MJ). In Case 4.4.1, as the syngas generated from biomass feedstock is used to meet heat and power demand, there are no GHG emissions by external energy sources, and feedstock-related GHG emissions have the highest impact (18.7 gCO_2e/MJ). In Case 4.4.2, as U.S. grid mix electricity is used for electricity demand, GHG emissions by electricity increased by 5.3 gCO_2e/MJ. In Case 4.4.3, the increased yield due to CO_2 utilization leads to a reduction in GHG emissions from the feedstock stage, but the GHG emissions by H_2 production increase significantly (39.2 g CO_2e/MJ).

For the renewable scenarios, using renewable electricity for feedstock preprocessing led to a 46% reduction of GHG emissions during the feedstock-related stage. Therefore, the CIs of Cases 4.4.1, 4.4.2, and 4.4.3 decreased by 8.6, 13, and 46 gCO_2e/MJ, respectively, compared to those cases in the conventional scenario. Case 4.4.3 has the lowest CI (9.3 gCO_2e/MJ), which is 90% lower than that of conventional HOG (E10).
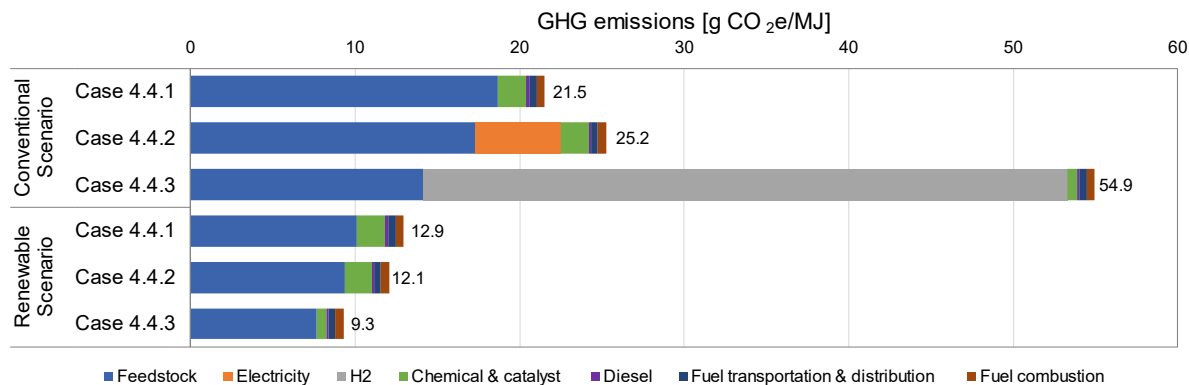
Figure 36. Life cycle GHG emissions (gCO_2e/MJ) of HOG production pathways (Case 4.4) from biomass using two scenarios (conventional and renewable)

3.4.3 TEA Results and Discussions on Key Metrics (Carbon Efficiency, Energy Efficiency, and Cost)

Methanol Minimum Selling Price (MSP) for Cases 4.1, 4.2, and 4.3

The TEA results for the renewable methanol pathways are summarized in Table 25. To the greatest extent possible, the TEA results and underlying assumptions presented in this work were held consistent with those presented elsewhere [53]. Notes are included within this work where differences exist.

The biomass gasification to methanol pathway achieves near-market costs with the MSP for the benchmark scenario of $0.39/kg. Cost reduction is achieved in both the renewable electricity scenario and the CO_2 utilization scenario when low-cost electricity and low-cost H_2 are utilized for each respective pathway. However, when high-cost renewable H_2 is utilized, the MSP of methanol increases from the benchmark case by 28% (to $0.50/kg). A summary of the cost contributions is included in Figure 37. The biomass feed rate in the biomass studies was fixed at 2,000 dry MT/day; therefore, MSP was primarily affected by total methanol yield and operating expenses. The productions in million gallons per year are also reported in Table 26.

Table 26. Summary of Case 4 TEA results

Case		Methanol MSP ($/kg) or MFSP for HOG ($/gge)	Production (MMgal/yr)	Carbon Efficiency
4.1.1	Benchmark, biomass to methanol, no external energy inputs	$0.39/kg	96.1	33.2%
4.1.2	Biomass to methanol, import renewable electricity	$0.36/kg	104.7	36.1%
4.1.3	Biomass to methanol, renewable H_2 import and CO_2 utilization	$0.35/kg	136.6	46.6%
4.2.1	Indirect CO_2-to-methanol via syngas, H_2:CO ratio = 1	$1.62/kg	95.8	43.8%
4.2.2	Indirect CO_2-to-methanol via syngas, H_2:CO ratio = 1.61	$1.05/kg	95.8	74.0%
4.2.3	Indirect CO_2-to-methanol via syngas, H_2:CO ratio = 2	$0.90/kg	95.8	91.5%
4.3.1	Direct CO_2-to-methanol, SOT	$12.74/kg	96.6	76.7%
4.3.2	Direct CO_2-to-methanol, future	$0.43/kg	97.0	94.7%
4.4.1	Benchmark, biomass to HOG, no external energy inputs	$3.29/gge	40.8	28.1%
4.4.2	Biomass to HOG, import renewable electricity	$3.09/gge	44.2	30.4%
4.4.3	Biomass to HOG, renewable H_2 import and CO_2 utilization	$3.17/gge	53.9	37.1%
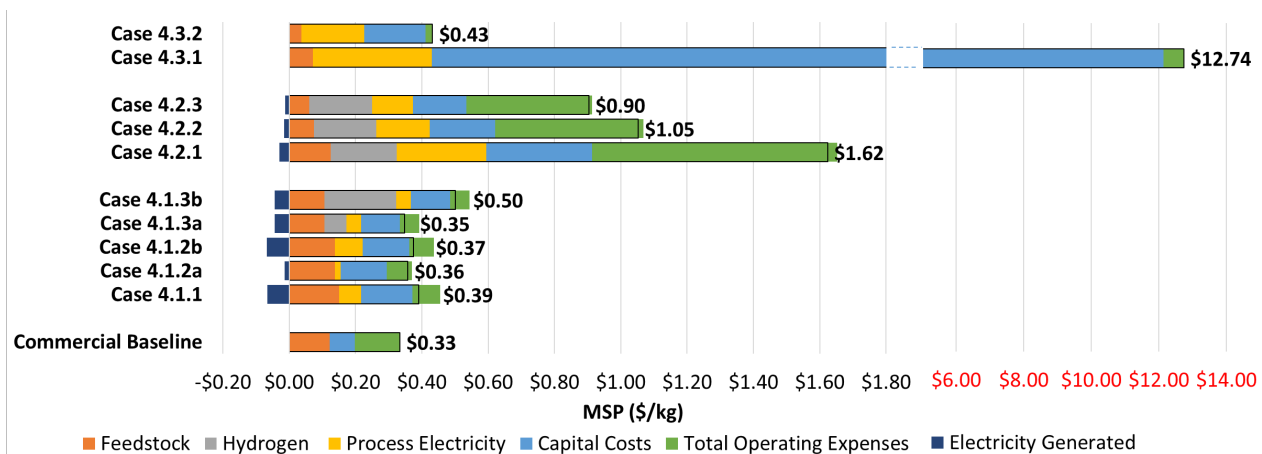
Figure 37. MSP comparison for Cases 4.1–4.3

In the indirect CO_2 to methanol case, separate electrolysis of CO_2 (for CO production) and H_2O (for H_2 production) allows for flexibility in the H_2:CO ratio fed to methanol synthesis. Investigation of the H_2:CO ratio shown in Figure 38 revealed increasing carbon efficiency and decreasing MSP as the ratio increased from 1:1 to 2:1. After a ratio of 2:1, minimal improvements in carbon efficiency and slight increases in MSP suggest an optimal ratio is obtained around 2:1, as suggested by the reaction stoichiometry. Therefore, both the SOT case and future case are set at a H_2:CO ratio of 2:1. This case was also selected as the basis for the two cases presented in the external publication. The SOT case for the indirect CO_2 to methanol pathway exhibits an MSP of $0.90/kg. Note, the external publication [53] utilizes a different baseline value for electricity ($0.068/kWh) and hydrogen cost ($4.50/kg), as such the MSP in the publication for the SOT case is $1.61/kg. Reducing cell voltage and keeping faradaic efficiency nearly constant reduces the electricity requirement of the process, decreasing both the operating expenses and capital expenses of electrolysis. Therefore, in this work, improvements from the SOT case to the future case reduces MSP by nearly 8%.
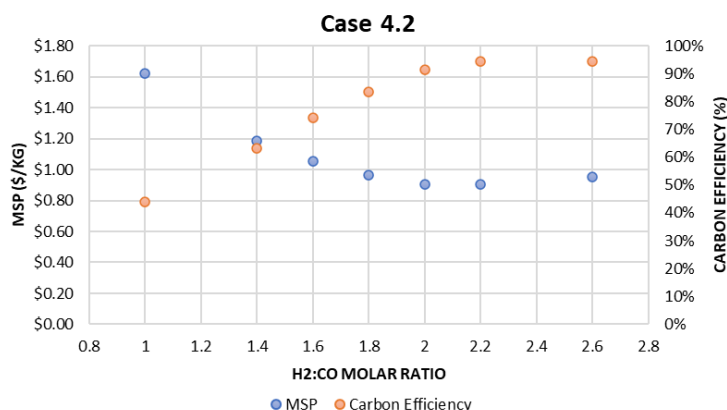
Figure 38. H_2:CO ratio study to observe the impacts on carbon efficiency and MSP for Case 4.2

The direct CO_2 to methanol pathway is in the very early stages of development. As such, methanol production via direct electrolysis exhibits variation across experimental SOT results.

Thus, the performance metrics for the SOT case were chosen to reflect the dataset that is most viable for scaleup [58]. Current SOT results for the direct pathway are extremely capital-intensive due to the low reported current densities. Our projections show the MSP of the SOT direct case (Case 4.3.1) as $12.74/kg with greater than 90% of the cost contributions coming from capital expenses associated with the electrolyzer. Like the indirect CO_2 case, the external publication uses a baseline value for electricity of $0.068/kWh, resulting in an MSP for the SOT case of $13.62/kg. In the future scenario, increasing the current density essentially increases the productivity. This results in greater yield of methanol per unit area, significantly reducing the capital expenses of the process. This results in a future MSP (Case 4.3.2) of $0.43/kg, approaching the current methanol market price.

Carbon Efficiency for Cases 4.1–4.3

Carbon efficiency highlights the technical limitations unique to each pathway as it applies to carbon loss due to selectivity, feedstock challenges, and maximum theoretical yield. Carbon flows normalized by carbon in the feedstock for each SOT scenario and a summary of the carbon efficiency for each scenario are shown in Figure 39. The exiting carbon flow as methanol, shown in red, is equal to the process carbon efficiency. As a benchmark for comparison, current commercial pathways exhibit carbon efficiencies ranging from 68%–75% [59].
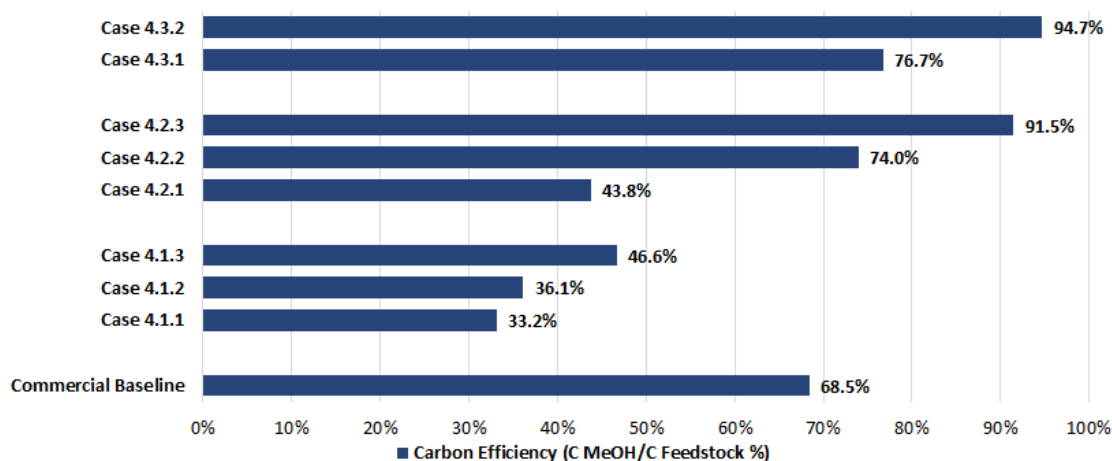
Figure 39. Carbon efficiency comparison for Cases 4.1–4.3

Out of the three sustainable cases, the biomass to methanol pathway displays the lowest carbon efficiency, regardless of scenario. The carbon efficiency of the biomass pathway in the base case was 33.2%, significantly lower than the commercial baseline. Importing H_2 into the synthesis loop to reincorporate carbon lost to CO_2 provides some improvement in carbon efficiency, up to 46.6%, whereas the renewable electricity case, which diverts less syngas to process fuel, only shows minimal gains in carbon efficiency (36.1%).

The indirect case achieves a carbon efficiency of 91.5% in Case 4.2.3, and carbon loss is primarily due to a small slipstream in the synthesis recycle loop and light hydrocarbons separated out in the methanol recovery step. Cases 4.2.1 and 4.2.2 have less optimized H_2:CO ratios and therefore exhibit lower carbon efficiencies. Carbon lost in the indirect case is routed to

the combined heat and power system and burned as process fuel. The SOT for the direct case (Case 4.3.1) has a carbon efficiency of 76.7%. In the future scenario (Case 4.3.2), the formation of formic acid and carbon monoxide byproducts is minimized, and the carbon efficiency has the potential to surpass each of the other Case 4 pathways at 94.7%.

Energy Efficiency

Calculated energy efficiencies displayed in Figure 40 are reported for the four studied methanol synthesis pathways, showing a range of 27.9%–58.1% depending on the specific case and assumptions. In comparing the three sustainable pathways to the commercial base case, we show that the energy efficiencies are all lower under both current SOT and future case assumptions. Among the sustainable cases, the direct CO_2-to-methanol future case (Case 4.3.2) was the highest-performing pathway at 58.1%, followed by biomass utilization at 47.8%–51.1% and then indirect CO_2-to-methanol at 27.9%–41.0%.
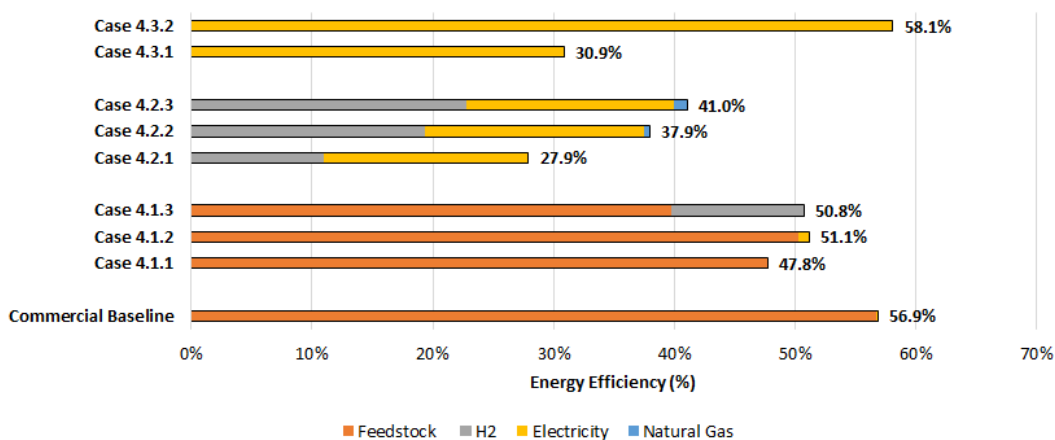
Figure 40. Energy efficiency comparison for Cases 4.1–4.3

With the benchmark biomass case relying predominantly on the energy inherent within the biomass as the main energy input, the lower energy efficiency can largely be traced back to the poor carbon efficiency as noted in Figure 29. Specifically, much of the inherent energy in the incoming feedstock is lost to char, tars, and other light species and not recovered for process use. Further, the biomass case employs several energy-intensive unit operations such as the tar reformer, acid gas removal, and methanol synthesis, which further drive-up energy usage. Process efficiencies are modestly improved through the use of renewable electricity; however, they are only expected to reach ~51.1%.

For the direct and indirect electrolysis CO_2 to methanol cases, the most significant differences in energy efficiency are related to the electrolysis operating assumptions. Although both processes require the transfer of six electrons to reduce CO_2 to methanol—shown in Equation 12 for the direct pathway and Equation 13, Equation 14, and Equation 15 for the indirect pathway—differences in assumed cell voltage significantly impact the total energy demand.

$$CO_2 + 6H^+ + 6e^- \rightarrow CH_3OH + H_2O \qquad \text{(Equation 12)}$$
$$4H^+ + 4e^- \rightarrow 2H_2 \qquad \text{(Equation 13)}$$
$$CO_2 + 2H^+ + 2e^- \rightarrow CO + H_2O \qquad \text{(Equation 14)}$$
$$CO + 2H_2 \rightarrow CH_3OH \qquad \text{(Equation 15)}$$
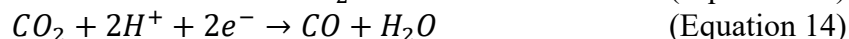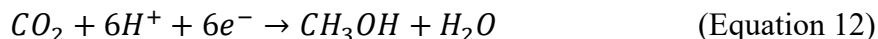
As shown in Table 22, the assumed cell voltage for direct methanol synthesis is 2.7 V based on recent experimental data, whereas the cell voltages for the H_2O oxidation and CO_2 to CO electrolysis are 2.0 and 3.0 V, respectively. Thus, despite requiring the same number of electrons per product (i.e., current), when multiplied by voltage to get total power demand, the differences in voltage significantly impact energy efficiency. Further, after forming the two syngas components via electrolysis, additional heat and pressure are required in the indirect case for the thermochemical conversion process to convert the syngas to methanol, whereas the direct case operates at near-ambient conditions.

Cross-Comparison of Cases 4.1–4.3

Analyzing minimum selling price, carbon efficiency, energy efficiency, and TRL simultaneously helps to identify the most important factors for near- or long-term deployment of sustainable methanol technologies (Figure 41).

The biomass gasification to methanol pathway has been highly optimized for cost efficiency. Comparatively, lower-TRL technologies such as the waste CO_2 pathways, which are more focused on proof-of-concept process design, are not yet optimized for cost or sustainability.

One of the challenges in comparing SOT data across products, such as CO and methanol, is that experimental conditions can be optimized for different metrics, which can highly impact TEA results. In the case of direct CO_2 to methanol synthesis (lowest in TRL), the reported current density, another key metric for commercialization, is comparably very low at only approximately 40 mA/cm^2. By contrast, the reported commercially relevant current densities for CO_2 to CO and H_2O to H_2 were on the scale of hundreds of mA/cm^2, which act to drive down both footprint of the electrolyzer and capital cost. This is illustrated in Figure 37 which shows that the indirect pathway has a significantly lower calculated production cost of $0.90/kg methanol compared to $12.74/kg methanol from direct conversion of CO_2. However, when comparing the future electrolysis cases, which account for improvements in technical parameters and a more like-for-like comparison, we find that the direct case approaches price parity with the indirect case while attaining a higher energy efficiency.

A significant limitation in the biomass to methanol pathway is carbon lost to tars and chars in the gasification step (about 31%). Higher operating temperatures could form less char, and thus would increase carbon efficiency of biomass to gaseous product, but gasification would require an external fuel source to provide heat, decreasing the energy efficiency of the process. In contrast, the CO_2-to-methanol pathways exhibit very high theoretical carbon efficiencies, accomplished through the elimination of other carbon sinks via highly selective electrocatalysts.

(A)

(B)

(C)
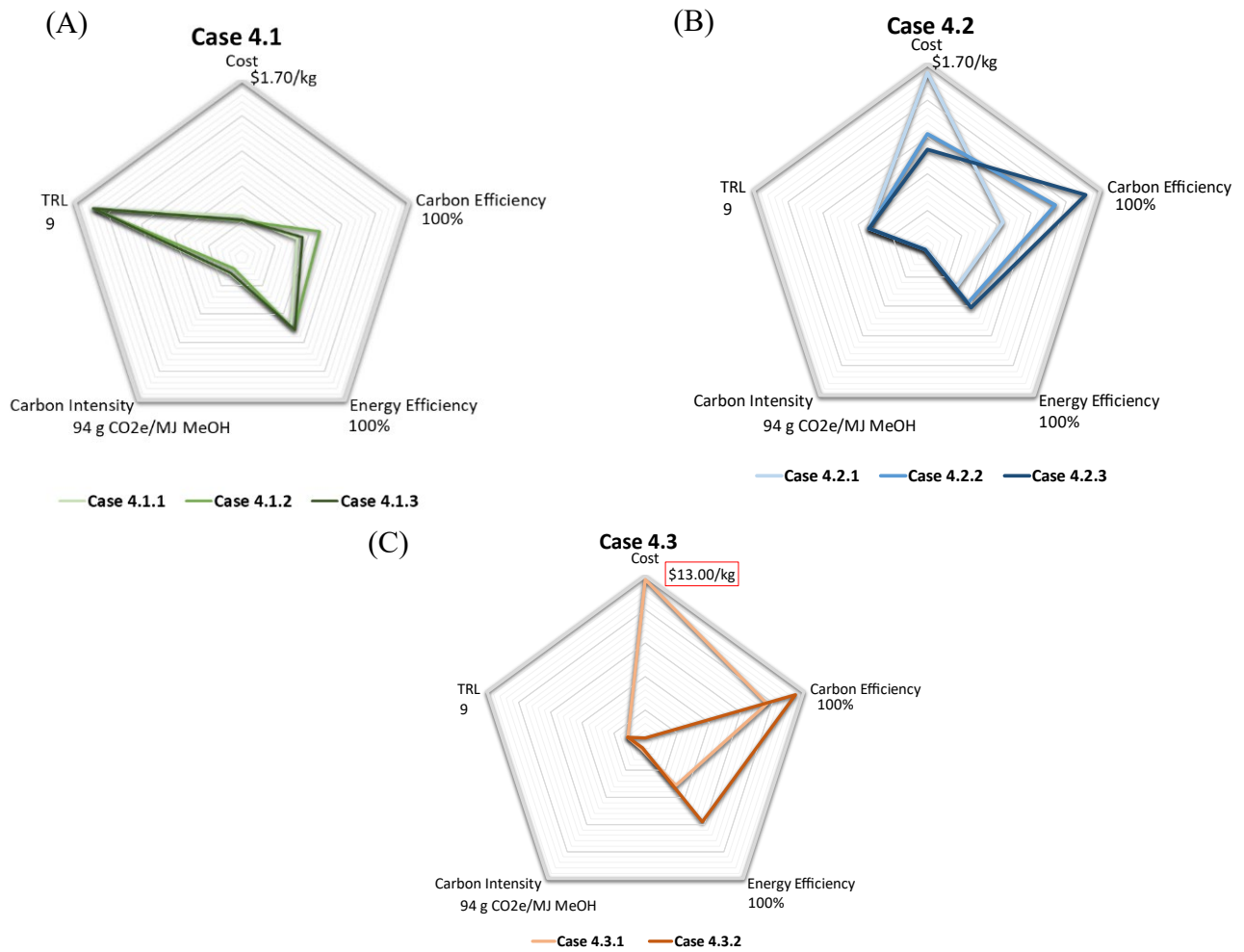
Figure 41. Cross-comparison of Cases 4.1–4.3
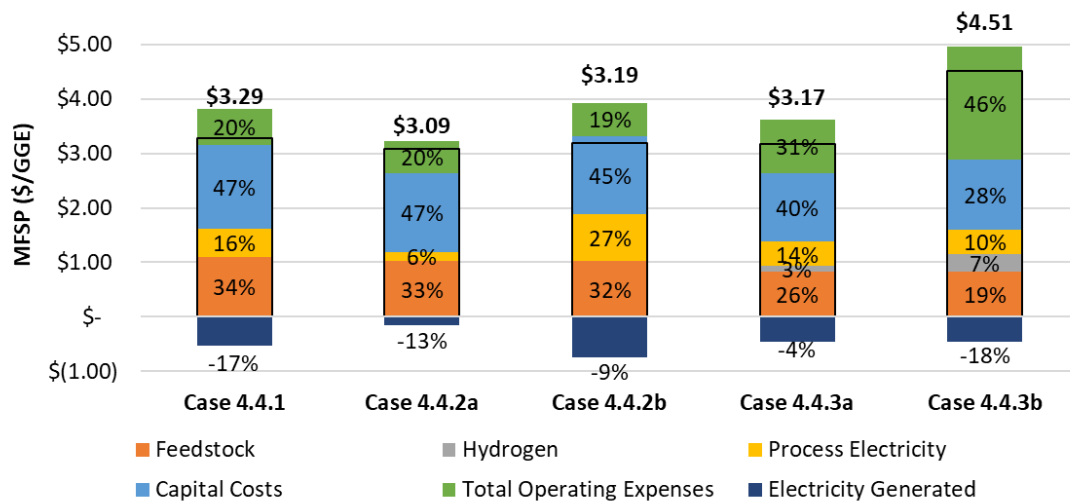
Figure 42. MFSPs ($/gge) of Case 4.4 scenarios

MFSP for Case 4.4

The benchmark scenario for the conversion of biomass to HOG via indirect gasification has a benchmark MFSP of \$3.29/gge, as seen in Figure 42. A 4% cost reduction is achieved by reincorporating CO_2 with low-cost (\$1.38/kg) renewable H_2 import; however, if high-cost (\$4.50/kg) H_2 is used, the MFSP increases by 37%. Further improvements are achieved in the renewable electricity case, in which MFSP reached \$3.09/gge in the low-cost electricity case (a 6% cost reduction). In addition, a high-level sensitivity case was run on the cost of imported renewable H_2 to identify the price required to reach HOG cost targets of \$2.50/gge (Figure 43).
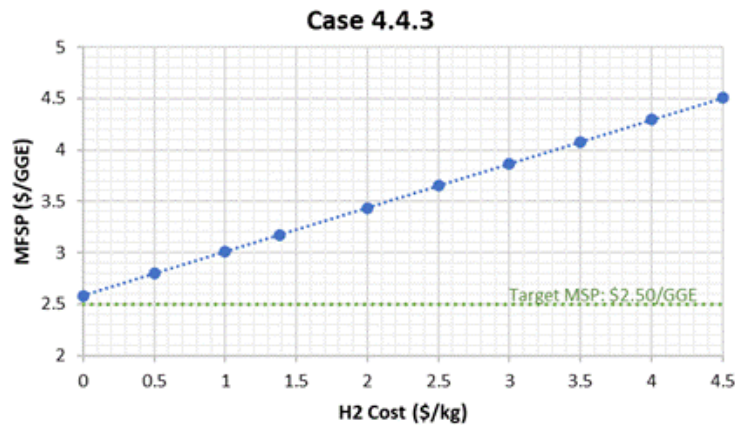
Figure 43. MFSP of HOG as a function of imported renewable H_2 cost

Decreasing H_2 costs significantly improves HOG MSP, but even with "free H_2" the target cost of \$2.50/gge is not possible under these operating conditions. However, further improvements in overall yield in conjunction with low H_2 prices could push the MSP past that target value. Additionally, although not considered in the Case 4.4 analysis, a combination of renewable electricity import along with CO_2 utilization could also have synergistic effects on both MSP and environmental metrics.

Carbon Efficiency and Energy Efficiency for Case 4.4
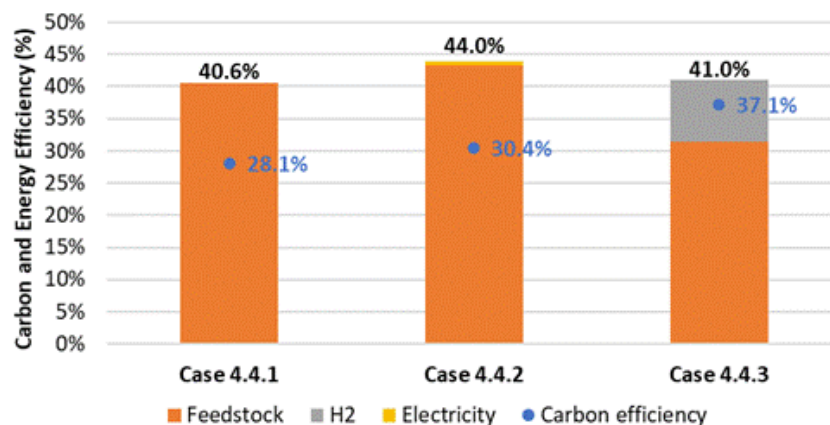
Figure 44. Carbon and energy efficiency of Case 4.4

Carbon and energy efficiencies for each Case 4.4 scenario are depicted in Figure 44. The calculated benchmark carbon efficiency and energy efficiency for the biomass to HOG pathway are 28.1% and 40.6%, respectively. The CO_2 utilization scenario shows the greatest improvement in carbon efficiency, similar to the trend seen in Case 4.1. Minimal improvements in carbon efficiency were shown in the renewable electricity import scenario. Similarly, only small improvements were achieved in energy efficiency, with the largest improvement in the renewable electricity case (up to 44%).

The biomass-to-HOG pathway is largely inhibited by the same factors mentioned for the biomass-to-methanol pathway described by Case 4.1. Significant tar, char, and CO_2 formation in the gasifier introduces a significant limitation in carbon efficiency in the upstream section of each process design. Further, because the biomass pathways rely significantly on biomass as both the energy and carbon source for the process, carbon efficiency losses can be closely tied to energy efficiency losses as well. Process improvements can be achieved, however, by reincorporating CO_2 via the reverse water gas shift reaction and imported H_2, and also with using renewable electricity for power rather than diverting syngas for power.

3.4.4 Key Learnings

Key Learnings – TEA

Commercial methanol pathways operate at large scale, at low cost, and with moderate carbon and energy efficiencies. Therefore, a viable sustainable methanol technology should meet or exceed the current commercial metrics to drive adoption at scale.

- Our analysis shows the biomass gasification to methanol pathway is capable of meeting market-competitive costs and displays a high TRL, and of the studied pathways is the most promising technology for the near term. However, sustainability metrics are key elements for impactful change in the ongoing global decarbonization efforts.
- Both indirect and direct CO_2-to-methanol pathways present energy efficiencies comparable to commercial pathways and exceptional carbon efficiencies, but at a cost. The direct CO_2 pathway is comparatively much lower in TRL and requires the most substantial R&D efforts pushing commercialization feasibility the farthest into the long term, whereas the indirect CO_2 pathway may be achievable in less R&D time if electrolysis costs can be reduced.
- Consequently, future analyses should consider process designs that are optimized across a variety of economic and environmental metrics rather than solely economic drivers.

Key Learnings – LCA

- Biomass-derived methanol via gasification and methanol synthesis using conventional energy inputs can achieve 80% of life cycle GHG emissions reductions than conventional fossil methanol (94 gCO_2e/MJ).
- Additional H_2 and CO_2 in waste stream from biomass gasification are converted into methanol to increase methanol yield. Using renewable energy sources can reduce the CI by 92% compared to conventional fossil methanol.
- CO_2-derived methanol cases require significant amounts of energy sources (electricity, H_2, and NG). Using low-CI energy sources is necessary to reduce life cycle GHG emissions; CO_2-derived methanol achieves net-zero-carbon fuel (1.3–3.9 gCO_2e/MJ) with renewable energy sources.

4. Discussion

4.1 LCA

The NZTT is tasked with investigating the potential to generate carbon-based fuels with much lower CIs compared to those of conventional fuels, approaching or exceeding net-zero GHG emissions. In this study, the life cycle GHG emissions of four main cases, 10 case variants, and dozens of sub-cases have been evaluated. These use the combinations of various carbon feedstocks (corn, algae, woody biomass, and CO_2 from some of these feedstocks), energy sources (intermediates from feedstock conversion, hydrogen, and electricity), and various conversion technologies (biomass fermentation, syngas fermentation, gasification, HTL, methanol synthesis, and methanol-DME-HOG conversion), which generate various energy products (ethanol, diesel, methanol, and HOG). To identify the potential reductions in CI, we evaluated the effects of substituting renewable inputs (electricity, hydrogen, and RNG) for traditional inputs. These net-zero-carbon fuel production pathways can help decarbonize the transportation and energy sectors. Table 27 presents the CIs of selected pathways, as well as electricity and H_2 requirements for the conversion processes in this study.

Our analysis shows that on a life cycle basis, there are multiple pathways to near-zero, zero, and net-negative hydrocarbon fuels. The biomass-derived fuel production pathways show life cycle GHG emissions reduction benefits compared to the fossil counterparts, mainly due to biogenic carbon uptake. With further reduction methods, we can achieve near-net-zero-carbon fuels. Case 1 starts from the CI of corn ethanol (53 gCO2e/MJ), which already achieves 42% reduction compared to E10 gasoline (91 gCO2e/MJ). We found this can be reduced by sequestrating CO_2 emissions from corn ethanol production (CCS), which leads to a CI of 15 gCO2e/MJ (Figure 6), and can be further reduced to −9 gCO2e/MJ through the use of RNG, renewable electricity, and green ammonia (Figure 7). Case 1 is unique among the four cases analyzed here in its use of carbon sequestration, and is therefore the only case capable of achieving negative emissions.

The benchmark scenario of Case 2, which uses algae for renewable diesel production, has 31 gCO2e/MJ (66% reduction compared to the CI of petroleum diesel [92 gCO2e/MJ]). This can be further reduced to 3 gCO2e/MJ when all available renewable energy options are fully used (Figure 17). Case 2 is unique in its employment of HTL, a technology being tested at scale for the production of drop-in fuels. Cases 3 and 4 use woody biomass for ethanol, methanol, and HOG production. Unlike other biomass feedstocks (corn or algae), these use 50 wt% of forest residue (waste stream) that do not involve upstream emissions from feedstock production stages except for the emissions related to feedstock collection; thus, the benchmark cases present lower CIs (17 and 18 gCO2e/MJ, respectively) (Figure 21 and Figure 35) compared to Cases 1 and 2. These can also reach near-net-zero-carbon fuels (7–8 gCO2e/MJ) by utilizing multiple renewable options such as RNG, renewable electricity, and renewable H_2.

We also evaluated two cases using CO_2 for fuel production (sub-scenarios of Cases 3 and 4). When converting CO_2 into fuels, the processes require significant electricity and/or H_2 inputs (Table 27). Thus, the CIs of CO_2-derived fuels highly rely on the CIs of electricity and H_2 used for the conversion processes. We found that the CO_2-derived fuel production pathways using conventional energy systems (e.g., U.S. electricity generation mix and H_2 from fossil natural gas) generate much higher life cycle GHG emissions even compared to conventional fossil fuels. However, when linked with renewable electricity and H_2, the pathways present the potential of achieving net-zero-carbon fuels mainly because of avoidance of the feedstock production-related emissions that happen in biomass-derived fuel production supply chains.

Although these net-zero-carbon fuel production pathways are all promising for decarbonizing the transportation and energy sectors, there are challenges to address and resolve in the future. First, renewable options such as renewable electricity, renewable H_2, and RNG that help reduce the CIs of various fuel production pathways are not all yet widely available at low cost and high reliability. For renewable electricity, the resource distribution (e.g., wind and solar) varies substantially by region, which may not necessarily be matched with the feedstock distribution (biorefineries, algae ponds, woody biomass, and CO_2). More importantly, renewable electricity has an intermittency issue that will drive up MFSP through underutilization of biorefinery equipment or the need for electricity or hydrogen storage. The near-term projected cost of renewable hydrogen is high because of both electrolyzer costs and potential underutilization of electrolyzer capital due to renewable electricity intermittency. Finally, the total available resource of RNG is limited.

For Case 1, CCS technology is well developed and proven at scale. Capture can be added to existing biorefineries, but there are potential challenges to connecting capture-enabled biorefineries to CO_2 disposal sites. If geologic formations appropriate for CO_2 sequestration are not sufficiently proximate to the biorefinery, significant additional cost and emissions will be associated with the transport of CO_2 from its source to the injection well. For all biomass-derived fuels, there may be logistic issues due to the spatial distribution of the biomass feedstocks (e.g., woody biomass) and preferred siting (e.g., algal ponds). For CO_2-derived fuel production pathways, the key challenge is its low technology readiness level.

Table 27 presents LCA results of various pathways evaluated in this study. It is important to remember that CI is but one of many fuel production pathway metrics. Other factors, such as the distribution and amount of the available resources (e.g., feedstocks and energy systems such as renewable electricity) to make the pathways feasible, need to be considered for successful net-zero-carbon fuel production. In terms of the conversion technologies, the cost and TRL should be considered along with the environmental benefits. We also found that many types of fuel products can be produced via various conversion routes, which means the market for the products and the infrastructure enabling use of the products should be considered.

In the LCA task, although we accounted for all GHG emissions throughout the supply chains of the fuel production pathways, the GHG emissions impacts of infrastructure build-out are not included. Because substantial electricity, H_2, and CO_2 capture demand may incur the demand for

additional infrastructure (e.g., wind turbines, solar panels, transmission, pipelines, electrolyzers for H_2 production, and H_2 storage tanks), further analyses are warranted to quantify these impacts.

The four cases evaluated in this study are not an exhaustive list of pathways; NZTT will explore more pathways (the combinations of feedstocks, conversion technologies, and products) to expand the coverage of net-zero-carbon fuel production pathways. Through continuous research efforts, we will identify new net-zero-carbon fuel production pathways and address the technical, logistic, and research challenges. LCA will be conducted along with TEA to help make strategic decisions on the development of future net-zero-carbon fuel production technologies.

In summary, the LCA task in this study has quantified two important aspects of net-zero-carbon liquid fuels. First, biomass through which atmospheric CO_2 is sequestered via biological photosynthesis is a key source for near-zero-carbon liquid fuel production. Second, further conversion of CO_2 produced from biological and chemical processes helps increase carbon conversion efficiencies. However, such conversion requires significant amounts of energy in terms of hydrogen and electricity. Net-zero-carbon liquid fuels become possible only when renewable electricity (and renewable hydrogen) is available and used for CO_2 conversion. The dual aspects show that biomass and renewable electricity can complement each other to produce net-zero-carbon liquid fuels that certain transportation subsectors still need.

Table 27. CIs of selected cases in this study, along with the electricity and H_2 inputs for the conversion processes

Case	Feedstock	Tech.	Product	Description [a]	CI (gCO2e/MJ)		Electricity Inputs (kWh/MJ)	H2 Inputs (MJ/MJ)
					Conventional Scenario [b]	Renewable Scenario [c]		
Case 1	Corn	CCS	Ethanol	Baseline (Corn ethanol CCS)	15		3	
				Corn ethanol CCS (RNG, ReElec., green ammonia)		−9	3	
Case 2	Algae	HTL	Renewable diesel	Base case	31		0.0052	0.051
				Case 2.1 — Using RNG for conversion		22	0.0052	0.051
				Case 2.2 — Case 2.1 + ReElec. for conversion		20	0.0052	0.051
				Case 2.3 — Case 2.2 + ReElec. for algae farm		13	0.0052	0.051
				Case 2.4 — Case 2.3 + ReElec. for CO2		3	0.0052	0.051
				Case 2.5 — Off-gas for H2 production		26	0.0027	0.044
				Case 2.6 — Case 2.5 + ReElec. for conversion		18	0.0027	0.044
				Case 2.7 — Case 2.6 + ReElec. for algae farm		11	0.0027	0.044
				Case 2.8 — Case 2.7 + ReElec. for CO2		2	0.0027	0.044
				Case 2.9 — Electrolysis for H2		53	0.00025	0.22
				Case 2.10 — Case 2.9 + ReElec. for conversion		18	0.00025	0.22
				Case 2.11 — Case 2.10 + ReElec. for algae farm		11	0.00025	0.22
				Case 2.12 — Case 2.11 + ReElec. for CO2		2	0.00025	0.22
Case 3	Woody biomass	Gas fermentation	Ethanol	Case 3.1.1 — Benchmark, no external energy inputs	17	10	0	0
				Case 3.1.2 — NG import	21	10	0	0
				Case 3.1.3 — Import H2	54	7	0	0.42
				Case 3.1.4 — Import H2 and NG	59	7	0	0.42
				Case 3.1.5 — Import H2 and electricity	55	7	0.0039	0.42
				Case 3.1.6 — Import H2, NG, and electricity	57	7	0.0033	0.42
	CO2	Gas fermentation	Ethanol	Case 3.2.1 — H2:CO2:CO = 3:1:0	444	5	0.86	0
				Case 3.2.2 — H2:CO2:CO = 2:0:1	247	5	0.31	0.88
				Case 3.2.3 — H2:CO2:CO = 5:0:3	194	5	0.17	1.08
Case 4	Woody biomass	Methanol synthesis	Methanol	Case 4.1.1 — Benchmark, no external energy inputs	18	11	0	0
				Case 4.1.2 — Import electricity	22	10	0.01	0
				Case 4.1.3 — Import H2/CO2 utilization	41	8	0	0.3
	CO2	Indirect methanol synthesis	Methanol	Case 4.2.1 — H2:CO = 1	350	1	0.59	0.87
				Case 4.2.2 — H2:CO = 1.61	238	2	0.35	0.83
				Case 4.2.3 — H2:CO = 2	209	2	0.28	0.83
		Direct methanol synthesis	Methanol	Case 4.3.1 — SOT	452	4	0.89	0
				Case 4.3.2 — Future	211	3	0.47	0
	Woody biomass	HOG production	HOG	Case 4.4.1 — Benchmark, no external energy inputs	22	13	0	0
				Case 4.4.2 — Import electricity	25	12	0.01	0
				Case 4.4.3 — Import H2/CO2 utilization	55	9	0	0.41

[a] ReElec = renewable electricity

[b] Using U.S. electric mix, fossil NG SMR H_2, and fossil NG (except as noted)

[c] Using renewable electricity, renewable H_2, and landfill-derived RNG (except as noted).

4.2 TEA

Even though many assumptions used for the TEA were kept consistent throughout this study, comparing TEA results across the four different cases can be difficult. This is because each pathway is analyzed based on different assumptions of process scale, product type and functional unit, and different TRLs. Production costs (and resultant MFSPs) comprise capital cost-related components (capital depreciation, income tax, and return on investment) and operating costs (materials, utilities, and labor). The production cost of all the case studies and scenarios analyzed are summarized in Table 28.

Table 28. Summary of TEA results positive cost impacts and negative cost impacts from the sensitivity study are presented in green and red, respectively.

	Scenarios	Product	Feedstock Rate	Product Rate	MSP ($/gge)	Reasons for Cost Changes from Baseline
Case 1	Baseline – corn ethanol with CCS	Ethanol	402,790 U.S. tons/yr	40 million gge/yr	2.95	N/A
Case 1.1	Ethanol with CCS and RNG	Ethanol	402,790 U.S. tons/yr	40 million gge/yr	3.35	RNG cost
Case 1.2	Ethanol with CCS and renewable electricity	Ethanol	402,790 U.S. tons/yr	40 million gge/yr	2.86	Renew. electricity cost
Case 1.3	Ethanol with CCS and green ammonia	Ethanol	402,790 U.S. tons/yr	40 million gge/yr	3.27	Feedstock cost
Case 2	Baseline – algae HTL	HC fuel	565 U.S. tons/day afdw algae	29 million gge/yr	4.27	N/A
Case 2.1	Using RNG	HC fuel	565 U.S. tons/day afdw algae	29 million gge/yr	4.50	RNG cost
Case 2.2	Using RNG + ReElec in conversion	HC fuel	565 U.S. tons/day afdw algae	29 million gge/yr	4.46	RNG cost
Case 2.3	Using RNG + ReElec in conversion and algae farm	HC fuel	565 U.S. tons/day afdw algae	29 million gge/yr	4.33	RNG cost
Case 2.4	Using RNG + ReElec throughout the process	HC fuel	565 U.S. tons/day afdw algae	29 million gge/yr	4.33	RNG cost
Case 2.5	No NG/off-gas to on-site H_2 prod. + renewable H_2	HC fuel	565 U.S. tons/day afdw algae	29 million gge/yr	4.24	Eliminate NG usage
Case 2.6	Case 2.5 + ReElec in conversion	HC fuel	565 U.S. tons/day afdw algae	29 million gge/yr	4.22	Eliminate NG usage
Case 2.7	Case 2.6 + ReElec in conversion and algae farm	HC fuel	565 U.S. tons/day afdw algae	29 million gge/yr	4.09	Eliminate NG usage + feedstock cost
Case 2.8	Case 2.7 + ReElec in CO_2 capture and transmission	HC fuel	565 U.S. tons/day afdw algae	29 million gge/yr	4.09	Eliminate NG usage + feedstock cost
Case 2.9	No NG/off-gas to on-site electricity generation + renewable H_2	HC fuel	565 U.S. tons/day afdw algae	29 million gge/yr	4.92	Renewable H_2 cost
Case 2.10	Case 2.9 + ReElec in conversion	HC fuel	565 U.S. tons/day afdw algae	29 million gge/yr	4.91	Renewable H_2 cost
Case 2.11	Case 2.10 + ReElec in conversion and algae farm	HC fuel	565 U.S. tons/day afdw algae	29 million gge/yr	4.78	Renewable H_2 cost
Case 2.12	Case 2.11 + ReElec in CO_2 capture and transmission	HC fuel	565 U.S. tons/day afdw algae	29 million gge/yr	4.78	Renewable H_2 cost
Case 3.1.1	Baseline – ReElec from syngas or CO_2	Ethanol	2,205 dry U.S. tons/day	48 million gge/yr	2.46	N/A
Case 3.1.2	w/ RNG	Ethanol	2,205 dry U.S. tons/day	51 million gge/yr	2.46	Yield, RNG
Case 3.1.3	w/ renewable H_2	Ethanol	2,205 dry U.S. tons/day	75 million gge/yr	2.20	Yield

	Scenarios	Product	Feedstock Rate	Product Rate	MSP ($/gge)	Reasons for Cost Changes from Baseline
Case 3.1.4	w/ renewable H_2 and RNG	Ethanol	2,205 dry U.S. tons/day	83 million gge/yr	2.18	Yield
Case 3.1.5	w/ renewable H_2 and renewable Electricity	Ethanol	2,205 dry U.S. tons/day	79 million gge/yr	2.12	Yield
Case 3.1.6	w/ renewable H_2, RNG, and renewable electricity	Ethanol	2,205 dry U.S. tons/day	83 million gge/yr	2.12	Yield
Case 3.2.1	Equation 6: $6 H_2 + 2 CO_2$ --> EtOH + $3 H_2O$	Ethanol	1,490 U.S. tons/day	48 million gge/yr	10.06	CO_2 electrolysis capital and operating costs
Case 3.2.2	Equation 7: $2 CO + 4 H_2$ --> EtOH + H_2O	Ethanol	1,490 U.S. tons/day	49 million gge/yr	7.36	CO_2 electrolysis capital and operating costs
Case 3.2.3	Equation 8: $3 CO + 5 H_2$ --> Bacteria + $2 H_2O$	Ethanol	1,490 U.S. tons/day	49 million gge/yr	6.56	CO_2 electrolysis capital and operating costs
Case 4.1.1	Baseline, biomass to methanol, no external energy inputs	Methanol	2,205 dry U.S. tons/day	47 million gge/yr	2.41	N/A
Case 4.1.2	Biomass to methanol, import renewable electricity	Methanol	2,205 dry U.S. tons/day	50 million gge/yr	2.22	Yield
Case 4.1.3	Biomass to methanol, renewable H_2 import and CO_2 utilization	Methanol	2,205 dry U.S. tons/day	67 million gge/yr	2.18	Yield
Case 4.2.1	Indirect CO_2-to-methanol via syngas, H_2:CO = 1	Methanol	3,048 U.S. tons/day	47 million gge/yr	9.99	CO_2 electrolysis capital and operating costs
Case 4.2.2	Indirect CO_2-to-methanol via syngas, H_2:CO = 1.61	Methanol	1,804 U.S. tons/day	47 million gge/yr	6.50	CO_2 electrolysis capital and operating costs
Case 4.2.3	Indirect CO_2-to-methanol via syngas, H_2:CO = 2	Methanol	1,459 U.S. tons/day	47 million gge/yr	5.57	CO_2 electrolysis capital and operating costs
Case 4.3.1	Direct CO_2-to-methanol, SOT	Methanol	1,751 U.S. tons/day	47 million gge/yr	78.82	CO_2 electrolysis capital and operating costs
Case 4.3.2	Direct CO_2-to-methanol, future	Methanol	1,424 U.S. tons/day	47 million gge/yr	2.66	CO_2 electrolysis capital and operating costs
Case 4.4.1	Baseline, biomass to HOG, no external energy inputs	HC fuel	2,205 dry U.S. tons/day	40 million gge/yr	3.29	N/A
Case 4.4.2	Biomass to HOG, import renewable electricity	HC fuel	2,205 dry U.S. tons/day	43 million gge/yr	3.09	Yield
Case 4.4.3	Biomass to HOG, renewable H_2 import and CO_2 utilization	HC fuel	2,205 dry U.S. tons/day	53 million gge/yr	3.17	Yield

RNG and renewable H_2 are assumed to have a higher price than fossil NG and fossil H_2. Higher prices of these renewable resources (compared to fossil base) increase the product selling price in Cases 1.1, 2.1–2.4, and 2.9–2.12. On the other hand, renewable electricity is assumed to be lower price compared to electricity from the grid, and therefore improves the process economics for Cases 1.2, 2.7, and 2.8. Impacts from the yield on the process economics are quite straightforward for the study of Cases 3.1.1–3.1.6. The process economics were improved in Cases 3.1.3–3.1.6 due to their significant increase in the product yields. The same yield impact on product selling price is also observed in the comparison between Cases 4.4.1 and 4.4.2.

The overall operating costs and capital costs are also very important cost drivers for process economics, especially for the case of utilizing low-efficiency processes. For example, the high capital and operating costs of CO_2 electrolysis in Case 3.2.2 can make the product selling price the least attractive, even though its process yield is comparable to the baseline Case 3.1.1. In addition, the sensitivity study of Case 4.3.2 shows the more attractive process economics when the process efficiency of CO_2 electrolysis is improved.

5. Conclusion

The analysis project team consists of team members from four national labs: the National Renewable Energy Laboratory, Pacific Northwest National Laboratory, Argonne National Laboratory, and Lawrence Livermore National Laboratory. The resulting analysis focused on the environmental and economic feasibility of net-zero-carbon fuels and identified the top challenges and opportunities of four representative pathway cases. Near-term commercialization will largely be driven by TRL and market acceptance through cost parity. As global priorities begin to shift and greater consideration is given to sustainability metrics for commercial deployment of technologies, long-term solutions will require improved environmental impacts such as CI, carbon efficiency, and energy efficiency. This report is designed to document LCA results first to determine the GHG emissions and other environmental impacts, then to look for TEA trade-offs in a consistent format across all four cases. All the key challenges and potential opportunities for achieving net-zero-carbon fuels with both environmental and economic viabilities are highlighted and summarized with comprehensive LCA and TEA data.

With intervention from renewable energy sources (renewable electricity, renewable H_2, and landfill-derived RNG), all cases studied in this report can approach near-zero CI values or near-100% carbon emissions reduction when compared with the petroleum gasoline baseline. For Case 1 and Case 2, renewable energy sources merely replace electricity and heat demands of the process. For Case 3 and Case 4, renewable energy sources not only replace electricity and heat demands of the process, but also provide processing strategies to significantly improve carbon efficiencies and product yields. In those case scenarios, the cost penalty of introducing expensive renewable energy sources may not be offset by product yield increases.

Specifically for Case 1, corn starch ethanol from state-of-the-art technologies can be net-zero with CCS (with a CI of -9 gCO_2e/MJ or near-100% GHG emissions reduction). Capture of fermentation CO_2 decreases ethanol CI by a net 29 gCO_2e/MJ to 15 gCO_2e/MJ. Three intervention scenarios (including importing renewable electricity, applying green ammonia, and renewable natural gas), when combined, can offset the remaining 15 g/MJ to near zero. However, getting corn starch ethanol to be net-zero CI comes with cost penalties. The cost of carbon capture was calculated at $0.15/gallon ethanol, equivalent to $52/ton of CO_2 in the baseline technology, without incentives or credits. Much higher cost penalties are expected with the other options, such as green ammonia and RNG. Thus, a carbon credit ranging from $50/ton up to $1,000/ton of CO_2 is required to trade off with cost for net-zero corn starch ethanol.

For Case 2, algae via HTL produces renewable diesel with the lowest GHG emissions for this case at 2 gCO_2e/MJ (near net zero, or equivalent to near-98% GHG emissions reduction), also by combining options using RNG, renewable electricity, and renewable H_2. Although RNG, electrolytically derived H_2, or combination of the two increases cost by about 5%–25%, the resulting MFSP stays in the range of $4–$5/gge for this algae to diesel pathway. If based on per-gge renewable diesel production, the heat demand for drying algae feedstocks is higher than process electricity or H_2 demand; therefore, replacing NG with RNG has the most significant

leverage on CI reduction in this case. Combing all three CI reduction strategies is necessary to approach near-net-zero renewable diesel fuel.

For Case 3, biomass-derived ethanol via gasification and gas fermentation using conventional energy inputs can achieve up to 85% of life cycle GHG emissions reduction (equivalent to 17 gCO_2e/MJ) compared to petroleum gasoline (91 gCO_2e/MJ), without considering importing renewable heat and power for process operation. Similar to Case 1 and Case 2, the CI could be reduced to near zero (93% GHG emissions reduction or 7 gCO_2e/MJ) by combining RNG, renewable H_2, and renewable electricity. The CI improvement is mainly due to higher yield of ethanol production by converting more carbon. If using cheaper renewable energy sources (such as $0.02/kWh electricity or $1.38/kg H_2), the cost of renewable energy sources would be break-even with the product yield improvement. Without cheap sources of electricity, RNG, or H_2, the cost penalty for CI improvement can be up to 50%. The CO_2-to-ethanol pathways require significant amounts of electricity and/or H_2 inputs (relative to Case 1 and Case 2). Therefore, if the grid electricity is used, the predicted CI could be near five times that of the petroleum gasoline baseline. By using renewable electricity and/or renewable H_2, the CI of CO_2-to-ethanol becomes near zero (down to 5 gCO_2e/MJ) with near-100% carbon efficiency utilizing CO_2 as a waste-to-energy feedstock. The cost for CO_2-to-ethanol is higher than baseline or corn ethanol studied in Case 1; thus, commercialization requires significant technological development to increase process efficiency and decrease the size and cost of the CO_2 electrolysis process.

For Case 4, biomass-derived methanol via gasification and methanol synthesis using conventional energy inputs can achieve 80% of life cycle GHG emissions reduction over conventional fossil methanol. The CI can be reduced to near net zero using renewable energy sources and H_2, like carbon-to-ethanol in Case 3. However, when high-cost renewable H_2 is utilized, cost of methanol increases from the benchmark case by near 30%, even with 40% carbon efficiency and product yield improvements. Our analysis shows the biomass gasification to methanol pathway is capable of meeting market-competitive costs and displays a high TRL, and of the studied pathways is the most promising technology for the near term. However, sustainability metrics are key elements for impactful change in the ongoing global decarbonization efforts. CO_2-derived methanol achieves net-zero-carbon fuel (1 gCO_2e/MJ or near-99% GHG emissions reduction from petroleum baseline) with renewable energy sources. Both indirect and direct CO_2-to-methanol pathways present energy efficiencies comparable to commercial pathways and present exceptional carbon efficiencies, but at a cost due to comparatively much lower TRL and demands for significant R&D improvements.

To approach net-zero-carbon emissions, most of the cases studied need to be green processes, meaning renewable energy resources are maxed out for all process heat and power and for fuel product carbon efficiency improvements. Obviously, curtailed and low-cost electricity is not a given and could be regionally specific across the country. Availability intermittency of all the renewable energy resources might increase operational cost for reduced fuel production and incur extra capital expenditures for on-site buffering capabilities and added complexity in integrating with existing infrastructure. Leveraging lessons learned from this analysis, the NZTT analysis team will continue to explore additional pathways (the

combinations of feedstocks, conversion technologies, and products) to expand the coverage of net-zero-carbon fuel production pathways, as well as to perform expanded analysis on the cases reported here to include logistic, system-level, and technical considerations. The uniqueness and key contribution of this study is that both LCA constraints and TEA perspectives are investigated simultaneously, so consequently this integrated study can quantify the impacts of a variety of economic and environmental metrics. Applying this simultaneous analysis approach to several highly varying technologies allows for the identification of overarching trends such as those highlighted in previous sections. This current analysis, together with future studies, can inform strategic decisions for development of future net-zero-carbon fuel production technologies.

6. References

1   International Energy Agency. 2020. *Global CO₂ emissions in 2019*.
    https://www.iea.org/articles/global-co2-emissions-in-2019
2   International Energy Agency. 2020. *United States*. https://www.iea.org/countries/united-states
3   National Oceanic and Atmospheric Administration. 2020. "Trends in Atmospheric Carbon
    Dioxide." https://www.esrl.noaa.gov/gmd/ccgg/trends/
4   Renewable Fuels Association. 2019. "Ethanol Biorefinery Locations."
    https://ethanolrfa.org/biorefinery-locations/
5   Zhang, Q. et al. 2017. "Carbon capture and utilization of fermentation CO_2: Integrated ethanol
    fermentation and succinic acid production as an efficient platform." *Applied Energy* 206: 364–
    371.
6   Wang, M., Elgowainy, Amgad, Lee, Uisung, Benavides, Pahola, Burnham, Andrew, Cai, Hao,
    Dai, Qiang, Hawkins, Troy, Kelly, Jarod, Kwon, Hoyoung, Liu, Xinyu, Lu, Zifeng, Ou,
    Longwen, Sun, Pingping, Winjobi, Olumide, Xu, Hui. 2019. *Greenhouse gases, Regulated
    Emissions, and Energy use in Transportation Model.* Lemont, IL: Argonne National Laboratory.
    https://doi.org/10.11578/GREET-EXCEL-2019/DC.20200706.1
7   Intergovernmental Panel on Climate Change. 2014. *Climate Change 2014: Synthesis Report*.
    [Core Writing Team, R.K. Pachauri and L.A. Meyer (eds.)]. IPCC, Geneva, Switzerland.
8   Jones, S. et al. 2014. *Process Design and Economics for the Conversion of Algal Biomass to
    Hydrocarbons: Whole Algae Hydrothermal Liquefaction and Upgrading*. Richland, WA: Pacific
    Northwest National Laboratory. PNNL-23227.
9   Phillips, S. D., Tarud, J. K., Biddy, M. J., Dutta, A. 2011. "Gasoline from Woody Biomass via
    Thermochemical Gasification, Methanol Synthesis, and Methanol-to-Gasoline Technologies: A
    Technoeconomic Analysis." *Industrial & Engineering Chemistry Research* 50: 14226–14226,
    doi:10.1021/ie2024992.
10 Davis, R. et al. 2016. *Process design and economics for the production of algal biomass: algal
    biomass production in open pond systems and processing through dewatering for downstream
    conversion*. Golden, CO: National Renewable Energy Laboratory. NREL/TP-5100-64772.
11 Dutta, A. et al. 2018. *High-Octane Gasoline from Lignocellulosic Biomass via Syngas and
    Methanol/Dimethyl Ether Intermediates: 2018 State of Technology and Future Research*.
    Golden, CO: National Renewable Energy Laboratory.
12 Tan, E. C. et al. 2018. *High-Octane Gasoline from Lignocellulosic Biomass via Syngas and
    Methanol/Dimethyl Ether Intermediates: 2018 State of Technology and Future Research*.
    Golden, CO: National Renewable Energy Laboratory.
13 Davis, R., Laurens, L. 2020. *Algal Biomass Production via Open Pond Algae Farm Cultivation:
    2019 State of Technology and Future Research*. Golden, CO: National Renewable Energy
    Laboratory.
14 ICF. 2020. *Study on the Use of Biofuels (Renewable Natural Gas) in the Greater Washington,
    D.C. Metropolitan Area*.
15 National Renewable Energy Laboratory. 2016. *H2A Production Model, Version 3*.
    http://www.hydrogen.energy.gov/h2a_production.html.
16 Klein-Marcuschamer, D., Simmons, B. A., Blanch, H. W. 2011. "Techno-economic analysis of a
    lignocellulosic ethanol biorefinery with ionic liquid pre-treatment." *Biofuels, Bioproducts and
    Biorefining* 5, 562–569.

17 Heydorn, B. 1998. *SRI Consulting Chemical Economics Handbook*. Menlo Park, CA: SRI Consulting.

18 International Energy Agency. 2016. *20 Years of Carbon Capture and Storage: Accelerating Future Deployment*. Paris, France: IEA. https://doi.org/10.1787/9789264267800-en

19 Liu, X., Elgowainy, A., Wang, M. J. G. C. 2020. "Life cycle energy use and greenhouse gas emissions of ammonia production from renewable resources and industrial by-products." *Green Chemistry* 22: 5751–5761.

20 U.S. Department of Agriculture National Agricultural Statistics Service. 2019. "Crop Production 2018 Summary."

21 Renewable Fuels Association. 2019. "World Fuel Ethanol Production." http://www.ethanolrfa.org/resources/industry/statistics/

22 U.S. Department of Agriculture Economic Research Service. 2019. "State Export Data: Agricultural Exports, U.S. agricultural cash receipts-based estimates." Retrieved October 28, 2019, https://www.ers.usda.gov/data-products/state-export-data/state-export-data/#State

23 Lin, T. et al. 2016. "Biomass feedstock preprocessing and long-distance transportation logistics." *GCB Bioenergy* 8: 160–170.

24 Baughman, W. F., Jamieson, G. S. 1921. "The Chemical Composition of Corn Oil." *Journal of the American Chemical Society* 43: 2696–2702.

25 Herron, S., Zoelle, A., Summers, W. M. 2014. *Cost of Capturing CO_2 from Industrial Sources*. National Energy Technology Laboratory. doi:10.2172/1480985.

26 McCoy, S. T., Rubin, E. S. 2008. "An engineering-economic model of pipeline transport of CO_2 with application to carbon capture and storage." *International Journal of Greenhouse Gas Control* 2: 219–229.

27 U.S. Department of Energy Bioenergy Technologies Office. 2016. *Multi Year Program Plan*.

28 Heath, L. S., Birdsey, R. A., Row, C., Plantinga, A. J. 1996. *Forest Ecosystems, Forest Management and the Global Carbon Cycle*. Springer, 271–278.

29 Lee, U., Han, J., Wang, M. 2016. *Well-to-Wheels Analysis of Compressed Natural Gas and Ethanol from Municipal Solid Waste*. Argonne, IL: Argonne National Laboratory.

30 Mintz, M., Han, J., Wang, M., Saricks, C. 2010. *Well-to-Wheels analysis of landfill gas-based pathways and their addition to the GREET model*. Argonne, IL: Argonne National Laboratory.

31 Lee, U., Han, J., Wang, M. J. 2017. "Evaluation of landfill gas emissions from municipal solid waste landfills for the life-cycle analysis of waste-to-energy pathways." *Journal of Cleaner Production* 166: 335–342.

32 Cai, H. et al. 2020. *Supply Chain Sustainability Analysis of Renewable Hydrocarbon Fuels via Indirect Liquefaction, Ex Situ Catalytic Fast Pyrolysis, Hydrothermal Liquefaction, Combined Algal Processing, and Biochemical Conversion: Update of the 2019 State-of-Technology Cases*. Argonne, IL: Argonne National Laboratory. ANL/ESD-20/2).

33 Daniell, J., Köpke, M., Simpson, S. 2012. "Commercial biomass syngas fermentation." *Energies* 5: 5372–5417.

34 Guo, Y. et al. 2010. "Medium optimization for ethanol production with Clostridium autoethanogenum with carbon monoxide as sole carbon source." *Bioresource Technology* 101: 8784–8789.

35 Simpson, S. D., Koepke, M., Smart, K. F., Tran, L. P., Sechrist, P. A system and method for controlling metabolite production in a microbial fermentation. WO Patent 2014151158A1, filed March 12, 2014, and issued September 25, 2014.

36 Handler, R. M. et al. 2016. "Life cycle assessments of ethanol production via gas fermentation: anticipated greenhouse gas emissions for cellulosic and waste gas feedstocks." *Industrial & Engineering Chemistry Research* 55: 3253–3261.

37 Dufek, E. J., Lister, T. E., McIlwain, M. E. 2011. "Bench-scale electrochemical system for generation of CO and syn-gas." *Journal of Applied Electrochemistry* 41: 623–631.

38 Yang, H., Kaczur, J. J., Sajjad, S. D., Masel, R. I. 2017. "Electrochemical conversion of CO_2 to formic acid utilizing Sustainion™ membranes." *Journal of CO_2 Utilization* 20: 208–217.

39 Steward, D., Ramsden, T., Zuboy, J. 2012. *H2A Central Hydrogen Production Model, Version 3 User Guide*. Golden, CO: National Renewable Energy Laboratory.

40 Jouny, M., Luc, W. W., Jiao, F. 2018. "A General Techno-Economic Analysis of CO_2 Electrolysis Systems." *Industrial & Engineering Chemistry Research*.

41 Li, X. et al. 2016. "Greenhouse gas emissions, energy efficiency, and cost of synthetic fuel production using electrochemical CO_2 conversion and the Fischer–Tropsch process." *Energy & Fuels* 30: 5980–5989.

42 Humbird, D. et al. 2011. *Process design and economics for biochemical conversion of lignocellulosic biomass to ethanol: dilute-acid pretreatment and enzymatic hydrolysis of corn stover*. Golden, CO: National Renewable Energy Laboratory.

43 Dutta, A. et al. 2011. *Process design and economics for conversion of lignocellulosic biomass to ethanol: thermochemical pathway by indirect gasification and mixed alcohol synthesis*. Golden, CO: National Renewable Energy Laboratory.

44 Rosen, B. A. et al. 2011. "Ionic liquid–mediated selective conversion of CO_2 to CO at low overpotentials." *Science*: 1209786.

45 Schultz, M. A., Raiser, T. E., Brenc, R. J. Product management in biological conversion processes. CA Patent 3013466C, filed February 3, 2017, and issued August 10, 2017.

46 Liew, F. et al. 2016. "Gas fermentation—a flexible platform for commercial scale production of low-carbon-fuels and chemicals from waste and renewable feedstocks." *Frontiers in microbiology* 7: 694.

47 Ueckerdt, F., Hirth, L., Luderer, G., Edenhofer, O. 2013. "System LCOE: What are the costs of variable renewables?" *Energy* 63: 61–75.

48 Saur, G. 2008. *Wind-to-hydrogen project: electrolyzer capital cost study*. Golden, CO: National Renewable Energy Laboratory.

49 Kalinci, Y., Hepbasli, A., Dincer, I. 2015. "Techno-economic analysis of a stand-alone hybrid renewable energy system with hydrogen production and storage options." *International journal of hydrogen energy* 40: 7652–7664.

50 Welch, A. J., Dunn, E., DuChene, J. S., Atwater, H. 2020. Bicarbonate or Carbonate Processes for Coupling Carbon Dioxide Capture and Electrochemical Conversion. *ACS Energy Letters* 5: 940–945.

51 Ma, S., Luo, R., Moniri, S., Lan, Y., Kenis, P. J. 2014. "Efficient electrochemical flow system with improved anode for the conversion of CO_2 to CO." *Journal of The Electrochemical Society* 161: F1124-F1131.

52 National Academies of Sciences, Engineering, and Medicine. 2019. *Gaseous carbon waste streams utilization: Status and research needs*. Washington, D.C. :National Academies Press.

53 Harris, K., Grim, R. G., Huang, Z., Tao, L. 2021. "A comparative techno-economic analysis of renewable methanol synthesis from biomass and CO2: Opportunities and barriers to commercialization." *Applied Energy* 303: 117637, doi:10.1016/j.apenergy.2021.117637.

54 Tan, E. C. D. et al. 2015. *Process Design and Economics for the Conversion of Lignocellulosic Biomass to Hydrocarbons via Indirect Liquefaction*. Golden, CO: National Renewable Energy Laboratory.

55 Tan, E. C. D. et al. 2020. *High-Octane Gasoline from Lignocellulosic Biomass via Syngas and Methanol/Dimethyl Ether Intermediates: 2019 State of Technology*. Golden, CO: National Renewable Energy Laboratory.

56 Ma, S. et al. 2016. "Carbon nanotube containing Ag catalyst layers for efficient and selective reduction of carbon dioxide." *Journal of Materials Chemistry A* 4: 8573–8578, doi:10.1039/c6ta00427j.

57 National Renewable Energy Laboratory. 2021. "H2A: Hydrogen Analysis Production Models." https://www.nrel.gov/hydrogen/h2a-production-models.html

58 Yang, D. et al. 2019. "Selective electroreduction of carbon dioxide to methanol on copper selenide nanocatalysts." *Nature Communications* 10: 677, doi:10.1038/s41467-019-08653-9.

59 IHS Markit. 2014. *Methanol Process Summary PEP Review - 2014-06*. IHS Markit. https://ihsmarkit.com/products/sricreport-pepreview2014-06-methanol-process-summary.html